Intermittent Electrical Stimulation as a Treatment Approach for Deep Tissue Pressure Injury after a Spinal Cord Injury

by

Hemalatha Velanki

A thesis submitted in partial fulfillment of the requirements for the degree of

Master of Science

Neuroscience

University of Alberta

ABSTRACT

The goal of this study was to investigate the effects and mechanisms of action of an intermittent electrical stimulation (IES) paradigm on the healing of deep-seated muscle injury. Electrical stimulation has been extensively studied for the treatment of open wounds, often with amplitudes lower than motor threshold. The effect of electrical stimulation producing palpable muscle contractions on the cellular events in deep-seated muscle injury has not been explored. In this study, an IES paradigm was tested in rats with complete spinal cord injury (SCI) in which a deep-seated muscle injury was induced. The goals of the study were to: *(i)* assess the natural progression of a muscle injury; and *(ii)* the role of IES in expediting the rate of healing. Three groups of rats were used: (a) muscle injury only, (b) IES only, and (c) muscle injury with IES. Magnetic resonance imaging monitored the extent and progression of muscle injury 1, 3, 5 and 7 days post-induction of injury and/or initiation of IES. Immunohistochemistry assessed the severity of injury and rate of healing by evaluating the presence of inflammatory and satellite cells, and embryonic myofibres. When applied on day 1 after the induction of muscle injury, IES significantly reduced the edema associated with the injury, increased M1 and M2 macrophages and increased satellite cell proliferation. It also decreased the overall size of injury. This suggested that when applied early after muscle injury, IES can expedite anti-inflammatory and pro-regenerative events, and may be an effective means for treating deep-seated muscle injury.

DEDICATION

To my mom & dad.

ACKNOWLEDGEMENTS

First and foremost, I would like to thank my supervisor Dr. Vivian K. Mushahwar for her extreme support and guidance during my Master's program at the University of Alberta. I am very grateful for her patience and understanding throughout. The skills learnt in her lab have developed my thinking as a scientist and growth at an individual level.

I would like to specially thank Neil Tyreman for being involved in every stage of my experiments. I would also like to thank Peter Seres, Kahir Rahemtulla, Steven Lu, and Dr. Leandro Solis who were involved in my experiments. Their immense support and contributions to this project were helpful. I want to thank them for reading my thesis and providing me with their valuable suggestions. I wish to thank my supervisory committee, Drs. Richard Thompson and Ming Chan for the suggestions during the meetings. Their ideas helped to develop the study from preliminary work. I acknowledge the funding agency Canadian Institute of Health Research (CIHR) for supporting my stipend throughout my program, without that support this work would not have been possible.

Sincere thanks to the HSLAS staff for their assistance during multiple experiments, especially Dr. Domahidi for her advice during animal care. I am grateful to Christian Barclay and Jennifer Sauve for the care and love during their daily visits to the animal house.

The Mushahwar lab has been a great place to work in. The time spent with Dr. Dirk Everaert, Ashley Dalrymple, and Amirali Toossi during the program has been memorable.

Special thanks to my mom and dad for their love and support, and being there for me always. I would like to thank my family and friends for their support.

More importantly, I would like to thank god for giving me strength throughout this journey.

TABLE OF CONTENTS

LIST OF FIGURES

LIST OF ABBREVIATIONS

AC - alternating current

ADP - adenosine di-phosphate

ANOVA - analysis of variance

ATP - adenosine tri-phosphate

BDNF - brain derived neurotrophic factor

BW - body weight

Ca^{2+} - calcium ion

CP - common peroneal nerve

CRP - C reactive protein

CSA - cross sectional area

DAPI - 4',6-Diamidino-2-Phemylindole, Dihydrochloride

DC - direct current

DTPI - deep tissue pressure injury

EGF - epidermal growth factor

eMHC - embryonic myosin heavy chain

ES - electrical stimulation

ETC - electron transport chain

HVPC - high voltage pulse current

ICAM - intracellular adhesion molecule

ICC - intraclass correlation coefficient

ICU - intensive care unit

IES - intermittent electrical stimulation

IGF-1 - insulin-like growth factor-1

IHC - immunohistochemistry

IL - interleukin

IRI - ischemic reperfusion injury

IT - ischial tuberosity

K^+ - potassium ion

LFSW - low frequency square wave pulse

MI - myocardial infarction

MRI - magnetic resonance imaging

Na^+ - sodium ion

NADH - nicotinic amide dehydrogenase

NGF - nerve growth factor

NPUAP - National Pressure Ulcer Advisory Panel

PI - pressure injury

ROM - reactive oxygen metabolites

RF - radiofrequency

SCI - spinal cord injury

sDTI - suspected deep tissue injury

TA - tibialis anterior

TE - echo time

TENS - transcutaneous electrical nerve stimulation system

TGF - transforming growth factor

TNF-α - tumor necrosis factor-α

TR - repetition time

TSE - turbo spin echo

US - ultrasound

UVC - ultraviolet-C

VAC - vacuum assisted closure

VCAM - vascular cell adhesion molecule

VEGF - vascular endothelial growth factor

XDH - xanthine dehydrogenase

XO - xanthine oxidase

1. Introduction

1.1. Problem definition

Pressure injury (PI), previously known as pressure ulcer (Edsberg et al., 2016), is a significant problem in Canada across the continuum of healthcare settings. They are among the common secondary complications that occur in populations with reduced mobility and/or sensation. Individuals at risk of developing PI include the elderly (Gorecki et al., 2009; Solis et al., 2011), patients in intensive care units (Shahin et al., 2008; Solis et al., 2011), and those with neurological insults (Krause et al., 2001; Garber and Rintala, 2003). A PI can also occur in individuals undergoing cardiac surgeries (Feuchtinger et al., 2005) and with orthoses and prostheses. Secondary complications like PIs lead to decreased quality of life, physical restrictions, loss of independence, social isolation, and financial stress (Gorecki et al., 2009). The resulting prolonged bed rest and restricted activity are among the factors that lead to clinical depression (Saunders et al., 2012).

A PI can initiate at the skin layer and progress towards the deep layers. These injuries are evaluated based on their involvement of the layers of the skin, subcutaneous tissue, and muscles (Black et al., 2007). Deep tissue pressure injury (DTPI) is a more recently studied form of PI that forms at the deep bone-muscle interface before progressing towards the epidermis (Edsberg et al., 2016). For example, in the recumbent position, the soft tissue between the external support and the sacral region is entrapped (Shahin et al., 2008). The common sites affected in the seated position include the region adjacent to the ischial tuberosities, shoulder blades, and posterior aspect of the arms and legs. The tissue compression and local obstruction in the blood supply can cause discomfort. This mechanoreceptor input is received by the central nervous system from the periphery to produce a suitable response (Marchand, 2008). Able-bodied individuals would

subconsciously reposition themselves to relieve the discomfort. The same would not be possible in individuals with disorders causing immobility or reduced sensation. The resulting compression of the tissue near the bony prominence over time can develop into a DTPI. The injury to deep structures puts patients at risk for additional complications such as septicemia (Galpin et al., 1976), osteomyelitis (Darouiche et al., 1994), and even premature death.

Despite the emergence of standard care interventions, the prevalence of PI decreased minimally over the last two decades (Thomas, 2010). The overall prevalence rate in all health facilities in the USA, Canada, and Europe ranges between 8 and 26% (Kaltenthaler et al., 2001; Woodbury and Houghton, 2004; Vanderwee et al., 2007). The prevalence in non-acute care facilities is the highest among all the hospital settings with a rate of 29.9%, followed by acute care and community care facilities (Woodbury and Houghton, 2004). The increase in the aging population attributes to the prevalence rates in the developed countries (Rasero et al., 2015). Studies indicate that more than two-thirds of hospitalized patients developing a PI are 70 years or older (Russo et al., 2006; Landi et al., 2007; Merten et al., 2015). The risk of developing a new PI also increases with advancing age.

The incidence rates of PI among acute care facilities range from 5 to 9% (Whittington et al., 2000; VanGilder et al., 2009). Acute care facilities include those who are severely ill or had recent surgery. A PI can develop within a few minutes of immobilization as a consequence of decreased mobility and loss of sensory perception after surgery.

The average length of hospital stay after developing a PI is 14.1 days (Russo and Elixhauser, 2006). During this single episode of hospitalization, the average cost to treat a full thickness PI in the United States was $ 129, 248 (Brem et al., 2010). In 2006, the minimal annual cost to treat a hospital-acquired PI was $9.2 – 11 billion in the United States (Russo

et al., 2006). These expenditures are related to diagnostic tests, monitoring, expensive preventive materials, extended inpatient stay, and re-hospitalization (Graves et al., 2005). The lengthy hospital stays coupled with the costs associated with the management are a significant concern in the Canadian health care system (Graves et al., 2005).

1.2. Significance of Pressure Injury on Spinal Cord Injury (SCI)

The incidence rates of PI are higher among people with chronic SCI than in the general population. In the United States, at least 35% of the people with SCI will develop a PI during the initial hospitalization, and the incidence rates rise with every year post injury (Krause et al., 2001). The prevalence of PI in SCI in the first year is 8%, and this can increase up to 32% a few years after SCI (Richardson and Meyer, 1981; Krause et al., 2001). Individuals with SCI are especially more vulnerable to PI because of loss of sensory, motor, and autonomic function (Carlson et al., 2017). They experience a change in the anatomical and physiological properties of the skin and the muscles after injury which can lead to health-related complications, including PI (Shields and Dudley-Javoroski, 2007). Some of the predisposing factors in SCI that cause a PI are duration after SCI, completeness of injury, spasticity, advancing age, urinary incontinence, and difficulty in performing routine skin care (Mawson et al., 1988). These factors contribute to a lifetime risk of developing a PI to 85% in individuals with SCI (Richardson and Meyer, 1981; Mawson et al., 1988; Fuhrer et al., 1993).

1.3. Classification of Pressure Injury

A PI is defined by the National Pressure Ulcer Advisory Panel (NPUAP), " as a localized damage to the skin and/or underlying tissue usually over a bony prominence or medical device, as a result of pressure in combination with shear and/or friction (Edsberg et al., 2016)." A PI can clinically present as intact skin or open ulcer (Edsberg et al., 2016). Based on where the injury originates the PI is classified into two main types: superficial PI and DTPI (Figure 1-1) (Black et al., 2007; Edsberg et al., 2016).

1.3.1. Superficial Pressure Injury

Superficial PI initiates at the epidermis as a result of friction and shear stress between the skin and the support surface (Dinsdale, 1974), and progress to underlying fat and muscle if unnoticed. The current numerical system by the NPUAP classifies superficial PI into five stages based on the involved tissue depth and extent of the damage (Shea, 1975; Black et al., 2007; Edsberg et al., 2016). Stage I is described as intact skin with a localized area of non-blanchable erythema (Black et al., 2007; Edsberg et al., 2016). Stage II, partial thickness skin loss, forms as a result of excessive moisture and shear in the skin (Black et al., 2007; Edsberg et al., 2016). Inadequate care to the skin may progress into a stage III (full thickness skin loss) or stage IV (full thickness skin and tissue loss), wherein deep structures such as fat and muscle are visible (Black et al., 2007; Edsberg et al., 2016). A newer addition to the 4-stage system is the unstageable PI, in which slough and eschar can make the staging of PI difficult (Black et al., 2007; Edsberg et al., 2016). In the past, the focus of prevention and treatment of PIs were concentrated on the skin to prevent a stage I from progressing into a full thickness

injury and skin loss (Bours et al., 2002).

1.3.2. Deep Tissue Pressure Injury (DTPI)

Early scientific literature described the differentiation between superficial PI and DTPI (Groth, 1942). However, DTPI only became clinically acknowledged in 2005 and was referred to as suspected deep tissue injury (sDTI) (Ankrom et al., 2005; VanGilder et al., 2010). In 2016, the NPUAP added DTPI into the revised staging classification of PI (Edsberg et al., 2016). A DTPI develops from prolonged entrapment or compression of soft tissue between a bony prominence and an external support surface (Dinsdale, 1973; Breuls et al., 2003a; Gefen, 2007; Stekelenburg et al., 2007; European Pressure Ulcer Advisory Panel et al., 2014) (Figure 1-2). In individuals with SCI, DTPI typically occurs in the muscles adjacent to the sacrum in supine and/or ischial tuberosities in seated position.

A DTPI is a serious form of PI due to its late detection and rapid deterioration. One challenge is the difficult detection at the time of injury initiation (Breuls et al., 2003b). As the DTPI progresses towards the skin, it presents as non-blanchable purple or localized maroon areas. This clinical presentation is often confused as a stage I or stage II PI, resulting in the management at the level of the skin. But, by then, the injury has involved the deep tissue and is approaching the epidermis. Other challenges include skin changes on a darkly pigmented skin which make the detection and differentiation difficult. Research studies have suggested the use of biomarkers in sweat or blood with infrared spectroscopy (Keller et al., 2006; Berg et al., 2010). Magnetic resonance imaging (MRI) and ultrasound are other methods that may be used for early detection (Bosboom et al., 2003). Still, these diagnostic techniques are under research and not practiced in hospital settings. Inappropriate

management and late detection of DTPI allow them to progress into stage IV PI with open wounds as deep as bone.

A prevalence study conducted in the US population in 2006 – 2009 showed a decrease in the proportion of stage I and stage II PI (VanGilder et al., 2010). In contrast, there was a 3-fold increase in the proportion of DTPI (VanGilder et al., 2010). This increase is due to staging education among the healthcare staff (VanGilder et al., 2010).

1.4. Magnetic resonance imaging for deep tissue pressure injury detection

Magnetic resonance imaging techniques were used to study the mechanisms of DTPI after application of compressive load (Bosboom et al., 2003; Solis et al., 2007 p.20, 2013; Stekelenburg et al., 2007). Of these techniques, the use of T_2-weighted MRI to detect the response of tissue to injury were well validated in previous studies (Bosboom et al., 2003; Solis et al., 2007, 2013; Stekelenburg et al., 2007).

The physics underlying MRI involves the application of radio frequency (RF) pulses at a resonant frequency leading to the oscillation of hydrogen ions from longitudinal to transverse plane. This helps generate a magnetic signal. When the RF pulse is turned off, the protons undergo dephasing resulting in decay of magnetic signal (T_2-relaxation time). The time constant for the protons to reach the state of equilibrium (longitudinal plane) is referred to as T_1-relaxation time. The response of these protons in different tissues (e.g., fat or water) are responsible for different relaxation times. For instance, water consists of protons that are freely mobile compared to fat, which leads to longer dephasing time and longer T_2-relaxation times. After DTPI, an increased mobility of protons in water of the affected region is associated with increased T_2- and T_1-relaxation time.

1.5. Etiopathogenesis of Pressure Injury

1.5.1. Etiology of Pressure Injury

The predisposing factors to the development of a PI are broadly classified into mobility/activity related, sensory perception, extrinsic, and patient-related (Defloor, 1999). Immobility is a contributing factor to PI formation because of its effect on various systems, including cardiovascular, musculoskeletal, and gastrointestinal (Topp et al., 2002). Cardiovascular manifestations are orthostatic hypotension, change in body fluid composition, and impairment in the peripheral blood flow (Greenleaf et al., 1992; Powell and Blair, 1994; Convertino, 1997; Krasnoff and Painter, 1999). Disuse of muscles leads to atrophy over time. Decreased appetite affects nutritional requirements leading to weight loss and malnutrition (Benati et al., 2001; Horn et al., 2004). Collectively, these consequences of immobility increase the predisposition to PI formation.

Some of the extrinsic factors are friction, shear stress, stiffness of support surface, and moisture (Defloor, 1999). Friction and shear stresses are primarily responsible for the development of superficial PI and maybe predisposing factors to DTPI formation (Gefen et al., 2005). Friction is the force that resists two surfaces. For instance, friction between the skin and the supporting surface occurs with repositioning in bed or wheelchair without completely lifting the body. Shear stress results when the externally applied load causes the tissue to move in the direction opposite and parallel to the supporting surface. These extrinsic factors also depend partially on properties of the mattress, wheelchair cushion, and/or operating room pads. If the support surface is stiff, then there is an increased risk of developing a PI. Moisture caused by urinary incontinence, fecal incontinence, and dual incontinence can exacerbate stage I/II injuries to stage IV injuries.

The intrinsic biomechanical factors that determine the risk of developing DTPI are the anatomy of the bone and the mechanical properties of the soft tissue affected by illness or age (Gefen et al., 2005). These biomechanical factors make certain individuals more susceptible than other individuals (Defloor, 1999; Gefen et al., 2005). Furthermore, premorbid conditions such as hypotension, anemia, and diabetes mellitus lead to an increase in the risk of PI (Fuoco et al., 1997; Scivoletto et al., 2004).

1.5.2. Mechanisms of Deep Tissue Pressure Injury

Muscle tissue comprises three components: bundles of muscle fibers (fascicles), connective tissue, and blood and lymph vessels. Each muscle fiber is a multinucleated syncytium made of myoblasts. Traditionally, the mechanism of DTPI formation was explained using the vascular and lymphatic components of the muscle tissue (Dinsdale, 1974; Daniel et al., 1981; Miller and Seale, 1981; Reddy and Cochran, 1981; Schultz et al., 1999). A recently emphasized mechanism is the role of mechanical tissue deformation in the development of DTPI (Bouten et al., 2003b; Breuls et al., 2003a; Stekelenburg et al., 2007). It is difficult to isolate these two mechanisms in understanding their effects on tissue damage (Figure 1-3) (Gawlitta et al., 2007; Stekelenburg et al., 2007).

1.5.2.1. Mechanical Deformation

The earliest literature on the etiology of PI dates back to the 19th century. The initial work suggested that the occurrence of PI was a result of prolonged pressure leading to ischemia (Kosiak, 1961). It was believed that if the pressure between the contact area i.e.,

skin and the support surface (interface pressure), exceeded the critical capillary closure pressure (32 mm Hg), ischemia occurs (Holloway et al., 1976; Bader et al., 1986; Benati et al., 2001). In addition, if this pressure is sustained for an extended period of time, tissue breakdown could occur (Kosiak, 1961; Dinsdale, 1973; Daniel et al., 1981; Bosboom, 2001). Conversely, another study indicated that the interfacial pressure causes the blood vessels in the skin and the subcutaneous tissue to be occluded and not the blood vessels in the muscle (Husain, 1953). The surface pressures (friction/shear) and the interfacial pressures are not solely responsible for the internal mechanical conditions that occur inside the tissue, which are crucial for tissue break down (Bosboom, 2001; Bouten et al., 2003a). The internal mechanical conditions are a result of tissue internal stresses/strain caused by the compression of tissue between the support surface and bony prominence (Gefen et al., 2005).

The relationship of the external load to local internal stresses/strain was studied using theoretical and numerical models (Todd and Thacker, 1994; Breuls et al., 2003b). One such model, a finite element model, provides the magnitude and the location of the internal stresses/strain (Oomens et al., 2003). The model consists of ischial tuberosities represented as rigid material; covered by muscle, fat, and skin (Todd and Thacker, 1994). From magnetic resonance imaging (MRI) data the thickness of these tissue layers is determined (Todd and Thacker, 1994). In short, the findings represent the transfer of interfacial pressures to the underlying tissues leading to greater extent of tissue deformation near the ischial tuberosities (Todd and Thacker, 1994). However, these models could not predict the internal pressures based on the interfacial pressure measurements (Galpin et al., 1976; Chow and Odell, 1978; Todd and Thacker, 1994; Oomens et al., 2003; Gefen, 2007).

An empirical model was used to demonstrate the relationship between external loads and internal stresses/strains using intact and SCI pigs (Solis et al., 2012). The levels of strain were quantified in the pig muscle around the ischial tuberosities during external loading using 25 % body weight (BW) and 50% BW (Solis et al., 2012). The strain measurements were performed at locations central, dorsal, and ventral to the ischial tuberosity on one side (Solis et al., 2012). The study showed that loading on the muscle tissue located between the apex of the ischial tuberosity and edge of the skin moves the tissue in the line of applied loading towards the ischial tuberosity, causing compressive deformation. It also generates shear stress in the tissue which moves the muscle tissue located near the ischial tuberosity in the transverse plane, leading to what is known as shear deformation. External loading (e.g., 50% BW) results in high peak strain deformation magnitudes in the tissue between an external support surface and the ischial tuberosities not only at the apex of the tuberosities but also 2 cm ventral to the bony prominence (Dodd and Gross, 1991; Oomens et al., 2010; Solis et al., 2012). Loading of tissue near an irregularly-shaped bony prominence (e.g., ischial tuberosities) results in internal stresses and strains that exceed the external load, causing greater muscle deformation near the bony prominence than measured at the surface of the skin (Solis et al., 2012).

Over the past decade, studies have focused on cell deformation within the tissue as a critical factor for cell damage after prolonged mechanical loading (Breuls et al., 2003b; Peeters et al., 2003). The threshold value of a cell indicates the time at which tissue deformation leads to cell damage (Stekelenburg et al., 2008). The estimated threshold value range for shear strain is 50 – 60%, indicating that beyond this level cell damage occurs. If the level of deformation is below this threshold level, cells are not affected (Stekelenburg et al., 2008). These cells can adapt to the physical deformation; however, if the cell deformation exceeds the adaptive capacity, cell damage occurs by apoptosis (programmed cell death) or

necrosis (final cell death) (Gawlitta et al., 2007; Stekelenburg et al., 2008) within 10 minutes (Loerakker et al., 2010). One study compared cell damage with compressive strains of 50% and 30%, and showed a higher percentage of cell damage at the 50% strain level (Breuls et al., 2003a).

The cells capable of adapting to physical deformation utilize circulating ATP as energy to maintain normal homeostasis. The energy is generated by a cytoplasmic pathway known as glycolysis, converting glucose into two pyruvates (Pronk, 2000; Barnett, 2003). During this pathway, two moles of ATP are generated. If a cell lacks mitochondria or oxygen, glycolysis occurs anaerobically (Pronk, 2000)(Figure 1-3). In the presence of cell mitochondria and oxygen, pyruvate enters the citric acid cycle leading to the oxidation of acetyl-CoA to carbon dioxide, generating energy in the form of ATP (Pronk, 2000; Barnett, 2003; Nelson and Cox, 2004). Enzymes in the mitochondria and those that are responsible for the citric acid cycle produce nicotinic amide dehydrogenase (NADH) (Barnett, 2003; Nelson and Cox, 2004). The oxidation of NADH to release NAD are reutilized by the mitochondrial enzymes as required followed by the delivery of electrons to the electron transport chain (ETC) (Nelson and Cox, 2004). The energy generated in this process can run proton pumps which drive the protons from the extracellular matrix space into intermembrane space (Nelson and Cox, 2004). It also helps in the transport of Na^+ ions, across the membrane to create a concentration gradient (Nelson and Cox, 2004). Overall, aerobic glycolysis and citric acid cycle produce ATP to meet the cell energy requirements and survival.

1.5.2.2. Ischemia

Muscle tissue is highly vascularized making it susceptible to perfusion changes during sustained loading (Linder-Ganz et al., 2006). Animal studies demonstrate that muscle tissue is capable of tolerating ischemia for four hours (Tupling et al., 2001a). The resulting decrease in blood supply leads to a state of ischemia and tissue hypoxia; wherein there is a deprivation in the transport of nutrients and oxygen to the cell and removal of metabolic wastes away from the cell in the tissue. Irreversible muscle cell damage starts at four hours of ischemia and is complete at six hours (Blaisdell, 2002).

Tissue hypoxia deprives the ETC of sufficient oxygen; therefore; decreasing the rate of ETC and ATP production. As the metabolic requirements of the tissue exceed the availability of oxygen, cells switch to anaerobic metabolism (Nelson and Cox, 2004). This leads to faster utilization of glucose stores, and an accumulation of lactic acid and inorganic phosphates in the tissue (Harris et al., 1986; Tupling et al., 2001b; Nelson and Cox, 2004). The resulting anaerobic by-products compromise cell viability and induce a state of lactic acidosis, which can lead to apoptosis and necrosis (Kabaroudis et al., 2003)(Figure 1-3). The resulting decrease in pH results in loss of H^+ ions by Na^+/H^+ exchanger followed by influx of Na^+ ions (Kalogeris et al., 2012). In addition, during the cell acidosis state the functioning of Na^+/K^+-ATPase pumps fail, causing intracellular accumulation of Na^+ and Ca^{2+} and in exchange, K^+ to diffuse out of the cell (Tupling et al., 2001b; Kabaroudis et al., 2003). This imbalance in electrolytes change the concentration gradient within the cell and therefore induces water to enter the cell through diffusion, causing cellular swelling and final cell rupture. An increase in Ca^{2+} by the mitochondrial permeability transition pore causes the Ca^{2+} in the cytosol to increase (Byrne et al., 1999; Tupling et al., 2001a). This leads to an increase in the Ca^{2+} dependent proteases (Byrne et al., 1999), endonucleases, phospholipases, and

production of toxic reactive oxidative species (Az-ma et al., 1999). The activation of Ca^{2+} dependent proteases causes the extracellular matrix to undergo degradation. The presence of endonucleases causes denaturation of proteins, clumping of nuclear chromatin, and inactivation of DNA and enzymes. Finally, phospholipase enzyme activation increases cell and organelle membrane permeability. The activation of these enzymes leads to irreversible cell death. This process is also referred to as cell degradation after injury.

1.5.2.3. Ischemia-Reperfusion Injury (IRI)

The removal of external load helps restore tissue perfusion as well as replenish nutrients and oxygen to the cells. Although restoration of blood flow causes some of the ischemic muscle to recover, a series of complex events of inflammation occur in the blood vessels and adjacent tissue (Diana and Laughlin, 1974; Gute et al., 1998; Blaisdell, 2002). The inflammatory events after ischemia include neutrophil accumulation, microvascular disruption, and edema formation.

In response to ischemia, the chemical mediators (e.g., tumor necrosis factor-α [TNF-α] and interleukins [IL-8, IL-6, IL-1]) recruit neutrophils (primary leukocytes) in the capillaries to post-ischemic tissue (Tidball, 1995, 1995, 2005; Gute et al., 1998; Ciciliot and Schiaffino, 2010; Grommes et al., 2014). P-selectin and E-selectin, the cell adhesion molecules, mediate the migration of the neutrophils in approximation to vascular endothelium at the site of ischemia. The neutrophils migrating along the central axial column of the capillary contribute to the circulating pool. The neutrophils that are in close proximity to the capillary wall are exposed to cytotoxic compounds to form activated neutrophils. The activated neutrophils contain NADPH oxidase which oxidizes $NADP^+$ and reduces

molecular oxygen to superoxide and hydrogen peroxide.

During sustained loading, tissue ischemia causes the cell to lose the ability to produce ATP from ADP (Parks and Granger, 1983; Granger, 1988). There is a substantial increase in ADP to produce hypoxanthine in a series of reactions (Parks and Granger, 1983; Granger, 1988). Hypoxanthine accumulates in ischemic conditions, leading to oxidative damage (Parks and Granger, 1983; Granger, 1988; Carden and Korthuis, 1989). Another enzyme, xanthine dehydrogenase (XDH) is present in the non-ischemic healthy cells. Hypoxic stress during ischemia results in the production of xanthine oxidase (XO) from xanthine dehydrogenase (XDH) (Parks and Granger, 1983; Granger, 1988).

Upon removal of an external load, reperfusion introduces molecular oxygen into the tissue. This molecular oxygen reacts with hypoxanthine and XO to produce a burst of reactive oxygen metabolites (ROM) such as superoxide anions and hydrogen peroxide (Parks and Granger, 1983; Granger, 1988; Carden Donna L. and Granger D. Neil, 2000; Kaminski et al., 2002). In the presence of iron, the superoxide anion and hydrogen peroxide convert into highly reactive hydroxyl ions (Haber Weiss reaction) (Granger, 1988). The release of ROM produces an acute inflammatory response that causes necrosis and irreversible cell death to both vascular endothelium and tissue (Hernandez et al., 1987). In contrast, reperfusion of the skeletal muscle with anoxic blood generates less tissue damage (Gute et al., 1998). Therefore, limiting the availability of oxygen to ischemic tissue during reperfusion can reduce tissue necrosis (Gute et al., 1998). The injury caused by three hours of ischemia followed by reperfusion was found to be higher than ischemia alone (Diana and Laughlin, 1974; Hernandez et al., 1987). In fact, IRI is a severe cause of DTPI thus making it an important underlying mechanism.

Once the pro-inflammatory level is achieved, the activated neutrophils release soluble factors such as tumor necrosis factor-α (TNF-α), thromboxane A2, and leukotriene A4 (Kaminski et al., 2002). They help initiate contraction of endothelial cells, further resulting in endothelial gaps. Moreover, the activated neutrophils with β-2 integrins modulate tight adhesion to the vascular endothelium. The vascular endothelial cells contain intracellular adhesion molecule (ICAM) and vascular cell adhesion molecule (VCAM). These adhesion molecules aid in increasing the adhesion of neutrophils and vascular endothelial cells. The β-2 integrin/ICAM interaction increases intracellular Ca^{+2}, mediating actin polymerization and vascular endothelial cell contraction (Kaminski et al., 2002). These mechanisms combine to increase the filtration of trans capillary fluid into the interstitial space known as edema (Gute et al., 1998).

Another phenomenon after IRI is failure in the restoration of blood flow upon reperfusion to ischemic tissue known as the no-reflow effect (Dahlbäck and Rais, 1966; Lindsay et al., 1989; Carden Donna L. and Granger D. Neil, 2000). The mechanism underlying this phenomenon is unclear. Various mechanisms have been proposed to explain the pathogenesis of this perfusion defect. One potential mechanism is the adhesion of activated neutrophils to the vascular endothelium (Schmid-Schoenbein et al., 1975; Carden and Korthuis, 1989; Gute et al., 1998) . The partial occlusion of the capillary by the adherent neutrophils affects blood flow dynamics in the capillaries at the ischemic site (Schmid-Schoenbein et al., 1975; Gute et al., 1998). Another mechanism is the release of ROM by the activated neutrophils causing the endothelial cell to swell (Gute et al., 1998). This can decrease the caliber of the capillary lumen (Gute et al., 1998). Use of antioxidants can decrease neutrophil and endothelial cell adhesion hence improving perfusion (Gute et al., 1998). A third mechanism is leucocyte adhesion to capillary endothelium leading to

microvascular disruption and increase in capillary permeability (Gute et al., 1998). Trans capillary fluid passes through the endothelial gaps into the interstitial space (Gute et al., 1998). The resulting increase in the interstitial fluid pressure compresses the capillaries preventing blood flow.

1.6. Healing after DTPI

The sequence of overlapping events that occur after DTPI include: i) degeneration and inflammation (described in section 1.4.2 and 1.4.2.3), ii) proliferation, differentiation, and fusion of satellite cells, iii) maturation of new myofibers into regenerated muscle fibers, and iv) formation of scar tissue (fibrosis) (Figure 1-4) (Ciciliot and Schiaffino, 2010). The termination of inflammation is marked by the release of anti-inflammatory macrophages (M2) between 2 to 4 days post injury (Ciciliot and Schiaffino, 2010; Hesketh et al., 2017). In addition to removal of necrotic tissue after injury, the macrophages have an important role in the muscle regeneration process (Mackey et al., 2017). They release anti-inflammatory cytokines such as interleukin-10 (IL-10), which help in myogenic precursor proliferation and differentiation (Ciciliot and Schiaffino, 2010; Mackey et al., 2017). Another event that occurs at the same time point as release of M2 macrophages is satellite cell activation, proliferation, and fusion (Ciciliot and Schiaffino, 2010). Satellite cells are muscle progenitor cells which contribute to muscle regeneration. They proliferate rapidly on day 2 after injury followed by fusion into multinucleated myotubes (Ciciliot and Schiaffino, 2010). The newly formed myotubes remodel into regenerated muscle fibers starting on day 3 post-injury (Huard et al., 2002). However, the regeneration process can vary based on the type and severity of injury with a peak at two weeks in humans (Huard et al., 2002). Muscle tissue repair is the final stage of tissue healing marked

by the formation of fibrosis or scar tissue beginning at 3 weeks after injury, and may continue to increase in size over time depending on the size and type of injury (Huard et al., 2002; Mackey et al., 2017).

1.7. Prevention of Deep Tissue Pressure Injury

1.7.1. Risk Assessment Scales

Risk assessment of PI is part of the screening process to identify individuals who are at risk (Lyder and Ayello, 2008). Early identification of risk is essential for prevention of DTPI. Particularly, risk assessment helps in identifying a prevention plan among the high-risk populations. Of the various scales, the most commonly used risk assessment scales in the clinic are the Braden (Bergstrom et al., 1987) , Norton, and Waterlow scales (Papanikolaou et al., 2007).

The Norton scale, developed in 1962, is the first risk assessment scale and comprises of 5 subscales evaluating the general physical condition, cognition, activity, mobility, and incontinence (Post, 1963; Mortenson and Miller, 2008a). The total score ranges from 5 to 20 with each subscale consisting of 4 points. A cut-off score defines those who are at risk from those who are not (van Marum et al., 2000); for instance, a score less than 12 indicates an inevitable risk of PI (van Marum et al., 2000). Another scale is the Braden scale used in research studies. This scale, developed in 1987, consists of 6 subscales: sensory perception, skin exposure to moisture, mobility, ability to change position, nutrition intake, and presence of friction and shearing force (Mortenson and Miller, 2008b). The total score ranges from 6 to 23, with a low score indicating a higher risk of developing a PI (Bergstrom et al., 1987;

Sundaram et al., 2017). The third risk assessment scale is the Waterlow scale, developed in 1985. The scale consists of 7 subscales: weight, height, visual assessment of skin, age, continence, mobility, and perception (Waterlow, 1985, 1988, 1991; Mortenson and Miller, 2008b). The score ranges from 10 to 20, with 10 being low risk and 20 being very high risk (Anthony et al., 2008). In contrast to the Norton and Braden scales, the Waterlow subscales have unequal weights coupled with a high score indicative of a greater risk of developing PI (Anthony et al., 2008).

A review was conducted to determine the effect of risk assessment scales on patient outcomes (Defloor and Grypdonck, 2004; Pancorbo-Hidalgo et al., 2006; Chou et al., 2013). The results indicated that the Braden and Norton scales had no additional benefit in comparison to routine inspection performed in the clinic (Defloor and Grypdonck, 2004; Pancorbo-Hidalgo et al., 2006; Chou et al., 2013). One reason could be that the prevention of DTPI requires early detection using risk assessment tools that allow for inspecting the health of deep tissue, and an appropriate plan to prevent its progression. A failure in one of these can result in the development of DTPIs that eventually develop into open wounds.

1.7.2. Prevention Strategies

It is critical to address the extrinsic and intrinsic factors to prevent the development and progression of DTPI into an open wound. Current preventive strategies focus on reducing the magnitude and duration of pressure between the body and an external support surface (McInnes et al., 2015). Commonly, manual repositioning and the use of pressure relieving support surfaces are strategies practiced by healthcare staff (McInnes et al., 2015). Recent advances in the prevention of DTPI modify the internal mechanical conditions by relieving and redistributing

the pressure around the bony prominences (Gyawali et al., 2011; Solis et al., 2011) in addition to pressure relief at the skin level.

1.7.2.1. Repositioning

Repositioning is a frequently used preventive strategy to redistribute the pressure from particular parts of te body (McInnes et al., 2015). A randomised controlled trial on the prevention of PI describes 3-hourly repositioning in a 30-degree tilt can improve tissue oxygenation by markedly reducing internal strains near the sacrum (Moore et al., 2011). A less frequent change in the position results in high incidence of PI.

The repositioning schedule depends on the health status of the individual and the costs associated with nursing time (Krapfl and Gray, 2008; Latimer et al., 2015). This includes the number of turns and nurses required for each turn. Currently, there is no fixed optimal repositioning regime for all individuals (Young, 2004; Krapfl and Gray, 2008; Miles et al., 2013). The clinical guidelines for prevention of PI require two-hourly repositioning (Miles et al., 2013). Similarly, wheelchair users are advised to perform push-ups and side-to-side leans with a minimal duration of pressure relief for 2 minutes (Latimer et al., 2015). If partial unloading occurs during repositioning, the supply of oxygen to tissues may be replenished; nonetheless, the persistence of tissue deformation can result in an irreversible injury. Moreover, repositioning increases the exposure of other sites to develop a PI (Oomens et al., 2016). For instance, a change from a supine to a lateral tilt position exposes the shoulder and greater trochanter to external loading and tissue damage (Oomens et al., 2016). As DPTI can initiate within 10 minutes of tissue loading (Loerakker et al., 2010), more

frequent repositioning is essential for the prevention of this inside-out PI. One of the disadvantages of frequent repositioning is sleep deprivation. The alteration of sleep-wake cycle affects the regulation of immune function (Besedovsky et al., 2012); in turn, slowing the healing process and recovery. Another drawback of repositioning is the additional discomfort because of wounds, stiff joints, and bony pain. Moreover, much of this preventive strategy depends on the efficiency to perform timely repositioning by patients, care providers, and healthcare staff.

1.7.2.2. Support Surfaces

The use of pressure relieving and redistributing devices such as cushions, mattresses, overlays, in conjunction with repositioning reduce the magnitude and the duration of external load (McInnes et al., 2015). They mold around the shape of the body to distribute the weight over a greater surface area (Clark, 2011). The devices are classified into low technology/non-powered surfaces or high technology surfaces based on their mode of operation (Clark, 2011; McInnes et al., 2015). The low technology surfaces have a static relief of pressure whereas the high technology surfaces have dynamic pressure relief (Clark, 2011; McInnes et al., 2015).

Often on admission to a hospital standard mattresses are used. The non-powered/static relief devices such as sheep skin, static air, gel, water, and bead filled supports replace standard mattresses when individuals are at risk of developing PI (Ewing et al., 1964; Cadue et al., 2008; Chou et al., 2013). During lengthy surgical procedures and postoperative period, these devices are laid on the bed to reduce the development of PI. Similarly, prescription of specialized cushions for wheelchair users prevent PI (Brienza et al., 2010).

These devices distribute the pressures over a larger area by fitting around the body surface (Clark, 2011). Some studies compared the incidence and severity of PI with the use of specialized devices (Gray and Campbell, 1994; Collier, 1996; Russell et al., 2003). One study reported a significant decrease in the incidence of stage II (43.6 %) to stage I PI (19.9%) in the group that used specialized cushions/mattresses (Russell et al., 2003). This indicates that the use of specialised devices were able to prevent the development of new cases of stage II PI. Importantly, there was no significant change in the progression from stage I to stage II PI indicating that specialised cushions prevent PI from developing into stage IV PI (Russell et al., 2003).

An example of a specialized device in the dynamic pressure relief group is the alternating pressure system (Andersen et al., 1983). These devices are connected to an external power source to generate an alternating inflation and deflation of the cells within the mattress/cushion (Andersen et al., 1983). The most commonly available devices are made of air and water (Andersen et al., 1983). These systems are made of cells in which of air/water is pumped at different cycles based on individual requirements (Andersen et al., 1983). The disadvantages of these systems are seasickness-like sensation, sleep disruption, and difficultly in cleaning. Newer devices are comprised of variable density foam within the air cells to avoid these unpleasant sensations.

The static and dynamic systems focus on reducing the interface pressure but have a minimal role on internal mechanical conditions around the bony prominence. Although prevention of superficial PI may be possible with these interventions (Allen et al., 2012), so far, there is no established evidence that these preventive methods will reduce the occurrence of DTPI (Atkinson and Cullum, 2018).

1.7.2.3. Electrical Stimulation as a Preventive Strategy

Simon Levine and coworkers studied the use of electrical stimulation to modify the internal mechanical conditions of soft tissue near the ischial tuberosities by redistributing and relieving pressures when individuals are seated (Levine et al., 1989, 1990). This group was among the first to quantify tissue deformation and shape in the presence of electrical stimulation using an eight transducer ultrasound imaging system (Levine et al., 1990). They also addressed the changes in the blood flow during muscle contraction by electrical stimulation in able-bodied and SCI individuals (Levine et al., 1990). The group demonstrated an increase in blood flow between rest and electrical stimulation (Levine et al., 1989, 1990). One drawback of these experiments was the use of continuous electrical stimulation which caused the onset of muscle fatigue within a few minutes of use.

Ferguson et al. used an alternative strategy of electrical stimulation in experiments involving nine persons with SCI (Ferguson et al., 1992). The electrical stimulation was applied bilaterally to the quadriceps muscle for 10 second intervals with a 20 second rest period. By restricting the knee extension movement during stimulation, the evoked muscle contractions were able to relieve pressure around the ischial pressures in the seated volunteers by lifting their buttocks above the support surface (Ferguson et al., 1992). However, the complex setting of the experiments, associated discomfort and potential for bone fractures made this approach unsuitable for the participants (Ferguson et al., 1992).

Paralyzed muscles undergo changes in cross-sectional area and enzymatic properties after a complete SCI, which maybe additional predisposing factors to DTPI formation (Burnham et al., 1997). Application of low frequency (10 Hz) electrical stimulation can increase oxidative enzyme activity and fatigue resistance (Trumble et al., 2001). In one

study, electrical stimulation was delivered for 6 weeks to the tibialis anterior muscle by subsequently increasing the duration of stimulation per day (Trumble et al., 2001). Surprisingly, the outcomes revealed no change in muscle fiber size and endurance. Another study showed that electrical stimulation applied for 8 weeks to the vastus lateralis, gluteus maximus, hamstrings, and erector spinae muscles increased muscle bulk. Moreover, a significant decrease in the interfacial pressure around the ischial tuberosity was seen during stimulation (Bogie and Triolo, 2003; Liu et al., 2006). The improvement in muscle mass could provide a cushioning effect that leads to static pressure relief near the ischial tuberosities (Bogie and Triolo, 2003; Bogie et al., 2006).

The Mushahwar lab applied intermittent electrical stimulation (IES) for the first time to prevent DTPI. The principle idea behind this technique is the use of periodical IES-induced contractions in the gluteus maximus muscles to counteract both the mechanical and vascular pathways leading to DPTI around the ischial tuberosities and sacrum. The paradigm tested in able-bodied study participants and participants with SCI was 10 seconds of electrical stimulation delivered every 10 minutes (Gyawali et al., 2011; Solis et al., 2011) (Figure 1-5). Contractions produced by IES changed the shape of the gluteus maximus muscle; thus reducing pressure around the ischial tuberosities (Solis et al., 2011) and the mechanical deformation in the deep tissue induced by loading (Gyawali et al., 2011; Solis et al., 2011). The IES-induced contractions also increased tissue perfusion and oxygenation in both able-bodied and SCI individuals (Solis et al., 2007, 2011; Gyawali et al., 2011). The long-term effectiveness of IES in preventing DTPI was demonstrated in pigs with SCI (Solis et al., 2013). The results showed a significant difference in muscle volume exhibiting tissue edema and damage in animals receiving IES relative to animals without IES (Solis et al., 2013). Animals receiving IES during loading did not develop a DPTI while all animals

without IES developed a DPTI.

The safety and feasibility of IES to prevent DTPI was conducted in a rehabilitation unit of general hospital, a tertiary rehabilitation hospital, a long term care facility, and a home care environment (Ahmetović et al., 2015). The treatment, delivered for 4 weeks, was proven to be safe, feasible, and acceptable by the participants and care givers (Ahmetović et al., 2015). Another feasibility study to prevent DTPI using IES in an intensive care unit (ICU) reported this technique as acceptable and safe (Kane et al., 2017). None of the study participants developed a DTPI while using IES in both studies (Ahmetović et al., 2015; Kane et al., 2017).

In summary, the work by various researchers demonstrate that electrical stimulation could relieve and redistribute pressure around bony prominences leading to reduced tissue deformation and necrosis. By improving tissue perfusion, electrical stimulation also helps maintain tissue viability.

1.8. Current treatment methods

The treatment of DTPI once it approaches the skin can be challenging because of the extensive damage to the underlying tissue. The failure of open wounds to heal, or if they become infected, increases the cost of an already expensive treatment. New strategies are needed to improve the clinical outcomes while also maintaining cost-effectiveness.

1.8.1. Conventional and Adjunctive Management for Pressure Injury

Conventional wound care regimes for open wounds include debridement, wound cleansing (Moore and Cowman, 2013), and regular dressing (Westby et al., 2017). Tissue debridement with surgical, mechanical, enzymatic or autolytic methods removes the dead necrotic tissue (Bradley et al., 1999; Bluestein and Javaheri, 2008; Choo et al., 2014). This process leads to new granulation tissue which, in turn, accelerates wound healing. Following debridement, the cleansing of wound with a neutral, non-irritant, and non-toxic agent is essential to maintain a healthy wound bed (Moore and Cowman, 2013). An example of commonly applied cleansing agents is normal saline at an irrigation pressure of 8 psi. Wound dressings help protect the physiological integrity of skin and underlying tissue and protect the wound against contamination (Westby et al., 2017). They also create a moist environment for easier subsequent debridement. Topical preparations such as Iodosorb (antiseptic) and collagenase are used in addition for maintaining a healthy wound bed (Westby et al., 2017). The wounds that are refractory to these conventional methods are managed surgically. This involves a surgical reconstruction followed by a myocutaneous/fasciocutaneous flap closure.

Adjunctive treatments include the use of low energy laser irradiation, ultrasound/ultraviolet C therapy (US/UVC), near-infrared light, and electromagnetic fields. Low energy lasers improve tissue health by non-thermal means (Hashmi et al., 2010; Farivar et al., 2014). Laser irradiation has been used as a treatment modality since the 1970s (Mester et al., 1968), and acts by promoting fibroblast activity and increasing granulation tissue (Farivar et al., 2014). Some benefits of low level laser therapy are reduction of pain and inflammation of open wounds (Farivar et al., 2014). One study reported that the use of laser did not show additional benefit to other standard of care/adjunctive interventions (Nussbaum

et al., 1994). While various case series have been published using this intervention, it appears that this method has not reached the clinical trial stages. Another study showed that the use of US/UVC when alternated over 5 days can improve the healing of an infected wound by reducing inflammation and infection (Honaker et al., 2016). Information on the individual effects of ultrasound or ultraviolet C are lacking in the published studies (Honaker et al., 2016).

Non-thermal near-Infrared light is used for refractory wounds (Braverman et al., 1989). It is hypothesized that its mechanism of action includes increasing perfusion and collagen synthesis (Braverman et al., 1989). Another adjunctive therapy is the use of electromagnetic fields for DTPIs reaching the epidermis (Olyaee Manesh et al., 2006). These act on the proliferative phase of wound healing, improving tissue perfusion and oxygenation, and increasing the formation of granulation tissue (Olyaee Manesh et al., 2006). Electromagnetic fields when applied for 1 week were able to increase significantly the rate of healing of stage II PIs. Complete healing was seen when the treatment was extended to 2 weeks (Comorosan et al., 1993).

Recent advances in the field of wound management have led to the development of a novel technique known as vacuum-assisted closure (VAC) for open wounds. The negative pressure generated with this technique reduces edema and improves microcirculation. Although there is not much literature supporting this method, one study compared the clinical outcomes of VAC with conventional management of open wounds. The blood marker levels of leucocytes, hemoglobin, C reactive protein (CRP) were measured in both groups before and after intervention (Fuchs et al., 2005). There was a faster decline in the leucocyte and CRP levels in the participants receiving VAC; however, the extent of decrease

in the blood markers was not different among the two groups (Fuchs et al., 2005).

In summary, some of the adjunctive treatment methods used for wound healing are supported by strong evidence. However, there is a lack of incorporation of these interventions in treatment plans because of the small sample sizes in their research studies and lack of further work on these interventions (Reddy et al., 2008; Boyko et al., 2016; Atkinson and Cullum, 2018).

1.8.2. Electrical Stimulation Therapy for Open Wounds

Electrical stimulation therapy is another adjunctive therapeutic method for DTPI's that reach the skin exposing the underlying muscle and bone (Thakral et al., 2013). Low amplitudes of electrical current are applied in and around an open wound to improve healing. Published reports on the benefits of electrical stimulation as a therapeutic modality date back to the 1960s (Wolcott et al., 1969; Kloth and Feedar, 1988; Kloth, 2005). Electrical stimulation therapy uses direct current (DC) (Wood et al., 1993; Adegoke and Badmos, 2001), alternating current (AC), and high-voltage pulse current (HVPC) delivered directly to the wound bed or with the use of devices within the dressings (Griffin et al., 1991).

The difference in the polarity of the healthy epidermis and the dermis allows the flow of natural monophasic current in the presence of an injury (Barker et al., 1982; Kloth, 2005). This endogenous monophasic current helps in the wound healing process (Barker et al., 1982; Kloth, 2005). The currents are disrupted if the wound is open for too long and affect tissue healing after PI. At a cellular level, an exogenously electrical current applied alters the ion channels to activate the cells and create small charges (Kloth, 2005). Electrical

current also aids in the migration of fibroblasts for granulation tissue formation, increases collagen synthesis, capillary density, and reepithelization (Kloth, 2005). In addition, electrical stimulation can combat bacterial resistance with long-term antibiotics due to its bactericidal and bacteriostatic properties.

Several research studies investigated the use of different types of electrical current and stimulation parameters (frequency, amplitude, duration) for treatment of open wounds. A study on the efficacy of HVPC one hour per day for 20 days showed a significant reduction in the size of pelvic PI (Griffin et al., 1991). Another double-blind, placebo-controlled study with 12-weeks of electrical stimulation showed a 65% closure of the wounds (Peters et al., 2001). Low frequency pulse current, DC, and asymmetrical biphasic currents are other types of currents proven to be better than conventional treatment alone.

Current electrical stimulation therapy targets DTPI that have reached the skin. By then, the underlying tissue has deteriorated leading to lengthy and expensive treatments. A better prognosis may be achieved by developing an intervention for DTPI before it reaches the skin

1.9. Overview of Masters Work

The Mushahwar lab developed a novel technique using electrical current in the form of IES for the prevention of DTPI. This technique works differently from the electrical stimulation therapy used to heal open wounds. The current-controlled stimulation causes muscles of interest to contract. Previous work on IES indicated that the periodical muscle contractions produced by electrical stimulation increase tissue oxygenation and

reduce/relieve internal pressure and mechanical deformation around bony prominences, thus preventing the formation of DTPI (Gyawali et al., 2011; Solis et al., 2012).

The goal of this study was to extend the application of IES to treat an already formed DTPI in a rat model. Based on previous work, I hypothesized that rats receiving IES will have a faster rate of tissue healing than rats not receiving IES. The specific aims of my thesis are twofold:

Identify when to intervene with IES after the induction of a DTPI; and

Assess the rate of muscle regeneration after injury with and without IES.

Chapter 2 describes the experiment I conducted to address the hypotheses of my thesis, and discusses the results and their significance.

Chapter 3 provides general conclusions and future directions for IES as a treatment strategy for DTPI.

Appendix 1 compares injury progression using T_2-weighted MRI and T_1-weighted contrast-enhanced MRI in skeletal muscle.

1.10. Figures and table

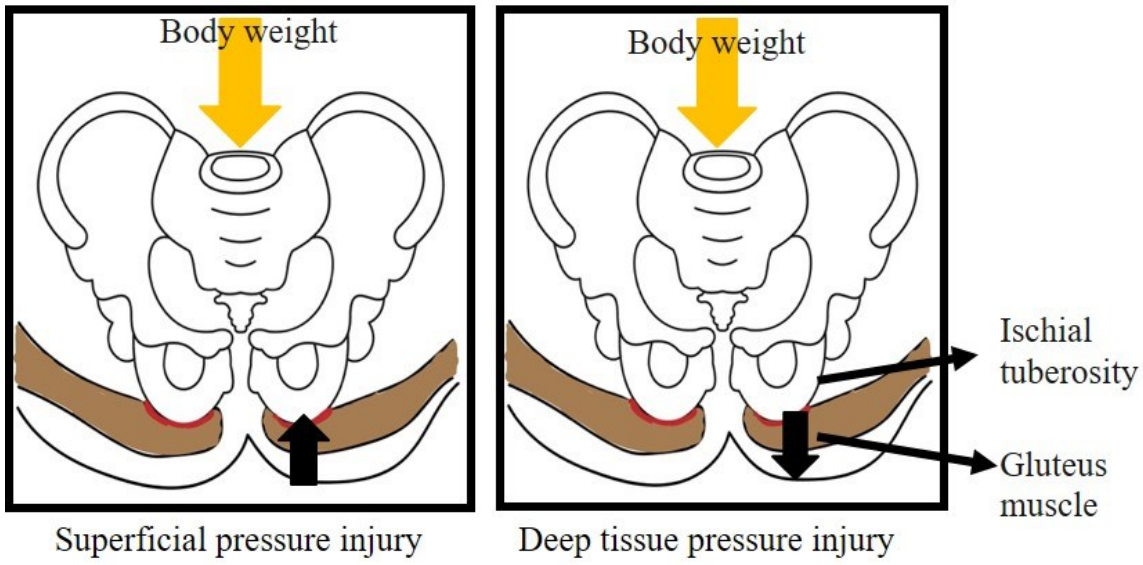

Figure 1-1: Classification of pressure injury. *A) Superficial pressure injury initiates at the skin surface and progresses towards the bone. B) Deep tissue pressure injury originates at the deep bone-muscle interface and progresses outwards towards the epidermis (created using Adobe stock).*

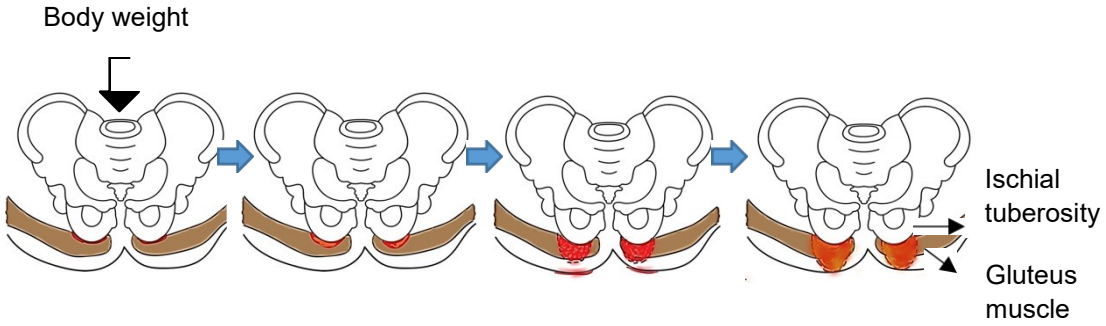

Figure 1-2: Progression of deep tissue pressure injury in seated position. *The injury begins at the gluteus maximus muscle near the ischial tuberosity before reaching the surface of the skin (created using Adobe stock).*

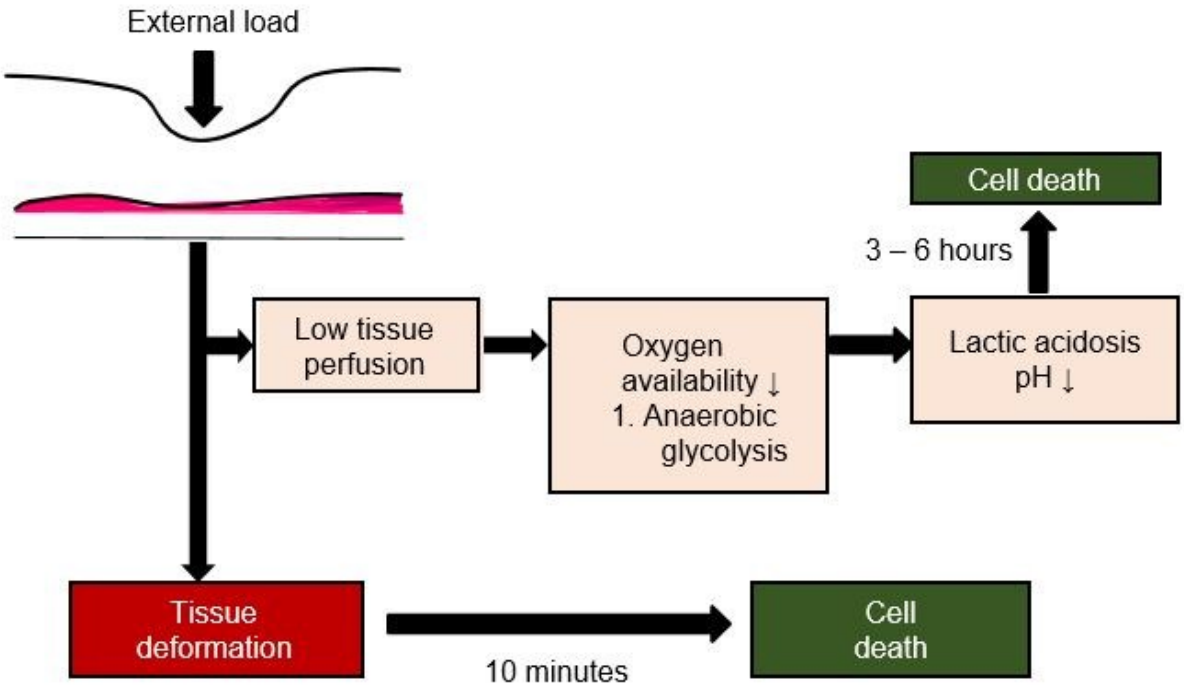

Figure 1-3: Etiopathogenesis of deep tissue pressure injury. *Sequence of events during tissue loading. The primary pathway is tissue deformation leading to cell death within 10 minutes. The secondary pathway is the vascular and metabolic pathway that leads to cell death 4 hours after the initiation of loading.*

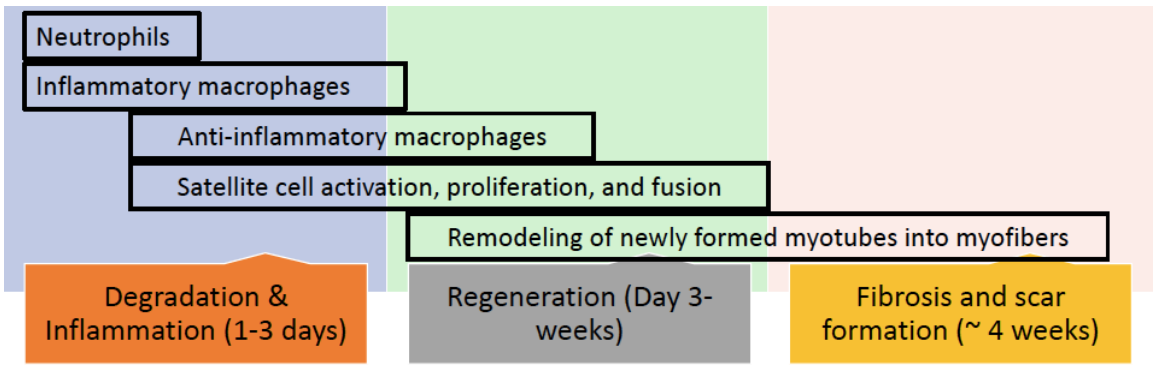

Figure 1-4: Deep tissue pressure injury and healing. *Stages of healing after deep tissue pressure injury. The first stage is the degeneration and inflammatory phase with invading neutrophils and macrophages. This is followed by muscle regeneration and fibrosis, which continues weeks after injury.*

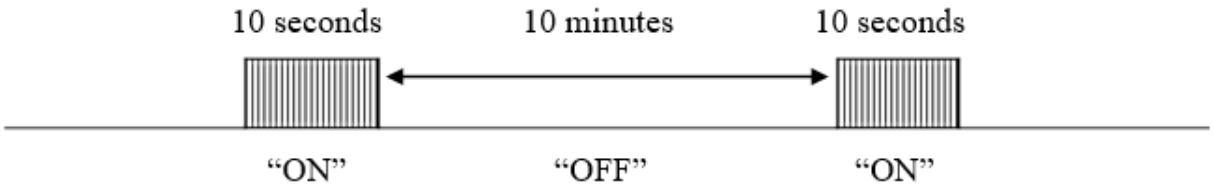

Figure 1-5: Intermittent electrical stimulation. *The intermittent electrical stimulation paradigm used for the prevention of deep tissue pressure injury. The paradigm consisted of an "on" duration of 10 seconds followed by "off" duration of 10 minutes, repeated throughout the duration of use.*

2. Contractions induced by Intermittent Electrical Stimulation Accelerate Pro-regenerative Processes and Reduce the Extent of Damage in Muscles with Deep Tissue Injury in Rats

Hemalatha Velanki,[1,2] Neil Tyreman,[2,3] Peter Seres,[4] Leandro R. Solis,[2,3] Steven Lu,[2,3] Kahir Rahemtulla,[2,3] Richard Thompson[2,4] and Vivian K. Mushahwar[1,2,3]

[1] Neuroscience & Mental Health Institute, University of Alberta

[2] Sensory Motor Adaptive Rehabilitation Technology (SMART) Network, University of Alberta

[3] Department of Medicine, Division of Physical Medicine & Rehabilitation, University of Alberta

[4] Peter S. Allen MR Research Centre, University of Alberta

AUTHOR CONTRIBUTION

The individual contribution of authors are:

Conception of experimental design and critical revision of thesis and manuscript - Dr. Vivian K. Mushahwar

Developed MRI protocol for study - Dr. Richard Thompson

Nerve cuff fabrication and implantation, tissue (sectioning/staining/imaging) for immunohistochemistry - Neil Tyreman

MRI imaging and technical support - Peter Seres

Spinalization surgery, loading procedure, delivery of electrical stimulation, conduction MRI experiments, and tissue extraction for immunohistochemistry - Hemalatha Velanki

MATLAB code for MRI data analysis - Dr. Leandro Solis

MRI data analysis - Steven Lu and Hemalatha Velanki

Immunohistochemistry analysis - Neil Tyreman, Kahir Rahemtulla, and Hemalatha Velanki

Manuscript revision - Dr. Vivian Mushahwar, Dr. Richard Thompson, Neil Tyreman, Peter Seres, Steven Lu, and Kahir Rahemtulla

2.1. Introduction

The benefits of electrical stimulation (ES) have been described since the 19th century, and ES is now employed as a common adjunctive treatment for many clinical conditions such as cancer, non-union bone fractures, soft tissue injuries, open wounds and muscle atrophy (Lente, 1850; Vodovnik and Karba, 1992; Stefanovska et al., 1993; Evans et al., 2001; Guo et al., 2012; Love et al., 2018). Different forms of ES have been used, commonly including direct current electrical fields and narrow pulses of various frequencies. Different parameters of electrical fields ranging between <1 mV/cm to 60 kV/cm, exhibit different roles on cell proliferation and apoptosis (Chen et al., 2005; Griffin et al., 2011; Love et al., 2018). High magnitude electrical fields induce cell apoptosis with no effect on cell proliferation, and are proposed as a potential treatment for different types of carcinoma (Chen et al., 2005). Lower magnitude electrical fields accelerate recovery from various conditions. For example, low magnitude fields applied on bone fractures with delayed union promote osteogenesis by generating electronegative potentials (Evans et al., 2001; Hess et al., 2012). These potentials, coupled with mechanical forces on the fracture site, expedite the healing process (Hess et al., 2012; Sundelacruz et al., 2013).

High voltage pulsed current (HVPC) reduces inflammation and swelling in the acute stages of soft tissue injuries such as tendon or ligament tears by minimising microvascular permeability and increasing lymphatic drainage (McLoughlin et al., 2004; Michlovitz, 2005; Snyder et al., 2010). HVPC also accelerates the closure of refractory open wounds, including pressure injuries (PIs). The use of high voltage galvanic stimulation and monophasic currents has also been shown to improve the rate of healing of open wounds but the mechanisms of action are not clearly understood (Polak et al., 2014). It is thought that the exogenously

applied electrical currents at amplitudes below motor activity form endogenous monophasic currents, which promote migration of fibroblasts for granulation tissue formation, and enhance angiogenesis and reepithelization, thus aiding in the healing of open wounds (Kloth, 2005; Kawasaki et al., 2014).

The effects of ES on counteracting atrophy in skeletal muscles after conditions such as spinal cord injury (SCI) and disuse atrophy have also been reported (Kim et al., 2008; Guo et al., 2012; Wan et al., 2016). A decrease in protein content, fibre size and overall muscle mass are characteristic features of muscle atrophy (Darr and Schultz, 1989; Siu and Alway, 2009). Decreased muscle mass is also the result of the depletion of satellite (muscle progenitor) cells coupled with their reduced ability to proliferate and fuse to develop into new muscle fibres (Mozdziak et al., 1998). Interestingly, electrical currents applied at amplitudes below motor activity to muscles with disuse atrophy cause protein synthesis, which is essential for regeneration, and enhance regrowth of the atrophied muscle (Ohno et al., 2013). Delivery of ES pulses at frequencies of 2-20 Hz with amplitudes causing visible contractions in muscles with disuse atrophy induced satellite cell proliferation (Guo et al., 2012; Wan et al., 2016). Similar effects of ES were seen for frequencies ranging from 20-100 Hz delivered at amplitudes causing motor activity in atrophied muscles after SCI (Kim et al., 2008; Becker et al., 2010).

To the best of our knowledge, very few studies have directly assessed the effect of ES-induced contractions on already injured tissue, and all such studies focused on the treatment of pressure injuries (PIs) with open wounds (Martínez-Rodríguez et al., 2013; Jercinovic et al., 1994). In the present study, we used deep tissue pressure injury (DTPI), a class of PI that originates at deep bone-muscle interfaces (Black et al., 2007; Edsberg et al., 2016), as a model of closed muscle injury with deep-seated damage. We induced

contractions in the injured muscle using a novel intermittent electrical stimulation (IES) pattern to assess the effect of ES-induced contractions on the cellular events after muscle injury, and on the rate of tissue regeneration and injury healing.

The sequence of cellular events associated with muscle injury such as DTPI are characterized by three phases. These are: *(i)* the inflammatory phase marked by invading neutrophils, activated macrophages and T lymphocytes; *(ii)* the resolution of inflammation by activation of anti-inflammatory macrophages; and *(iii)* regeneration described by activation and differentiation of muscle progenitor cells (satellite cells), and maturation of new myofibres into adult muscle fibres (Ciciliot and Schiaffino, 2010).

The invasion of neutrophils, inflammatory macrophages (M1) and T lymphocytes occurs ~24 hours after the onset of injury (Savill et al., 1989). The inflammatory cells help in the removal of necrotic debris after injury, release adhesion molecules (e.g., P-selectin, L-selectin, and E-selectin), pro-inflammatory cytokines (e.g., tumor necrosis factor-α [TNF-α] and interleukins [IL-8, IL-6, IL-1]) which are responsible for a series of vascular events (Huard et al., 2002). This includes vascular endothelial cell contraction coupled with filtration of transcapillary fluid into the interstitial space resulting in tissue edema.

Although the phases overlap, the activation of the anti-inflammatory macrophages (M2) and satellite cells follow the inflammatory phase (Ciciliot and Schiaffino, 2010). The M2 macrophages help in resolving inflammation by the release of anti-inflammatory cytokines (e.g., IL-10) (Ciciliot and Schiaffino, 2010). The satellite cells develop into new myofibres in response to growth factors such as insulin-like growth factor-1 (IGF-1), epidermal growth factor (EGF) and transforming growth factor (TGF-α and TGF-β), which then undergo remodeling to become regenerated muscle 7–10 days after injury (Huard et al.,

2002; Mackey and Kjaer, 2017). In brief, muscle injury initiates a heightened inflammatory response on days 1-3 followed by resolution of inflammation and muscle regeneration (Mackey and Kjaer, 2017).

The main goal of the current study was to determine the effect of IES-induced muscle contractions on modulating the cellular consequences of DTPI in rats with hind limb paralysis, and its capacity to prevent the progression of the injury into an open wound. We hypothesized that animals receiving IES would have a faster rate of DTPI healing in comparison to animals without IES. IES was initiated at 3 different time points after the induction of DPTI in rats with complete SCI, and the extent of tissue damage and healing were assessed. The size of muscle injury was examined using magnetic resonance imaging (MRI), and the cellular events associated with tissue regeneration and healing after DTPI were assessed with immunohistochemistry.

2.2. Methods

Experiments were conducted in 85 adult female Sprague Dawley rats weighing 250-375g. All procedures were approved by the Animal Care and Use Committee at the University of Alberta. All animals received a spinal cord injury (SCI) at the 8th thoracic level (T8) to reduce the effect of voluntary movements on tissue healing. Animals were then divided into control and experimental groups to assess the effect of IES on expediting tissue healing and investigating the underlying mechanisms of action of IES.

2.2.1. Spinal cord transection

Anesthesia was induced and maintained using isoflurane (2-3 %; 1L/min oxygen). Under aseptic conditions, a 2cm incision was made around T8 and a laminectomy was performed to expose the spinal cord. A complete SCI was induced by transecting the cord, and the muscle layers of the back and skin were sutured closed. Post-surgery, Temegesic (buprenorphine, 0.05 mg/kg subcutaneously, 3x/day) was administered for analgesia for the first 3 days post-SCI, and Baytril (enrofloxacin, 5mg/kg subcutaneously, 2x/day) was administered for the entire duration post-SCI for preventing infections. The bladders were manually expressed 4-5 times per day. Post-SCI, the rats were randomly assigned to control and treatment groups (Figure 2-1) as follows:

1. Loading only control (Lc; n=32): All rats in this group received a one-time load to the tibialis anterior (TA) muscle of one hind leg 14 days after SCI, resulting in a DTPI. These rats were then divided into 4 subgroups based on the duration they were maintained after the loading procedure (1, 3, 5 and 7 days; referred to as LD1, LD3, LD5 and LD7, respectively). The extent of the resulting tissue damage was compared to the intact contralateral legs on days 1, 3, 5 or 7 after DTPI using T_2-weighted and T_1-weighted contrast-enhanced MRI. The animals in the different subgroups were euthanized on the corresponding days to allow for muscle extraction for immunohistochemical analysis.
2. Stimulation only control (Sc; n=20): The rats in this group received IES only starting 14 days after the induction of SCI. IES was applied to the common peroneal (CP) nerve through a nerve cuff, activating the TA muscle of one hind limb. The rats were divided into 4 subgroups based on the duration of stimulation (1, 3, 5 and 7 days; referred to as SD1, SD3, SD5 and SD7, respectively). The extent of tissue damage in the leg with

implanted nerve cuff and stimulation was compared to the sham contralateral leg which received nerve cuff but no stimulation on days 1, 3, 5 or 7 using T_2-weighted and T_1-weighted contrast-enhanced MRI. The animals in the different subgroups were euthanized on the corresponding days to allow for muscle extraction for immunohistochemical analysis.

3. Loading and IES treatment (LSt; n=33): All rats in this group received a one-time load to the TA muscle of one hind leg to induce DPTI 14 days after SCI, similar to the Lc group. The rats were then divided into three subgroups based on the time of initiation of IES post-induction of DPTI (1, 3 and 5 days; referred to as LSD1, LSD3 and LSD5, respectively). The application of IES initiated on days 1, 3 or 5 continued until day 7 after the induction of DTPI. The extent of tissue damage was compared to the sham contralateral leg with implanted nerve cuff and no stimulation using T_2-weighted and T_1-weighted contrast-enhanced MRI on days 1, 3, 5 or 7. All animals were euthanized on day 7 except for one additional LSDI group that was euthanized on day 3. The TA muscles from both hind legs were extracted for immunohistochemical analysis.

2.2.2. Loading procedure

Two weeks post-SCI, the rats in the Lc and LSt groups were subjected to a one-time load applied to the TA muscle of one hind leg for 2 hours to induce a DTPI. The rats were weighed and the experimental leg was shaved under isoflurane anesthesia. The load was then applied through a 3mm-diameter indenter centered 1cm below the tibial tuberosity using a custom-built apparatus (Figure 2-2). The diameter of the indenter represented the cross-sectional area of the rat's ischial tuberosity (Curtis et al., 2011). The one-time load was

equivalent to 44% of each rat's body weight. This represented the level at which the deep tissues adjacent to the ischial tuberosities are subjected to in humans when seated on a hard surface (Curtis et al., 2011). The indenter was attached to a transducer to measure the applied load, and the force trace was digitized and recorded on a personal computer using a CED analog-to-digital converter and Spike 2 software (Cambridge Electronic Design Limited, Milton, Cambridge, England). The one-time constant application of pressure on the TA muscle led to the development of a DTPI.

2.2.3. Nerve cuff fabrication and implantation for delivery of IES

Nerve cuffs (2 per rat) were constructed using a 4mm piece of Silastic tubing (Dow Corning; #2415542, Midland, MI, USA) with a 1mm groove cut out (Figures 2-3A and B). Three lengths (26cm) of multi-stranded stainless steel wire (Cooner Wire; AS631, Chatsworth, CA, USA) with 1cm of the Teflon insulation removed from the end were used as the conductors. The uninsulated wire tips were threaded through the top of the tubing and out the other side. The cuff was placed around an 18G needle to form the wire against the inside wall of the cuff. Silicon gel (Dow Corning #732) was applied to the outside of the Silastic cuff and 2 braided 7-0 silk sutures (Ethicon, Somerville, NJ, USA) were embedded into the silicon ~1.5mm from each end. Teflon tape was wrapped around the cuff to smooth out the silicon gel and the cuff was placed in an oven at 37^{o}C for 24 hours to cure. After 24 hours, the Teflon tape was removed and the free ends of the stainless steel wire were soldered to gold pins (Plastics One; E363-0, Roanoke, VA, USA). The pins were inserted into a 6-pin plastic headpiece (Plastics One; MS363) and affixed to the headpiece with epoxy (Figure 2-3C).

To implant the nerve cuffs, the rats in the Sc and LSt groups were anaesthetized with isoflurane (2-3 %; 1L/min oxygen). The top of the head, back, and both hind limbs were shaved and sterilized with Betadine scrub. Incisions, 2cm-long, were made in the skin on top of the skull, midway down the back and above the femur in both hind limbs. The nerve cuffs were tunneled under the skin from the incision on the skull to the incisions in each hind limb. The CP nerve was isolated from the tibial nerve and placed inside the Silastic cuff. The nerve cuff was stabilized using the two embedded 7-0 silk sutures, and the muscle and skin were sutured closed. Three holes were drilled in the skull forming a triangular shape across the midline of the parietal bone, and 3 stainless steel screws were threaded into the holes. The headpiece was placed in the middle of the 3 screws and anchored with orthodontic resin (Dentsply, Milford, DE, USA), and the skin incision was sutured shut. Post-surgery, the rats received Temegesic (buprenorphine, 0.05 mg/kg) and Baytril (enrofloxacin, 5mg/kg).

Electrical stimulation was delivered using a constant current stimulator (model number: MCSSTG4008) from Multi Channel Systems (Reutilgen, Baden-Wurttemberg, Germany). The TA muscle of one hind limb received IES via the implanted nerve cuff (Figure 2-3C). The stimulation paradigm consisted of a 2 s "ON" period followed by a 5 min "OFF" period repeated for 4 hours every day from the time of initiation of the IES intervention to the end point of all animals. The stimuli were biphasic and charge balanced with a 300 ∝s pulse width delivered at a frequency of 30 Hz (Figure 2-3D). The amplitude of stimulation was chosen to induce palpable contraction of the TA muscle. The contractions in TA and the activity of the rat were monitored throughout the duration of stimulation.

2.2.4. Assessments of tissue injury using MRI

MRI assessments were performed using a 3T Siemens Prisma full body magnet at the Peter S Allen MR Research Centre, University of Alberta. Rats were positioned within a hand/wrist radio-frequency (RF) coil, with their legs stretched using Velcro straps. The body and head were outside the RF coil, allowing for unrestricted breathing and for placing a gas mask when isoflurane anesthesia was used. Rats were imaged on days 1, 3, 5 and 7 after loading or initiation of IES as depicted in Figure 1. A subset of animals was euthanized on each imaging day to provide tissue for immunohistochemical analyses.

MRI assessments on the days prior to the end point were performed under isoflurane (1.5-2 %; 2L/minute oxygen). The assessment on the final day was performed under sodium pentobarbital (intraperitoneal, 40mg/kg). Thirty consecutive transverse slices, 1 mm thick, were acquired from the knee to the ankle bilaterally for each rat (Figure 2-4). Three sequences were used: T_2-weighted turbo spin echo (TSE), T_1-weighted 2D FLASH and T_1-weighted 2D FLASH contrast-enhanced MRI. The contrast agent was Magnevist administered intravenously through a catheter in the jugular vein in a bolus of 0.1mmol/kg. The parameters of the sequences were as follows: T_2-weighted TSE: echo time (TE) = 396 ms; repetition time (TR) = 3570ms; field of view = 67x80mm; acquisition matrix = 192x192; in-plane resolution (interpolated) = 0.2mm x 0.2mm; slice thickness = 1mm; flip angle = 152°; averages = 6; and total scan time = 10min 30s. T_1-weighted 2D FLASH: TE = 6.35 ms; TR= 460ms; field of view = 67x80mm; acquisition matrix = 192x192; in-plane resolution (interpolated) = 0.2mm x 0.2mm; slice thickness = 1 mm; flip angle = 90°, averages = 1; total scan time = 3min 30s. T_1-weighted contrast-enhanced MRI sequences were obtained after intravenous administration of contrast agent with parameters as follows: TE = 6.35 ms; TR = 460ms; field of view = 67x80mm; acquisition matrix = 192x192;

in-plane resolution (interpolated) = 0.2mm x 0.2mm; slice thickness = 1 mm; flip angle = 90°, averages = 1; total scan time = 3min 30s. The T_2-weighted MRI images were used to detect the extent of tissue edema within the TA muscle in the limb that received loading, with the contralateral limb serving as control. The T_1-weighted MRI images were used to delineate the TA muscle in the experimental and contralateral control limbs for image analysis. The T_1-weighted contrast-enhanced images were used to identify the region of TA with irreversible injury (or scar formation) in the chronic stage of DTPI.

The MR images were analyzed by two observers (3 repetitions each) blinded to the animal groups using custom written scripts in MATLAB (Mathworks, Cambridge, MA). The MR images were imported to MATLAB as DICOM files. The region of interest representing the TA muscle was selected in both limbs using the T_1-weighted images, and superimposed on the T_2-weighted images. The pixel intensity in T_2-weighted images within the selected region of interest in the experimental limb was compared to the intensity in the region of interest chosen in the contralateral limb. If the signal intensity in the experimental limb exceeded mean + 2 SD of the intensity in the contralateral limb, the increased signal intensity indicated the presence of tissue edema/damage. The total pixels exhibiting tissue edema/damage across the slices from the knee to ankle were used to determine the percentage of muscle volume that was affected by DTPI. Outliers in the total of 6 repetitions of analysis per animal by the two observers were statistically removed, and averages were calculated for each rat (Figure 2-4)

2.2.5. Immunohistochemistry (IHC)

Immediately after the final MRI assessment, the rats were deeply anesthetized and the TA muscle was extracted from both hind limbs. The rats were euthanized following tissue extraction. The TA muscle from the experimental leg was marked with an India ink line denoting the level where the highest signal intensity was observed during the final MRI assessment. The muscles from both hind limbs were weighed, frozen in liquid nitrogen- cooled melting isopentane and stored in a -80°C freezer. Serial 12 µm-thick transverse sections were collected at -23°C from the India ink marked area of each muscle and transferred onto Superfrost Plus microscope slides (Fisher Scientific, Hampton, New Hampshire, USA). Two sections each for the experimental and contralateral control muscle per animal were mounted on a slide. The slides were air dried for 30-45 mins at room temperature and stored at -80°C.

Embryonic myosin heavy chain (eMHC) immunofluorescence was performed with a primary antibody (anti-mouse IgG_1, MYH3; Santa Cruz Biotechnology, Dallas, Texas, USA) against eMHC. To determine whole muscle cross-sectional area (CSA) and fiber CSA, individual muscle fiber boundaries were identified with a rabbit polyclonal IgG antibody against laminin (Millipore-Sigma, Burlington, Massachusetts, USA). Macrophages and satellite cells were identified using a combination of anti-CD68 (ED1) antibody (anti-mouse monoclonal IgG_1; Abcam, Cambridge, UK) and anti-Mannose Receptor (CD206) antibody (anti-rabbit polyclonal IgG; Abcam, Cambridge, UK). Alexa Fluor® 488 and 568 secondary antibodies were purchased from Thermo Fisher Scientific. Nuclei on all sections were stained with DAPI (4',6-Diamidino-2-Phemylindole, Dihydrochloride; Molecular Probes, Eugene, Oregon, USA) (Figure 2-5).

Serial sections for either MYH3/laminin or CD68/CD206 labelling were briefly air

dried, fixed in 100% acetone at -20°C for 10 min, washed once in phosphate-buffered saline (PBS, pH 7.4) with 0.1% (v/v) Tween-20 (PBS-T, pH 7.4) and twice in PBS at room temperature for 5 min each, before incubating in a blocking solution [1% (w/v) bovine serum albumin and 10% (v/v) normal goat serum in PBS-T, pH 7.4] overnight at 4°C in a humidity chamber. Sections were washed 3 times in PBS for 5min each and then co-incubated with primary antibodies diluted in blocking solution containing anti-laminin (1:100) and anti-MYH3 (1:50), or CD68 (1:200) and CD206 (1:200) for 2 hours at room temperature. After several washes in PBS-T followed by PBS, sections were co-incubated with secondary antibodies diluted in blocking solution containing goat anti-mouse IgG Alexa Fluor 488 (1:400) and goat anti-rabbit IgG Alexa Fluor 568 (1:400) for 2 hours at room temperature. After several washes in PBS-T followed by PBS, sections were exposed to a 14.3 mM solution of DAPI in ddH_2O for 3min followed by 3 rinses in PBS, mounted with VectaShield® HardSet mounting medium and stored according to manufacturer directions (Vector Laboratories).

Muscle sections of the experimental and contralateral control TA were visualized with a spinning disk inverted confocal microscope (Leica TCS-SPE; Leica Microsystems, Wetzlar, Germany). A Leica Application Suite X (LAS-X; Leica Microsystems) was used to capture and export images as jpegs for later analysis.

The muscle images were analyzed using ImageJ 1.51K (NIH). The system was calibrated using a scale bar embedded in each image. The merged images from the LAS-X software were opened in ImageJ and split into the red, blue and green channels. The CD68/CD206/DAPI-labelled muscle sections were split into their component channels to measure the percentage of whole muscle CSA occupied by the DAPI-labelled nuclei, M1 macrophages, M2 macrophages and satellite cells. Cell counts were not expressed as a

density (# of cells/known area) due to the large number of overlapping cells in high density areas.

The % of CSA occupied by DAPI labelled nuclei was measured using the blue channel. The % of CSA occupied by M1 macrophages was measured by *subtracting* the red channel from the green channel. The % of CSA occupied by M2 macrophages was measured by *combining* (using the AND function in the ImageJ calculator) the green and red channels. The % of CSA occupied by satellite cells was measured by *subtracting* the green channel from the red channel. Whole muscle fiber CSA and CSA of both the MYH3 positive (eMHC MHC isoform) and negative (adult MHC only isoforms) fibers were analyzed using the red and green channels from the MYH3/laminin double-labelled sections.

2.2.6. Statistical analysis

The outcome measures were twofold: 1) muscle volume with increased signal intensity; 2) % of CSA with positive staining for satellite cells, M1 and M2 macrophages, and regenerating muscle fibers.

The reliability of MRI results conducted by two observers were assessed using intraclass correlation coefficient (ICC) (random mixed model; absolute agreement). The % he % of muscle volume with increased signal intensity were represented as mean ± standard error (SE). The change in signal intensity was compared across assessment time points using one-way analysis of variance (ANOVA). Muscle volume exhibiting increased T_2 signal intensity was normalised to day 1 for between group comparisons, and a two-way ANOVA was performed for which group and time were the independent variables, and muscle volume with increased signal intensity was the dependent variable. If significant changes were

observed ($p \leq 0.05$), post-hoc analyses was conducted using Tukey's Honestly Significant Difference for multiple comparisons.

The IHC counts of positively and negatively-stained cells in the experimental leg were normalised to the counts in the contralateral control leg, and represented as mean ± SD. The eMHC fibre CSA for Lc, Sc and LSt subgroups were represented as mean ±SE. The values of %CSA with positive labelling for all cell types were compared across time points using t-tests or one-way ANOVA. A two-way ANOVA was used for between group comparisons. The value of α was 0.05 for all statistical tests, and differences were considered significant for ≤ 0.05.

2.3. Results

2.3.1. Tissue damage assessed using T_2-weighted MRI

Assessments of muscle volume with increased signal intensity from T_2-weighted MR images were obtained on days 1, 3, 5 and 7 after the induction of DPTI and/or initiation of IES. One rat from the Lc group was excluded from the MRI analysis because of technical issues on the day 1 assessment time point. All animals that received the one-time 2hr-loading on the TA muscle showed an increase in signal intensity in the muscle of the loaded leg, indicating the presence of a DPTI. A typical example of a TA muscle with increased signal intensity in one rat from the Lc group is shown in Figure 2-4. Each trace in Figure 2-4E represents a blinded analysis performed by an observer. The reliability analysis for all trials indicated an absolute agreement between the single and average measures with ICC score of 0.984 and 0.997, respectively ($*p \leq 0.05$).

The % of muscle volume exhibiting increased signal intensity for the Lc group was substantially reduced over time (from day 1 to 7). In Figure 2-6A, the raw data represent the % of muscle volume with increased signal intensity across assessment time points in the presence of statistically-identified outliers, which were then removed (Figure 2-6B). The leg that received loading (experimental) had a significantly larger % of muscle volume with increased signal intensity relative to the leg that did not receive loading (contralateral control) at all time points. Moreover, the % of muscle volume with increased signal intensity was significantly higher on day 1 compared to days 3, 5 and 7 ($*p \leq 0.005$). The significant reduction in the % of muscle volume with increased signal intensity over time was due to natural healing after DTPI.

The IES intervention showed no change in the % of muscle volume with increased signal intensity for all Sc subgroups (Figure 2-7). There was no statistical difference between the experimental leg (nerve cuff + stim) and sham contralateral control leg (nerve cuff only) across all time points ($p \geq 0.513$). Furthermore, there was no statistical difference in the % of muscle volume with increased signal intensity between the sham contralateral control leg in the Sc group and the contralateral control leg (no cuff) in the Lc group ($p \geq 0.991$). This demonstrated that neither the nerve cuff nor the application of IES caused tissue damage in the paralyzed TA muscles.

Initiation of IES on day 1 after DTPI (LSD1) showed a marked reduction in the % of muscle volume exhibiting increased signal intensity compared to the Lc group without IES (Figure 2-8). Figure 2-8A shows the % of muscle volume with increased signal intensity (normalised to day 1) for the Lc and LSD1 groups on days 1, 3, 5 and 7 post-induction of DTPI and initiation of IES. There was a significant reduction in % of muscle volume with increased signal intensity on days 3, 5 and 7 compared to day 1 for the control Lc and LSD1

groups (*$p \leq 0.001$). Importantly, the % of muscle volume with increased signal intensity was significantly smaller on day 3 in the LSD1 group than the Lc group (*$p \leq 0.01$). Although there was no statistical significant difference on the subsequent assessment time points, the trend of reduced % of muscle volume with increased signal intensity continued in the LSD1 group on the day 5 time point ($p = 0.062$).

A comparison of Lc and LSt subgroups with IES initiated in day 3 (LSD3) and day 5 (LSD5) after the induction of DTPI is shown in Figures 2-8B and C, respectively. There was no significant difference between the Lc and LSt groups when IES was initiated on day 3 or later after the induction of DTPI ($p \geq 0.671$). Figure 2-8D merges the T_2-weighted MRI results from the Lc and LSt subgroups. The Lc, LSD3 and LSD5 groups were not significantly different from each other for any assessment time point ($p \geq 0.520$). In addition to the statistical difference between the Lc and LSD1 groups, there was a significant difference between the LSD1 and LSD3 groups ($p \leq 0.019$). However, there was no statistically significant difference between LSD1 and LSD5 ($p = 0.075$).

While increased signal intensity in T_2-weighted MR images indicates increases in water content (i.e., edema), increased signal intensity in T_1-weighted contrast-enhanced MR images delineates scar formation (Abdel-Aty et al., 2004; Kelle et al., 2009). Figure 2-9 shows the % of muscle volume with increased signal intensity in T_1-weighted contrast-enhanced MR images for the Lc and LSD1 groups at two time points post-induction of DTPI: day 3 (LD3 and LSD1-3) and day 7 (LD7 and LSD1-7). There was a significant reduction in the % of muscle volume with increased signal intensity on day 7 in the LSD1 group (LSD1-7) relative to the Lc group (LD7) (*$p \leq 0.026$).

2.3.2. Immunohistochemistry Outcomes

The cellular events after DTPI were quantified by immunolabelling muscle fibers, nuclei, inflammatory cells and regenerating muscle fibers. After injury, activation of chemokines recruits two macrophage subpopulations—pro-inflammatory or early macrophages (M1) which are identified by CD 68^{+} CD 206^{-} immune-labelling, and anti-inflammatory or late macrophages (M2) identified by CD 68^{+} CD 206^{+} immune-labelling. Another overlapping event is the activation, differentiation and fusion of satellite cells that are marked by $CD68^{-}CD\ 206^{+}$ immunolabelling (Figure 2-5A-D). The satellite cells fuse into new myofibers which express developmental markers, such as embryonic MHC (Figure 2-5E-G).

Figure 2-10 shows the IHC results from the contralateral control TA muscles extracted on day 7 from the Lc (LD7) and Sc (SD7) groups. There was no significant difference between the contralateral control leg in the Lc group (no nerve cuff), the sham contralateral control leg in the Sc group (nerve cuff, no stim) and the experimental leg in the Sc leg (nerve cuff + stim) for any of the stained cells ($p \geq 0.228$). This demonstrated that the implantation of the nerve cuffs and IES applied for 4 hr/day did not cause damage in the paralyzed TA muscled.

Macrophage cell groups and satellite cells are shown in Figure 2-11A for TA muscles extracted on day 3 from the Lc group (LD3) and the LSt group with IES initiated on day 1 post-induction of DTPI (LSD1-3). There was a statistically significant increase in satellite cells, M1 and M2 macrophages in the group that received stimulation ($*p \leq 0.0432$), but no significant increase in the nuclei stained with DAPI between the groups ($p = 0.129$) (Figure 2-11B). When, tissue was extracted on day 7 after DTPI induction from the Lc and LSt

groups (LD7 and LSD1-7, respectively), there was no statistical difference in the satellite, M1 and M2 cells ($p \geq 0.274$) between the groups (Figure 2-12).

Figure 2-13 shows the CSA of the positive and negative-labelled eMHC fibres in the experimental and contralateral control legs for the Lc, Sc, and LSt groups in muscles extracted on days 3 or 7 post-induction of DTPI and/or IES. Figure 2-13A shows that the LD7 group had a significantly larger CSA of positively-labelled eMHC fibers than the LD1 group for both hind limbs, and the LD3 group for the experimental hind limb ($*p \leq 0.001$), suggesting growth of eMHC fibres over time. Simultaneously, there was a significant reduction in CSA of negatively-labelled eMHC fibers in LD7 relative to LD1 ($p = 0.013$), potentially indicating increased atrophy of muscle fibres over time in the paralyzed TA muscles.

The CSA of positively-labelled and negatively-labelled eMHC fibres was not significantly different between the LD7 and SD7 groups for the contralateral (no cuff) and sham contralateral (nerve cuff, no stim) control legs (Figure 2-13B). It was also not significantly different for the negatively-labelled fibres in the experimental legs of the two groups ($p \geq 0.136$). Furthermore, there was no difference in the positively-labelled fibres between the experimental (nerve cuff + stim) and sham contralateral control (nerve cuff, no stim) legs of the SD7 groups ($p = 0.999$). This suggests that 7 days of stimulation did not result in tissue damage. However, the CSA of the positively-labelled eMHC fibres significantly increased in the LD7 relative to the SD7 group ($p = 0.001$), indicating that the proliferation of new muscle fibres due to injury. Interestingly, there was no statistical difference in the CSA of the positively and negatively-labelled eMHC fibres in the TA muscles from both hind limbs between the LD3 and LSD1-3 groups ($p \geq 0.949$) (Figure 2-13C). Similarly, there was no statistical difference between the CSA of the muscle fibres

between the LD7 and LSD1-7 groups ($p \geq 0.277$) (Figure 2-13D).

2.4. Discussion

2.4.1. Overview

The overall goal of this study was to investigate the role and underlying mechanisms of a novel IES paradigm in accelerating healing after tissue injury. DTPI, a class of PIs, was chosen as an example of deep-seated tissue injury that currently has no treatment. The progression of DTPI in the TA muscle caused by a one-time 2hr-application of loading was assessed using MRI and IHC. The findings demonstrate, for the first time, that brief (2s), low-level contractions of the injured muscle, repeated every 5min for 4 hours/day, significantly accelerate the rate of healing and reduce the size of tissue damage when applied early after DTPI formation.

2.4.2. Susceptibility of muscle to damage due to loading and electrical stimulation

Across all animals in the Lc and LSt groups, loading the TA muscle for a duration of 2 hours was sufficient to cause a DTPI. The injury was deep in the muscle, below the skin, and despite involving nearly 40% of the muscle volume, showed no signs of damage on the surface of the skin in any of the animals. This demonstrates the higher susceptibility of muscle tissue to damage by mechanical loading than the skin (Daniel et al., 1981; Bouten et al., 2003b, 2003a; Solis et al., 2007; Loerakker et al., 2013), and underscores the danger of

this class of PIs which currently progresses unbeknownst to the affect individual or their caregiver. The initiation of DTPI within 2 hours of loading also suggests that current clinical guidelines of 2 hourly repositioning of patients with reduced mobility and impaired sensation may be ineffective for the prevention of DTPI (Miles et al., 2013).

In contrast to previous records (e.g., Bickel et al., 2004 and Slade et al., 2004), the ES paradigm used in this study did not cause damage in the target muscle. The MRI findings showed no IES-induced damage in the Sc group (Figure 2-7), which were confirmed immunohistochemically (Figure 2-12), thus making this IES paradigm a safe treatment for injured muscles. The primary differences with studies showing damage caused by ES-induced contractions are likely to be the magnitude and type of ES-induced contractions. Typically, large contractions (e.g., 60% of maximal voluntary contraction) are induced in an isometric fashion (Bickel et al., 2004; Slade et al., 2004). These contractions may cause micro-tears in muscle fibers, leading to local inflammation that subsequently appears as increased edema (water content) in T_2-weighted MR images (Slade et al., 2004). In the present study, low-level, concentric muscle contractions were induced by IES, causing no damage in the atrophied TA muscle after SCI.

2.4.3. Use of MRI for detection of damage progression in injured muscles

In the current study, edema in the damaged tissue was assessed using T_2-weighted MRI, which was validated by previous studies as an accurate measure for quantifying tissue beak down (Solis et al., 2007, 2013; Curtis et al., 2011). An increase in the intensity of the T_2 signal in the damaged region of the experimental leg is due to increased water content within the intracellular and/or extracellular environment following an injury, and is indicative of tissue edema (May et

al., 2000) caused by an acute inflammatory response. The percentage of muscle volume with increased signal intensity across the entire region of interest (TA muscle) helped determine the extent of tissue damage.

In addition, the current study investigated for the first time, the progression of skeletal muscle injury using T_1-weighted contrast-enhanced MRI to delineate the size of the scar formed in the chronic stages of injury. Previously, the progression of edema and infarct size in cardiac muscle after myocardial injury (MI) was assessed with T_2-weighted MRI and T_1-weighted contrast-enhanced MRI (Abdel-Aty et al., 2004; Klocke, 2010; Raman et al., 2010). To date, however, these techniques have not been used in skeletal muscle. The T_2-weighted and T_1-weighted contrast-enhanced MRI findings in this study demonstrated that IES reduces both inflammation (edema) and the overall size of a muscle injury (DTPI) when applied one day after the induction of the injury.

2.4.4. Mechanism of action of IES

Recently, our lab developed IES as a novel technique for preventing the formation of DTPI (Solis et al., 2007, 2012, 2013; Curtis et al., 2011). In contrast to ES for open wounds, IES functions by application of pulses of electrical current to the muscles that are loaded while sitting and lying down (Solis et al., 2012). The electrical stimuli are applied for 10s every 10min resulting in periodical muscle contractions throughout the duration of sitting or lying down (Curtis et al., 2011; Solis et al., 2012). These muscle contractions prevented the formation of DTPI by periodically redistributing and relieving pressure and mechanical deformation in tissue near bony prominences, and improving tissue perfusion (Solis et al., 2007, 2012, 2013; Gyawali et al., 2011).

The current study investigated the effects of IES delivered at low amplitudes for a brief duration of 2s every 5min (4hr/day) on muscles affected with DTPI. In contrast to the IES technique used for the prevention of DTPI, the ES paradigm in this study applied low-amplitude and shorter-duration contractions on already injured tissue to resolve edema and expedite the healing process. The mechanisms of action of IES-induced contractions on expediting the healing of injured muscles are likely two-fold: 1) acceleration of anti-inflammatory mechanisms, and 2) increase in the proliferation of satellite cells.

2.4.4.1. Acceleration of anti-inflammatory mechanisms

Clinicians have used different forms of ES to control edema after musculoskeletal injuries. In particular, HVPC is commonly used to treat musculoskeletal injuries by athletic trainers and physical therapists (Reed, 1988). These studies reported a treatment benefit on acute edema when ES was applied at amplitudes lower than visible motor activity. However, while ES applied at amplitudes below motor threshold was effective in resolving edema (Man et al., 2007), ES-induced muscle contractions during the acute phase of ankle injury showed minimal resolution of edema which was possibly due to the compression of lymphatic and venous vessels (Man et al., 2007; Feger et al., 2015). In those studies, the ES amplitudes were adjusted to the maximal level of tolerance (typically generate large muscle contractions), and resulted in no to little effect on edema clearance. The present study showed that the use of balanced, biphasic electrical stimulation at amplitudes titrated to produce palpable contractions cause a significant reduction in edema on the day after the application of IES.

The T_2-weighted MRI findings in the present study showed a significant decrease in

edema when IES was initiated on day 1 and ending on day 7 (LSD1). A trend showing a reduction in edema on the subsequent time points in the same group was also seen, although it was not significant (Figure 2-8A). However, there was no change in damage progression when the IES was initiated on days 3 and 5 compared to the Lc group because of the spontaneous resolution of edema over time.

The sequential and overlapping roles of macrophage subpopulations after DTPI are shown using IHC. In this study, IES significantly increased the M1 and M2 macrophages when the tissue was extracted on day 3. The balance between these two macrophage subpopulations in tissue plays a role in the degeneration or healing processes (Leibovich and Ross, 1975, 1976; Willenborg et al., 2012; Novak et al., 2014). Interestingly, Hesketh et al suggested that the macrophage subpopulations switch from M1 to M2 5–7 days after injury (Hesketh et al., 2017). In the present study, the switch occurred on the day 3 time point when the IES intervention was initiated one day after the induction of DTPI (Figure 2-11B). The M2 macrophage subpopulation plays a critical role in the removal of apoptotic cells, promotion of angiogenesis and fibroplasia, which collectively promote tissue healing and regeneration (Koh and DiPietro, 2011; Hesketh et al., 2017).

2.4.4.2. Increase in satellite cell proliferation

Initial work on ES demonstrated a decrease in cell death by altering cell signalling pathways such as kinase pathways (Huang et al., 2010; Qi et al., 2013; Love et al., 2018). Much of the effects on cell survival also depend on stimulation parameters. Li et al. showed that the use of unbalanced biphasic ES (25mV/mm) significantly increases the survival of neural progenitor cells (Li et al., 2007). This was proposed to be the result of increased

production of trophic factors [nerve growth factor (NGF), brain derived neurotrophic factor (BDNF), vascular endothelial growth factor (VEGF)] through the activation of the kinase pathway by ES. The increase in trophic factors inhibits cell apoptosis (Li et al., 2007).

There is also strong evidence that low frequency ES pulses delivered to atrophied muscles inhibits apoptosis of satellite cells (Guo et al., 2012; Wan et al., 2016). More importantly, the same study showed that ES helps skeletal muscle regeneration, supported by the ability of ES to increase satellite cell proliferation and inhibit apoptosis (Guo et al., 2012).

In contrast to previous studies, the current study used IES to produce small visible contractions in already injured muscle. There was a significant increase in satellite cells on day 3 in the group of rats that received stimulation starting on day 1 after the induction of DPTI. This demonstrated that the IES-induced contractions in the injured muscled inhibited apoptosis of satellite cells (Figure 2-11), which likely resulted in a significant decrease in the size of injury (Figure 2-9).

Interestingly, IES alone (Sc group) did not produce any changes in satellite cell counts in atrophied but uninjured muscles (Figure 2-10). The absence of increase in satellite cells in the Sc group may be due to the short duration (7 days) of IES application. In studies where ES showed increases in satellite cells in atrophied muscles, the duration of application spanned multiple weeks (Becker et al., 2010). Importantly, however, is the effect of IES on satellite cell proliferation in the injured muscle. IES caused a significant increase in the number of satellite cells soon after its initiation (i.e., by the day 3 time point) in the injured muscles (Figure 2-11).

Secondly, there was no difference in the regenerating muscle fiber size with IES

when tissue was extracted on days 3 and 7 compared to the Lc subgroups (Figure 2-13C, D). One possible reason could be that satellite cells fuse into new myofibers on day 3, the time they begin to express the developmental marker eMHC. This suggests that the day 3 time point may be too early to see regenerating muscle fibres. Collectively, IES may be a technique that can help in resolving inflammation and promote an increase in M2 macrophages. These findings, coupled with a significant increase in satellite cells, may be responsible for tissue regeneration after DTPI.

2.4.5. Clinical applicability

In humans, a DTPI can initiate after 10 min of immobility and loading (Loerakker et al., 2010). A change in the position can relieve tissue compression between the external surface and an underlying bony prominence, which can help in the natural healing of a DTPI. Nonetheless, absence of frequent repositioning subjects a site to prolonged loading. Paradoxically, even with repositioning, a site prone to injury is subjected to loading multiple times per day. Over time, the persistent injury at the deep bone-muscle interface progressestowards the skin surface.

In this experiment, the loading procedure was performed once for a duration of 2hr to induce a DTPI. The resulting decrease in damage in the Lc group over the 7 day testing period represents the natural healing process from a single episode of loading, in contrast to multiple loading episodes that would occur in a clinical setting. The IES paradigm used in this study demonstrated that healing of an impending DPTI can be expedited, thus preventing the progression of the injury to the skin surface where it develops into a large open wound.

2.5. Conclusion

This study demonstrated that IES-induced muscle contractions reduce tissue edema coupled with an acceleration of pro-regenerative processes such as proliferation of satellite cells, M1 and M2 macrophages. These cellular events suggest that IES is a safe intervention for treating muscle injury by targeting on stages of acute inflammation and promoting tissue regeneration in rats.

2.6. Acknowledgements

The authors would like to thank the staff of Health Sciences Laboratory Animal Services (HSLAS) staff for their support. The work was funded by the Canadian Institutes of Health Research (CIHR) and the Sensory Motor Adaptive Rehabilitation Technology (SMART) Network.

2.7. Figures

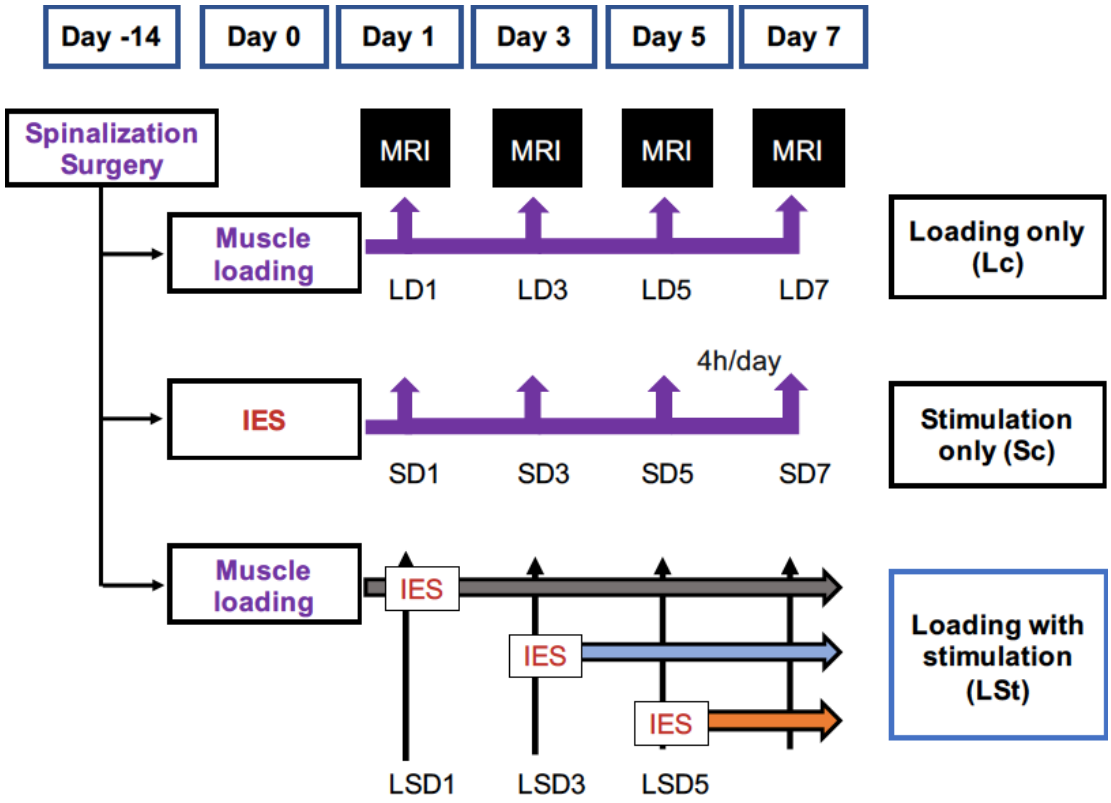

Figure 2-1: Overview of experimental protocol. *Shown are the groups and timelines of assessments. LD1, LD3, LD5 and LD7 are the subgroups of Lc with MRI assessments and tissue extraction on days 1, 3, 5 and 7, respectively. SD1, SD3, SD5 and SD7 are the subgroups of Sc with IES initiated on day 1 (4hr/day) and MRI assessments and tissue extraction obtained on days 1, 3, 5, and 7, respectively. LSD1, LSD3 and LSD5 are the subgroups of LSt with IES initiated on days 1, 3 and 5 after the induction of DTPI, respectively. MRI assessments were performed on days 1, 3, 5 and 7, and tissue was extracted on day 7. For LSD1 (LSD1-3) tissue was also extracted on day 3 in a separate group.*

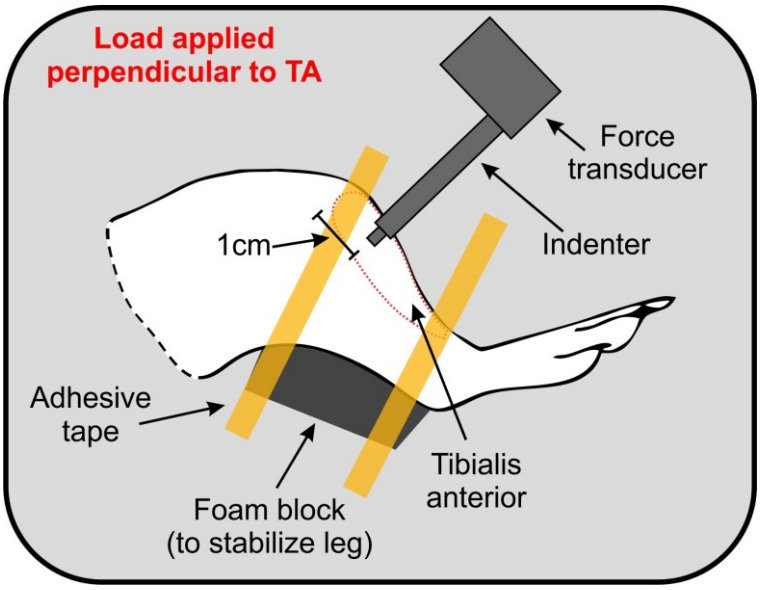

Figure 2-2: Loading procedure on an anaesthetized rat for induction of DTPI. *The rat was positioned in a custom built apparatus. A 3 mm indenter connected to a force transducer was used to apply 44% of the rat's body weight 1cm below the tibialis tuberosity.*

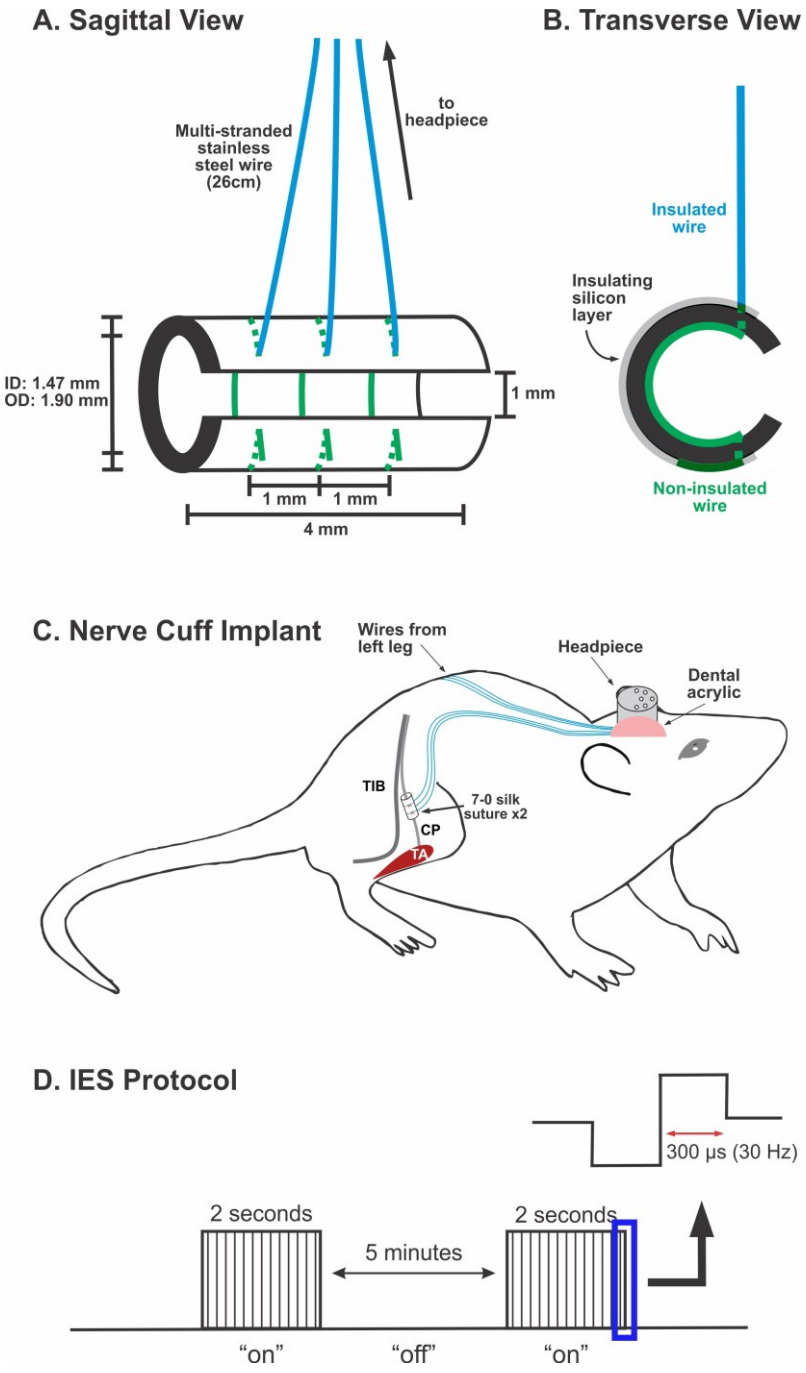

Figure 2-3 :Bilateral nerve cuff implants. *Nerve cuff in (A) sagittal view and (B) transverse view (C) Nerve cuffs are implanted bilaterally around the CP nerve. (D) IES protocol consisted of a 2 s "on" period and 5 min "off" period, delivered 4h/day.*

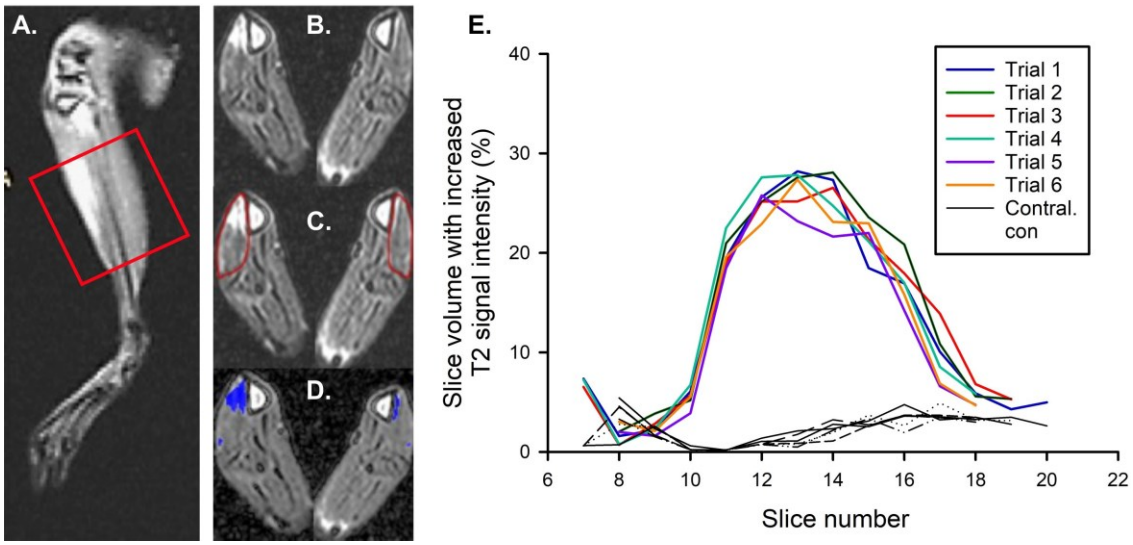

Figure 2-4: MRI image acquisition and analysis. *(A) Sagittal view of rat leg from the loading only group (Lc) showing the region of TA with DTPI (blue box) in the experimental leg. Cross-sectional MR slices were acquired from knee to ankle, covering the full extent of the TA muscle. (B) Cross- sectional slices of the TA from the experimental leg (left) and the contralateral control leg (right); the region of DTPI is the region with the bright signal in the experimental leg. (C) Region of interest for analysis (TA in both legs) is shown in red. (D) Pixels within the region of interest with signal intensity > (mean ± 2SD) of the signal intensity of all pixels in the contralateral control TA are marked in blue. (E) Percent volume with increased signal intensity across sequential MRI slices of the experimental and contralateral control legs in one animal. The traces represent the three repetitions of measurements obtained by two blinded assessors. Colored traces (trials 1-6) are from the experimental leg; black traces (different line types for the 6 overlaid traces) are from the contralateral control legs.*

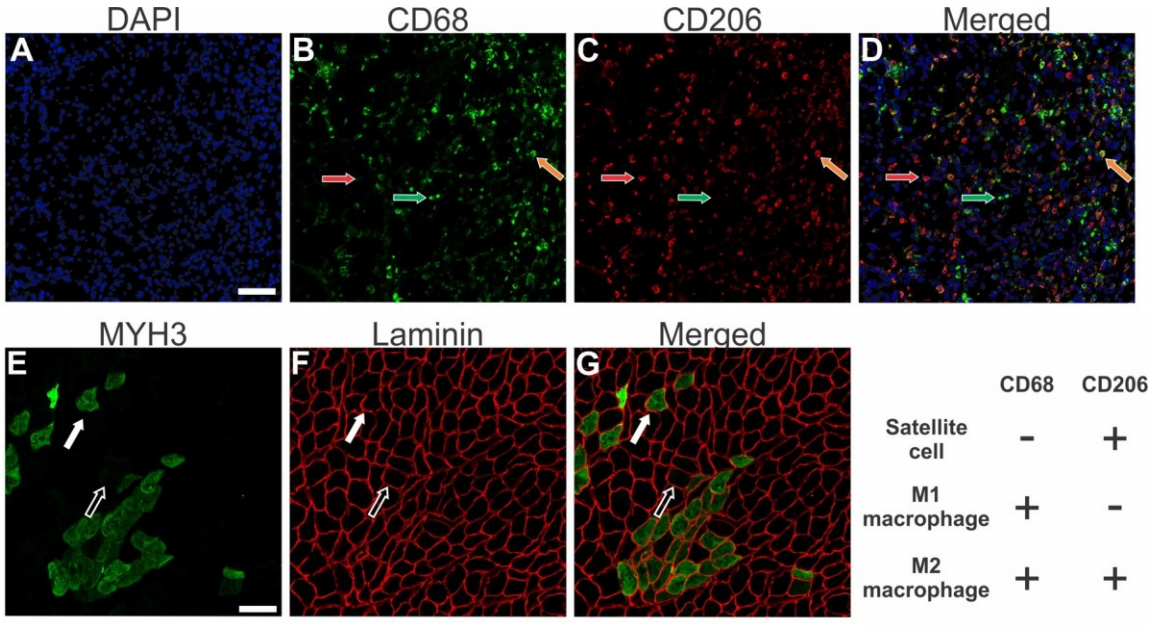

Figure 2-5: IHC staining on 12 µm cryosections of the rat TA muscle showing the cellular events after DTPI. *The invasion of cells into the damaged region of TA is shown in panels (A-D). Clusters of nuclei stained positively with DAPI in the damaged region are shown in A. (B-D) Macrophage subpopulations and satellite cells. CD 68^{+} CD 206^{-}—M1 macrophages (indicated by green arrows), CD 68^{+} CD 206^{+}—M2 macrophages (indicated by orange arrows), and CD 68^{-} CD 206^{+}—satellite cells (indicated by red arrows). Regenerating embryonic myosin heavy chain (eMHC) muscle fibers are recognised in panels (E-G) – MYH3 stains for eMHC fibres. Scale bars = 75 µm.*

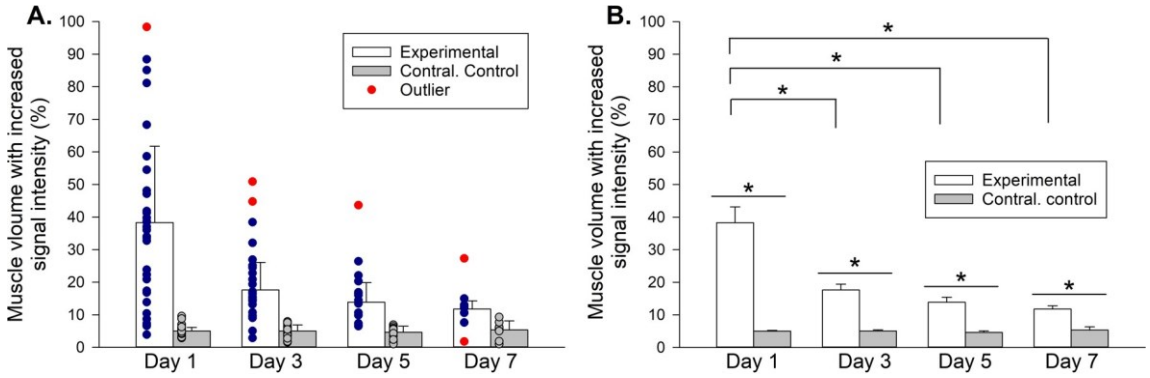

Figure 2-6: Progression of DTPI after a one-time application of loading. *(A) Muscle volume with increase in signal intensity on days 1, 3, 5 and 7 MRI assessments in the loading only group (Lc) with outliers (red). (B) Muscle volume with increase in signal intensity after DTPI in the Lc group after removal of outliers. Values are mean ± SE. The muscle volume with increased signal intensity was higher in the experimental leg (white bars) during all the analysed time points compared to the contralateral control leg (grey bars). Mean signal intensity was significantly higher on day 1 in comparison to days 3, 5 and 7 ($^{*}p \leq 0.005$).*

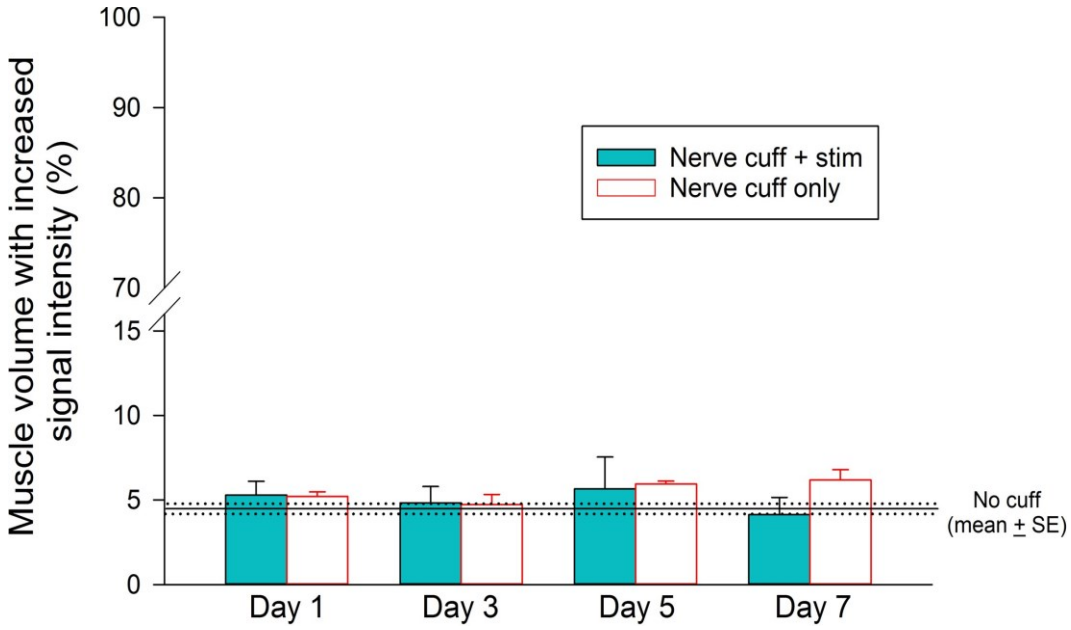

Figure 2-7: Effect of IES on the atrophied TA muscle. *Shown is the muscle volume with increased signal intensity across time points for the stimulation only group (Sc). Values are mean ± SE. The volume with increased signal intensity in the experimental leg receiving nerve cuff and stimulation (blue column) was not significantly different from the contralateral control leg that received a nerve cuff and no stimulation (white column) at all assessment time points ($p \geq 0.513$). Horizontal lines represent the mean ± SE of volume with increased signal intensity in the contralateral control legs for all animals without a nerve cuff. The signal intensity between the experimental legs that received neve cuffs and stimulation (blue column) was not different from the contralateral control legs in animals that did not receive nerve cuffs ($p \geq 0.991$).*

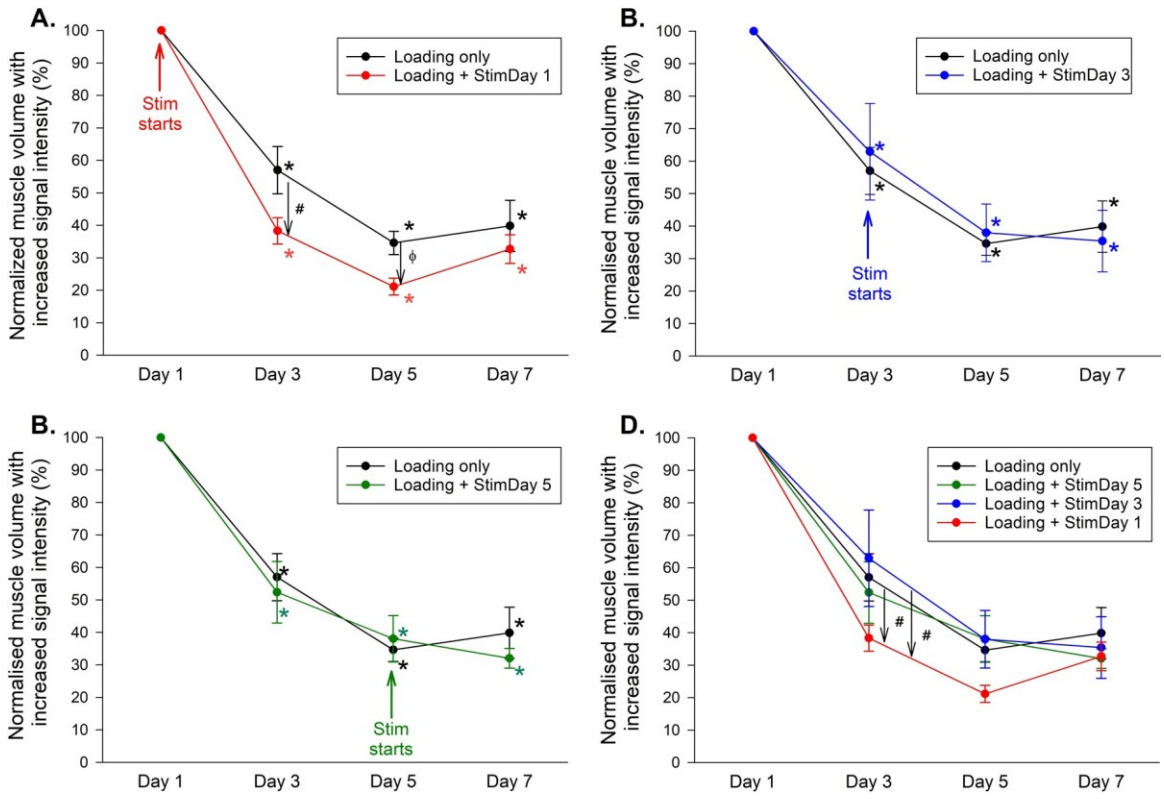

Figure 2-8: Comparisons of muscle volume with increased signal intensity between the control and treatment subgroups. *Shown are the [loading only control (Lc), load with stim starting on day 1 (LSD1), load with stim starting on day 3 (LSD3) and load with stim starting on day 5 (LSD 5)] groups. Values are mean ± SE. (A) Muscle volume with increased signal intensity across all assessment time points normalised to day 1 for the Lc and LSD1 subgroup. The control and treatment subgroup show a significant reduction in muscle volume with increased signal intensity on days 3, 5 and 7 relative to day 1 ($^{*}p \leq 0.001$). Moreover, there was a significant decrease in muscle volume with increased signal intensity on the day 3 time point when stimulation started on day 1 after DTPI (LSD1, n=18) compared to the Lc group (n=8) ($^{\#}p = 0.01$). The trend of reduction in muscle volume with increased signal intensity in the LSD1 subgroup relative to the Lc group continued on the subsequent time point (day 5;$^{\phi}p = 0.062$). (B) No significant difference between Lc and LSD3 (stim starting on day 3 after induction of DTPI; n=8) (p = 0.671). (C) No significant difference between Lc and LSD5 (stim starting on day 5 post induction of DTPI; n=9) (p = 0.605). (D) Merge (control and all treatment subgroups) – Lc and LSD3 were significantly different from LSD1 ($^{\#}p \leq 0.01$).*

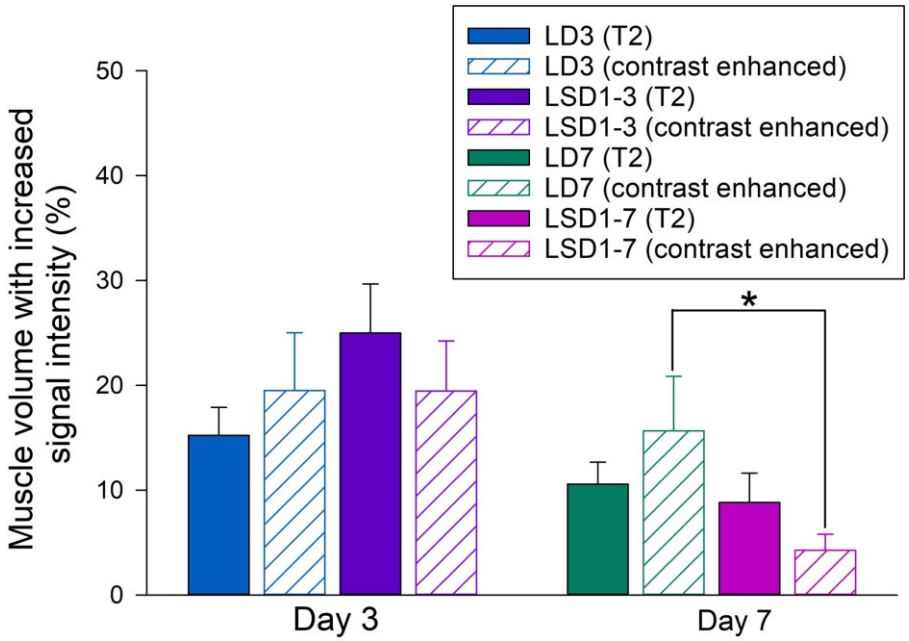

Figure 2-9: Comparison of muscle volumes with increased signal intensity in T_2-weighted images and T_1-weighted contrast-enhanced images. *Shown are the muscle volumes with increased T_2 (solid bars) or T_1 contrast-enhanced (hashed bars) signal intensity for the loading only group on days 3 and 7 (LD3 and LD7; blue and green solid bars, respectively) and the group with stim initiated on day 1 post induction of DTPI (LSD1-3 and LSD1-7; purple and pink bars, respectively). Muscle volume with increased signal intensity was significantly smaller in the LSD1- 7 group relative to the LD7 group in T_1-weighted contrast-enhanced images ($^*p= 0.026$) indicating and smaller DTPI size.*

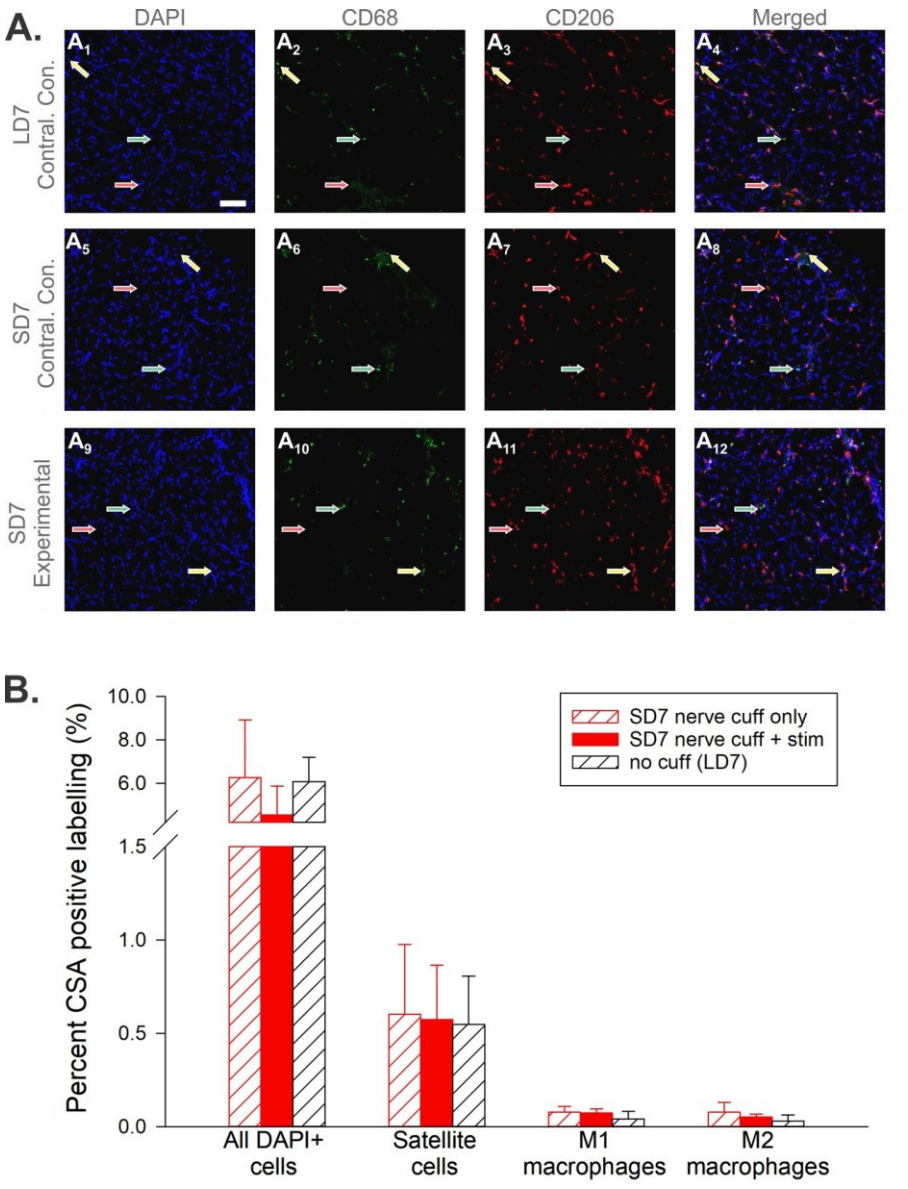

Figure 2-10: IHC of tissue extracted on day 7 from the loading only control (LD7) and the stim only control (SD7). *(A) Satellite cells, M1 and M2 macrophages are shown in panels (A1-12). Satellite cells: CD68^{-} 206^{+} (red arrows); M1 macrophages: CD 68^{+} CD 206^{-} (green arrows); M2 macrophages: CD 68^{+} CD 206^{+} (orange arrows). Scale bar = 75 μm. (B) Percent of cross sectional area (CSA) with positive staining for both Lc and Sc groups (means ± SD). No statistical significance between %CSA with positive staining for all cell groups ($p \geq 0.228$) between LD7 and SD7.*

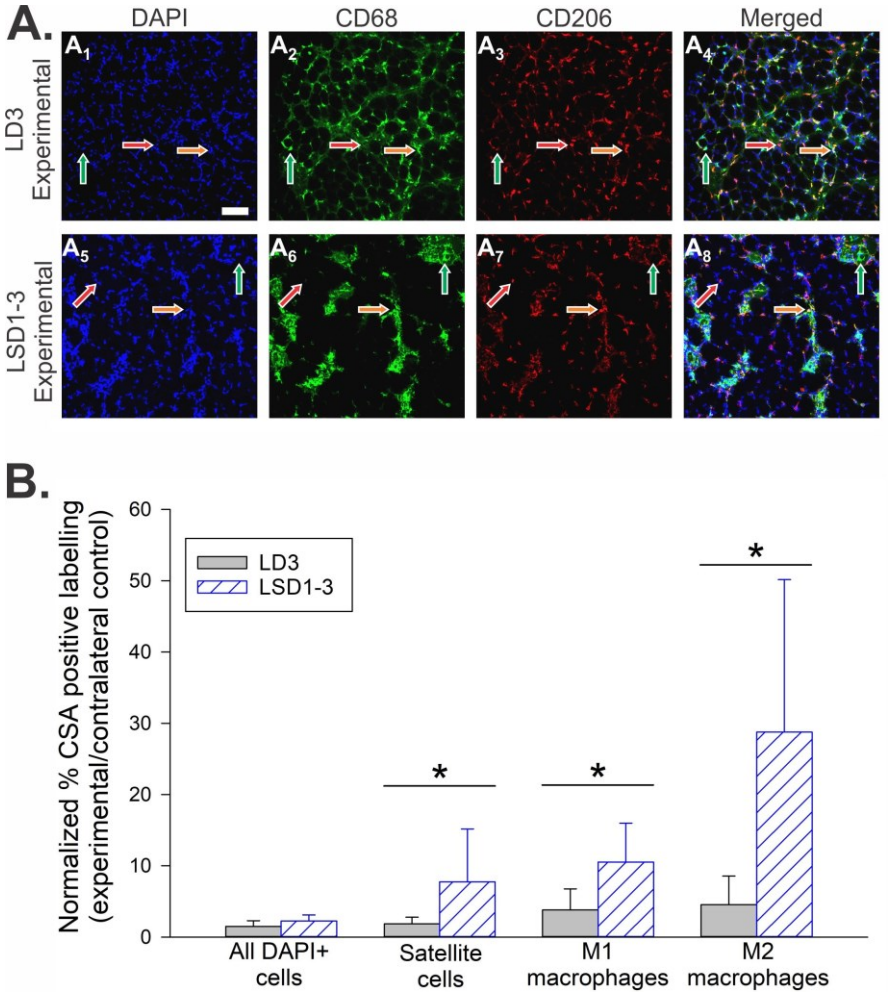

Figure 2-11: IHC of tissue extracted on day 3 from the loading only control (LD3) and the loading with stim initiated on day 1 post induction of DTPI (LSD1-3). *(A) Satellite cells, M1 and M2 macrophages are shown in panels (A1-8). Satellite cells: CD68$^-$ 206$^+$ (red arrows); M1 macrophages: CD 68$^+$ CD 206$^-$ (green arrows); M2 macrophages: CD 68$^+$ CD 206$^+$ (orange arrows). Scale bar = 75 μm. (B) Percent of cross sectional area (CSA) with positive staining for all cell types in the LD3 (gray bars) and LSD1-3 (blue, hashed bars) groups normalized to the %CSA with positive staining in the contralateral leg (means ± SD). $^*p \leq 0.0432$.*

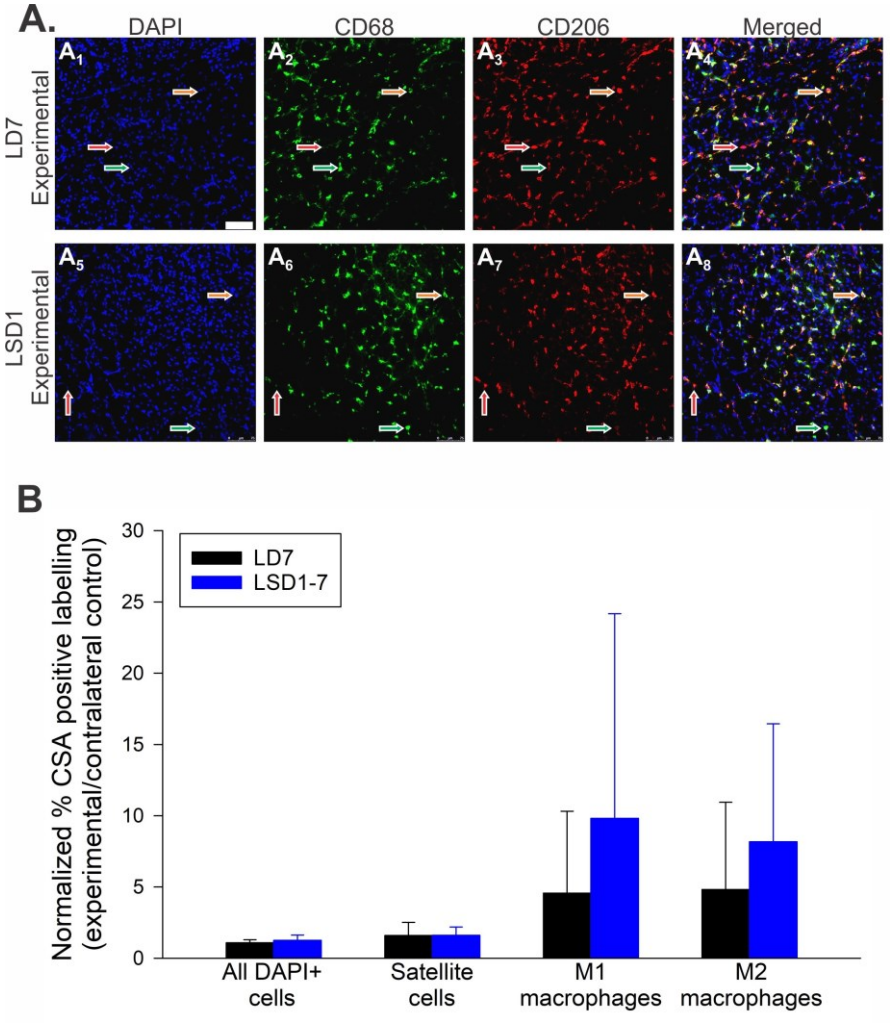

Figure 2-12: IHC of tissue extracted on day 7 from the loading only control (LD7) and the loading with stim initiated on day 1 post induction of DTPI (LSD1-7). *(A) Satellite cells, M1 and M2 macrophages are shown in panels (A1-8). Satellite cells: CD68$^-$ 206$^+$ (red arrows); M1 macrophages: CD 68$^+$ CD 206$^-$ (green arrows); M2 macrophages: CD 68$^+$ CD 206$^+$ (orange arrows). Scale bar = 75 μm. (B) Percent of cross sectional area (CSA) with positive staining for all cell types in the LD7 (black bars) and LSD1-7 (blue bars) groups normalized to the %CSA with positive staining in the contralateral leg (means ± SD). No significant difference between LD7 and LSD1-7 for any cell type (p ≥ 0.274).*

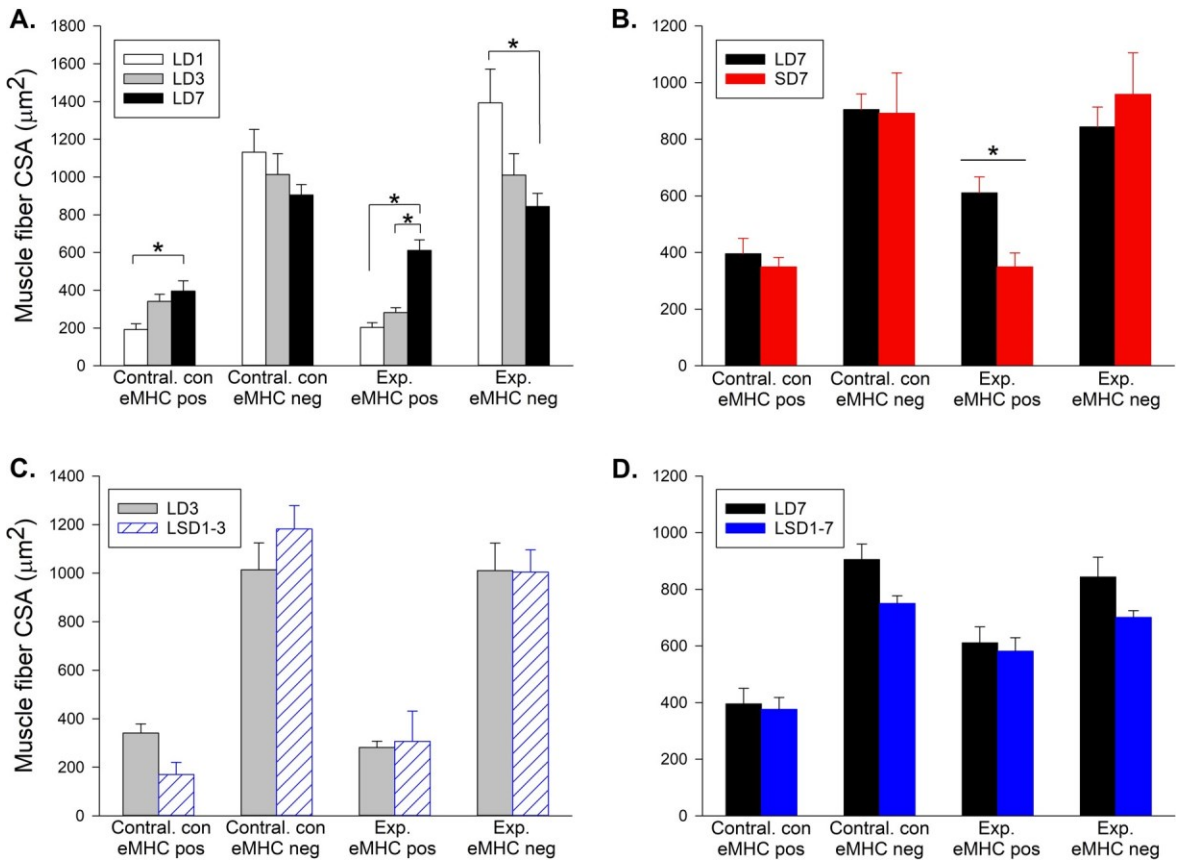

Figure 2-13: Cross sectional area (CSA) of embryonic myosin heavy chain (eMHC) fibres in control and treatment groups. *(A) CSA of positive and negative eMHC stained fibers from the experimental and contralateral legs for animals in the loading only group with tissue extracted from both the experimental and contralateral control legs on days 1, 3 or 7 (LD1, white bars; LD3, gray bars; LD7, black bars).* $^{*}p \leq 0.001$*. (B) CSA of positive and negative eMHC stained fibers from the experimental and contralateral legs for animals in the loading only and stimulation only groups with tissue extracted on day 7 (LD7, black bars; SD7, red bars).* $^{*}p = 0.001$*. (C) and (D) CSA of positive and negative eMHC stained fibers from the experimental and contralateral legs for animals in the loading only and loading with stim initiated on day 1 post induction of DTPI with tissue extracted on days 3 (LD3, gray bars; LSD1-3, blue, hashed bars) or 7 (LD7, black bars; LSD1-7, blue bars). There was no significant difference in the size of positive and negative eMHC stained fibers between the groups (*$p \geq 0.277$*).*

3. Conclusions and Future Directions

3.1. Summary

Despite advances in the treatment of pressure injuries over the past 60 years, there is no one method that is proven beneficial over the other, the incidence rate has not changed. Moreover, treatments for DPTI that prevent its progression to an open wound currently do not exist. The underlying mechanisms for the formation of DTPI involve mechanical and vascular (ischemia and ischemia/reperfusion injury) pathways as a result of prolonged pressure (Kosiak, 1961; Dinsdale, 1973; Bouten et al., 2003a).

Previously, IES was shown to be an effective preventive method for DTPI that directly addressed both pathways leading to its formation. IES delivered in bouts of 10 s-duration followed by 10 min-rest periods produce muscle contractions that mimic the fidgeting movements performed by able-bodied individuals to relieve discomfort while seated or lying down (Solis et al., 2007, 2011). Specifically, the IES-induced contraction of gluteus maximus muscle relieve pressure around the ischial tuberosities and improve tissue oxygenation in able-bodied and SCI individuals (Solis et al., 2007, 2011; Gyawali et al., 2011). IES was also effective in preventing the onset of DTPI in partially SCI pigs subjected loading for 4h/day for 4 weeks (Solis et al., 2013). In addition, the IES intervention was applied for an extended period in clinical settings, and was found to be safe, feasible and acceptable among the study participants and clinical staff (Ahmetović et al., 2015; Kane et al., 2017). Collectively, IES is a technique for preventing the formation of DTPI.

The overall goal of my project was to develop for the first time, IES as a treatment technique for an already formed DTPI to halt and reverse its advancement towards the skin. The current study looked at DTPI progression with/without IES in a rat model with SCI. The IES stimulation paradigm consisted of low amplitudes of electrical current causing minimal

contractions in the muscle with DTPI. My IES paradigm differed substantially from the paradigm used for the prevention of DPTI formation. Specifically, I used a 2s "on" period followed by a 5 min "off" period for 4 hours/day after a DPTI had already formed, and monitored the rate of DTPI healing. I compared the rate of healing with IES to that without IES.

The short bouts of IES at low amplitudes were intended to prevent already damaged tissue from worsening. I posited that the frequent small muscle contractions would diffuse edema from the site of injury and improve tissue oxygenation; therefore, expediting the healing process.

MRI results demonstrated a significant decrease in edema on day 3 post-induction of DTPI (T_2-weighted MRI) and a significant decrease in the size of injury on day 7 (T_1-weighted contrast-enhanced MRI) when the delivery of IES started on day 1 post-DTPI induction and ended on day 7. IHC results showed a significant increase in satellite cells, M1, and M2 macrophages on day 3 after DTPI. The results of this thesis propose a potential treatment option at an early stage of DTPI that may prevent the progression of injury towards the skin by reducing edema in the acute phase, and over time decrease the overall extent and size of DTPI.

3.2. Limitations

The loading only control group (Lc) underwent a natural healing process that reduced the extent of edema over time as demonstrated using T_2-weighted MRI. This was because a one-time load application to induce DTPI was used. Nonetheless, persistent edema and injury in the Lc group was seen with both the T_2-weighted and T_1-weighted contrast-

enhanced MRI, respectively. The effects of IES on the healing of a DPTI were likely smaller than would have been seen had multiple loading sessions been administered. Moreover, the effects of IES application at time points other than the first day post-DTPI induction may have been more substantial had multiple loading sessions been used.

While T_2-weighted MRI was obtained for all animal subgroups, T_1-weighted contrast-enhanced MRI indicating the size of persistent injury (Appendix 1) could not be obtained for all animals in the stimulation only (Sc) and loading with IES (LSt) groups. This was because the contrast agent for T_1-weighted contrast-enhanced MRI was administered intravenously on the final assessment day in each subgroup, during which an intravenous catheter was inserted in the jugular vein. Therefore, comparisons between Lc and LSt using T_1-weighted contrast-enhanced MRI could not be performed at all time points. It may have been possible to detect a significant difference in the size of a DPTI on day 5 between the Lc and LSt groups with T_1-weighted contrast-enhanced MRI indicating an earlier effect of IES. Nonetheless, a difference was detected on day 7.

IHC showed satellite cells fused into new myofibers (identified by the developmental marker, eMHC) in tissue extracted on day 3, and mature myofibers in tissue extracted on day 7. On these days, no significant difference was detected in the eMHC-labeled fibers between the Lc group and the LSt subgroup with IES starting on day 1. This is likely because day 3 is too early for the detection of eMHC-labeled fibers in both groups. Moreover, day 7 may have either also been too early for the development of regenerated myofibers since tissue regeneration and remodelling can extend to 4 weeks depending on the severity of injury (Mackey et al., 2017), or the natural healing process after the one-time application of loading obscured the effect of IES.

3.3. Future directions

An extension to this study would be to look at a paradigm with multiple loading sessions followed by application of IES to study the effectiveness of the intervention. This would be a closer model to DTPI occurrence in clinical settings. Previously, application of IES to prevent DTPI formation as a result of daily loading was studied in paralyzed pigs (Solis et al., 2013). The results showed that IES, when applied every day for one month, prevented the formation of DTPI (Solis et al., 2013). A similar model could be used to study the effectiveness of the IES intervention as a treatment technique on the progression of an already formed DTPI. In addition, the current study looked at a single stimulation paradigm that was applied after DTPI formation. The effect of other stimulation parameters (e.g., pulse width, pulse frequency, durations of "on" and "off") may have an effect on the rate of healing.

In Chapter 2, the T_2-weighted MRI findings for DTPI progression in paralyzed rats were emphasized to compare the control and treatment subgroups. T_1-weighted contrast-enhanced MRI sequences were acquired at one time-point (i.e., day 7) for the treatment subgroups. Information from T_2-weighted and T_1-weighted contrast-enhanced MRI sequences are useful to provide a more in depth knowledge regarding the effects of IES in the acute and chronic stages of DTPI. A larger animal model (e.g., pig model) may be used to address this limitation in future studies.

The IHC results showed an increase in satellite cells, M1, and M2 macrophages in tissue collected on day 3 after DTPI. However, there was no difference in these cells on day 7 after DTPI. While the peak in the satellite cell response is at 7-8 days after injury in humans (Mackey et al., 2017), a peak in animal studies were observed between 2-7 days (Ciciliot and

Schiaffino, 2010). We were not able to address the difference in eMHC on day 3 as this time point is too early for the formation of new myofibers. Some papers suggest that the peak in regenerating fibers is seen at two weeks in animals (Ciciliot and Schiaffino, 2010). A long term animal model (i.e., weeks) will be able to address these limitations related to changes in the regenerating fibers.

Although previous studies have shown the rate of tissue regeneration in various animal models such as mouse, rat, and pigs, there appears to be limited information about human muscle regeneration. This can make the direct comparison between animal models and humans challenging. The stimulation parameters and results from the animal work could be consolidated to develop a device that is non-invasive and user friendly for use in humans. The progression of DTPI with the application of IES intervention using these devices in humans is a realistic future development. IES may prove to be an innocuous yet effect means for treating DTPI, a devastating condition that currently has no known treatment.

Bibliography

Abdel-Aty H, Zagrosek A, Schulz-Menger J, Taylor AJ, Messroghli D, Kumar A, Gross M, Dietz R, Friedrich MG (2004) Delayed enhancement and T2-weighted cardiovascular magnetic resonance imaging differentiate acute from chronic myocardial infarction. Circulation 109:2411–2416.

Adegoke BO, Badmos KA (2001) Acceleration of pressure ulcer healing in spinal cord injured patients using interrupted direct current. Afr J Med Med Sci 30:195–197.

Ahmetović A, Mushahwar VK, Sommer R, Schnepf D, Kawasaki L, Warwaruk-Rogers R, Barlott T, Chong SL, Isaacson G, Kim S, Ferguson-Pell M, Stein RB, Ho C, Dukelow S, Chan KM (2015) Safety and Feasibility of Intermittent Electrical Stimulation for the Prevention of Deep Tissue Injury. Adv Wound Care 4:192–201.

Allen L, McGarrah B, Barrett D, Stenson B, Turpin PG, Vangilder C (2012) Air-fluidized therapy in patients with suspected deep tissue injury: a case series. J Wound Ostomy Cont Nurs Off Publ Wound Ostomy Cont Nurses Soc 39:555–561.

Andersen KE, Jensen O, Kvorning SA, Bach E (1983) Decubitus prophylaxis: a prospective trial on the efficiency of alternating-pressure air-mattresses and water-mattresses. Acta Derm Venereol 63:227–230.

Ankrom MA, Bennett RG, Sprigle S, Langemo D, Black JM, Berlowitz DR, Lyder CH, National Pressure Ulcer Advisory Panel (2005) Pressure-related deep tissue injury under intact skin and the current pressure ulcer staging systems. Adv Skin Wound Care 18:35–42.

Anthony D, Parboteeah S, Saleh M, Papanikolaou P (2008) Norton, Waterlow and Braden scores: a review of the literature and a comparison between the scores and clinical judgement. J Clin Nurs 17:646–653.

Atkinson RA, Cullum NA (2018) Interventions for pressure ulcers: a summary of evidence for prevention and treatment. Spinal Cord 56:186–198.

Az-ma T, Saeki N, Yuge O (1999) Cytosolic Ca2+ movements of endothelial cells exposed to reactive oxygen intermediates: Role of hydroxyl radical-mediated redox alteration of cell-membrane Ca2+ channels. Br J Pharmacol 126:1462–1470.

Bader DL, Barnhill RL, Ryan TJ (1986) Effect of externally applied skin surface forces on tissue vasculature. Arch Phys Med Rehabil 67:807–811.

Barker AT, Jaffe LF, Vanable JW (1982) The glabrous epidermis of cavies contains a powerful battery. Am J Physiol-Regul Integr Comp Physiol 242:R358–R366.

Barnett JA (2003) A history of research on yeasts 6: the main respiratory pathway. Yeast 20:1015–1044.

Becker D, Gary DS, Rosenzweig ES, Grill WM, McDonald JW (2010) Functional electrical stimulation helps replenish progenitor cells in the injured spinal cord of adult rats. Exp Neurol 222:211–218.

Benati G, Delvecchio S, Cilla D, Pedone V (2001) Impact on pressure ulcer healing of an arginine-enriched nutritional solution in patients with severe cognitive impairment. Arch Gerontol Geriatr 33:43–47.

Berg G, Nyberg S, Harrison P, Baumchen J, Gurss E, Hennes E (2010) Near-infrared spectroscopy measurement of sacral tissue oxygen saturation in healthy volunteers immobilized on rigid spine boards. Prehospital Emerg Care Off J Natl Assoc EMS Physicians Natl Assoc State EMS Dir 14:419–424.

Bergstrom N, Braden BJ, Laguzza A, Holman V (1987) The Braden Scale for Predicting Pressure Sore Risk. Nurs Res 36:205–210.

Besedovsky L, Lange T, Born J (2012) Sleep and immune function. Pflugers Arch 463:121–137.

Bickel CS, Slade JM, Dudley GA (2004) Long-term spinal cord injury increases susceptibility to isometric contraction-induced muscle injury. Eur J Appl Physiol 91:308–313.

Black J, Baharestani M, Cuddigan J, Dorner B, Edsberg L, Langemo D, Posthauer ME, Ratliff C, Taler G, National Pressure Ulcer Advisory Panel (2007) National Pressure Ulcer Advisory Panel's updated pressure ulcer staging system. Dermatol Nurs 19:343–349; quiz 350.

Blaisdell FW (2002) The pathophysiology of skeletal muscle ischemia and the reperfusion syndrome: a review. Cardiovasc Surg Lond Engl 10:620–630.

Bluestein D, Javaheri A (2008) Pressure ulcers: prevention, evaluation, and management. Am Fam Physician 78:1186–1194.

Bogie KM, Triolo RJ (2003) Effects of regular use of neuromuscular electrical stimulation on tissue health. J Rehabil Res Dev 40:469–475.

Bogie KM, Wang X, Triolo RJ (2006) Long-term prevention of pressure ulcers in high-risk patients: a single case study of the use of gluteal neuromuscular electric stimulation. Arch Phys Med Rehabil 87:585–591.

BOSBOOM E (2001) Deformation as a trigger for pressure sore related muscle damage. PhD Diss Tech Univ Eindh Available at: https://ci.nii.ac.jp/naid/10018026647/ [Accessed March 15, 2018].

Bosboom EMH, Bouten CVC, Oomens CWJ, Baaijens FPT, Nicolay K (2003) Quantifying pressure sore-related muscle damage using high-resolution MRI. J Appl Physiol 95:2235–2240.

Bours GJJW, Halfens RJG, Abu-Saad HH, Grol RTPM (2002) Prevalence, prevention, and treatment of pressure ulcers: descriptive study in 89 institutions in the Netherlands. Res Nurs Health 25:99–110.

Bouten CV, Oomens CW, Baaijens FP, Bader DL (2003a) The etiology of pressure ulcers: Skin deep or muscle bound? Arch Phys Med Rehabil 84:616–619.

Bouten CVC, Breuls RGM, Peeters EAG, Oomens CWJ, Baaijens FPT (2003b) In vitro models to study compressive strain-induced muscle cell damage. Biorheology 40:383–388.

Boyko TV, Longaker MT, Yang GP (2016) Review of the Current Management of Pressure Ulcers. Adv Wound Care 7:57–67.

Bradley M, Cullum N, Sheldon T (1999) The debridement of chronic wounds: a systematic review. Centre for Reviews and Dissemination (UK). Available at: https://www.ncbi.nlm.nih.gov/books/NBK67945/ [Accessed April 24, 2018].

Braverman B, McCarthy RJ, Ivankovich AD, Forde DE, Overfield M, Bapna MS (1989) Effect of helium-neon and infrared laser irradiation on wound healing in rabbits. Lasers Surg Med 9:50–58.

Brem H, Maggi J, Nierman D, Rolnitzky L, Bell D, Rennert R, Golinko M, Yan A, Lyder C, Vladeck B (2010) High Cost of Stage IV Pressure Ulcers. Am J Surg 200:473–477.

Breuls RGM, Bouten CVC, Oomens CWJ, Bader DL, Baaijens FPT (2003a) Compression Induced Cell Damage in Engineered Muscle Tissue: An <Emphasis Type="Italic">In Vitro</Emphasis> Model to Study Pressure Ulcer Aetiology. Ann Biomed Eng 31:1357–1364.

Breuls RGM, Bouten CVC, Oomens CWJ, Bader DL, Baaijens FPT (2003b) A Theoretical Analysis of Damage Evolution in Skeletal Muscle Tissue With Reference to Pressure Ulcer Development. J Biomech Eng 125:902–909.

Brienza D, Kelsey S, Karg P, Allegretti A, Olson M, Schmeler M, Zanca J, Geyer MJ, Kusturiss M, Holm M (2010) A randomized clinical trial on preventing pressure ulcers with wheelchair seat cushions. J Am Geriatr Soc 58:2308–2314.

Burnham R, Martin T, Stein R, Bell G, MacLean I, Steadward R (1997) Skeletal muscle fibre type transformation following spinal cord injury. Spinal Cord 35:86–91.

Byrne AM, Lemasters JJ, Nieminen AL (1999) Contribution of increased mitochondrial free Ca2+ to the mitochondrial permeability transition induced by tert-butylhydroperoxide in rat hepatocytes. Hepatol Baltim Md 29:1523–1531.

Cadue J-F, Karolewicz S, Tardy C, Barrault C, Robert R, Pourrat O (2008) [Prevention of heel pressure sores with a foam body-support device. A randomized controlled trial in a medical intensive care unit]. Presse Medicale Paris Fr 1983 37:30–36.

Carden DL, Korthuis RJ (1989) Mechanisms of postischemic vascular dysfunction in skeletal muscle: implications for therapeutic intervention. Microcirc Endothelium Lymphatics 5:277–298.

Carden Donna L., Granger D. Neil (2000) Pathophysiology of ischaemia–reperfusion injury. J Pathol 190:255–266.

Carlson M, Vigen CL, Rubayi S, Blanche EI, Blanchard J, Atkins M, Bates-Jensen B, Garber SL, Pyatak EA, Diaz J, Florindez LI, Hay JW, Mallinson T, Unger JB, Azen SP, Scott M, Cogan A, Clark F (2017) Lifestyle intervention for adults with spinal cord injury: Results of the USC-RLANRC Pressure Ulcer Prevention Study. J Spinal Cord Med:1–18.

Chapman AR, Adamson PD, Mills NL (2017) Assessment and classification of patients with myocardial injury and infarction in clinical practice. Heart 103:10–18.

Chen C-H, Wang W-J, Kuo J-C, Tsai H-C, Lin J-R, Chang Z-F, Chen R-H (2005) Bidirectional signals transduced by DAPK-ERK interaction promote the apoptotic effect of DAPK. EMBO J 24:294–304.

Choo J, Nixon J, Nelson EA, McGinnis E (2014) Autolytic debridement for pressure ulcers. In: The Cochrane Library. John Wiley & Sons, Ltd. Available at: http://cochranelibrary-wiley.com/doi/10.1002/14651858.CD011331/full [Accessed April 24, 2018].

Chou R, Dana T, Bougatsos C, Blazina I, Starmer AJ, Reitel K, Buckley DI (2013) Pressure ulcer risk assessment and prevention: a systematic comparative effectiveness review. Ann Intern Med 159:28–38.

Chow WW, Odell EI (1978) Deformations and Stresses in Soft Body Tissues of a Sitting Person. J Biomech Eng 100:79–87.

Ciciliot S, Schiaffino S (2010) Regeneration of mammalian skeletal muscle. Basic mechanisms and clinical implications. Curr Pharm Des 16:906–914.

Clark M (2011) TECHNOLOGY UPDATE: Understanding support surfaces. 2:5.

Collier ME (1996) Pressure-reducing mattresses. J Wound Care 5:207–211.

Comorosan S, Vasilco R, Arghiropol M, Paslaru L, Jieanu V, Stelea S (1993) The effect of diapulse therapy on the healing of decubitus ulcer. Romanian J Physiol Physiol Sci 30:41–45.

Convertino VA (1997) Cardiovascular consequences of bed rest: effect on maximal oxygen uptake. Med Sci Sports Exerc 29:191–196.

Curtis CA, Chong SL, Kornelsen I, Uwiera RRE, Seres P, Mushahwar VK (2011) The effects of intermittent electrical stimulation on the prevention of deep tissue injury: varying loads and stimulation paradigms. Artif Organs 35:226–236.

Dahlbäck LO, Rais O (1966) Morphologic changes in striated muscle following ischemia. Immediate postischemic phase. Acta Chir Scand 131:430–440.

Daniel RK, Priest DL, Wheatley DC (1981) Etiologic factors in pressure sores: an experimental model. Arch Phys Med Rehabil 62:492–498.

Darouiche RO, Landon GC, Klima M, Musher DM, Markowski J (1994) Osteomyelitis Associated With Pressure Sores. Arch Intern Med 154:753–758.

Darr KC, Schultz E (1989) Hindlimb suspension suppresses muscle growth and satellite cell proliferation. J Appl Physiol Bethesda Md 1985 67:1827–1834.

Defloor T (1999) The risk of pressure sores: a conceptual scheme. J Clin Nurs 8:206–216.

Defloor T, Grypdonck MFH (2004) Validation of pressure ulcer risk assessment scales: a critique. J Adv Nurs 48:613–621.

Diana JN, Laughlin MH (1974) Effect of Ischemia on Capillary Pressure and Equivalent Pore Radius in Capillaries of the Isolated Dog Hind Limb. Circ Res 35:77–101.

Dinsdale SM (1973) Decubitus ulcers in swine: light and electron microscopy study of pathogenesis. Arch Phys Med Rehabil 54:51-56 passim.

Dinsdale SM (1974) Decubitus ulcers: role of pressure and friction in causation. Arch Phys Med Rehabil 55:147–152.

Dodd KT, Gross DR (1991) Three-dimensional tissue deformation in subcutaneous tissues overlying bony prominences may help to explain external load transfer to the interstitium. J Biomech 24:11–19.

Edsberg LE, Black JM, Goldberg M, McNichol L, Moore L, Sieggreen M (2016) Revised National Pressure Ulcer Advisory Panel Pressure Injury Staging System: Revised Pressure Injury Staging System. J Wound Ostomy Cont Nurs Off Publ Wound Ostomy Cont Nurses Soc 43:585–597.

European Pressure Ulcer Advisory Panel, National Pressure Ulcer Advisory Panel (U.S.), Pan Pacific Pressure Injury Alliance (2014) Prevention and treatment of pressure ulcers: quick reference guide.

Evans RD, Foltz D, Foltz K (2001) Electrical stimulation with bone and wound healing. Clin Podiatr Med Surg 18:79–95, vi.

Ewing MR, Garrow C, Pressley TA, Ashley C, Kinsella NM (1964) FURTHER EXPERIENCES IN THE USE OF SHEEPSKINS AS AN AID IN NURSING. Med J Aust 2:139–141.

Farivar S, Malekshahabi T, Shiari R (2014) Biological effects of low level laser therapy. J Lasers Med Sci 5:58–62.

Feger MA, Goetschius J, Love H, Saliba SA, Hertel J (2015) Electrical stimulation as a treatment intervention to improve function, edema or pain following acute lateral ankle sprains: A systematic review. Phys Ther Sport Off J Assoc Chart Physiother Sports Med 16:361–369.

Ferguson AC, Keating JF, Delargy MA, Andrews BJ (1992) Reduction of seating pressure using FES in patients with spinal cord injury. A preliminary report. Paraplegia 30:474–478.

Feuchtinger J, Halfens RJG, Dassen T (2005) Pressure ulcer risk factors in cardiac surgery: a review of the research literature. Heart Lung J Crit Care 34:375–385.

Fuchs U, Zittermann A, Stuettgen B, Groening A, Minami K, Koerfer R (2005) Clinical Outcome of Patients With Deep Sternal Wound Infection Managed by Vacuum-Assisted Closure

Compared to Conventional Therapy With Open Packing: A Retrospective Analysis. Ann Thorac Surg 79:526–531.

Fuhrer MJ, Garber SL, Rintala DH, Clearman R, Hart KA (1993) Pressure ulcers in community-resident persons with spinal cord injury: prevalence and risk factors. Arch Phys Med Rehabil 74:1172–1177.

Fuoco U, Scivoletto G, Pace A, Vona VU, Castellano V (1997) Anaemia and serum protein alteration in patients with pressure ulcers. Spinal Cord 35:58–60.

Galpin JE, Chow AW, Bayer AS, Guze LB (1976) Sepsis associated with decubitus ulcers. Am J Med 61:346–350.

Garber SL, Rintala DH (2003) Pressure ulcers in veterans with spinal cord injury: a retrospective study. J Rehabil Res Dev 40:433–441.

Gawlitta D, Li W, Oomens CWJ, Baaijens FPT, Bader DL, Bouten CVC (2007) The relative contributions of compression and hypoxia to development of muscle tissue damage: an in vitro study. Ann Biomed Eng 35:273–284.

Gefen A (2007) The biomechanics of sitting-acquired pressure ulcers in patients with spinal cord injury or lesions. Int Wound J 4:222–231.

Gefen A, Gefen N, Linder-Ganz E, Margulies SS (2005) In vivo muscle stiffening under bone compression promotes deep pressure sores. J Biomech Eng 127:512–524.

Gorecki C, Brown JM, Nelson EA, Briggs M, Schoonhoven L, Dealey C, Defloor T, Nixon J, European Quality of Life Pressure Ulcer Project group (2009) Impact of pressure ulcers on quality of life in older patients: a systematic review. J Am Geriatr Soc 57:1175–1183.

Granger DN (1988) Role of xanthine oxidase and granulocytes in ischemia-reperfusion injury. Am J Physiol 255:H1269-1275.

Graves N, Birrell FA, Whitby M (2005) Modeling the economic losses from pressure ulcers among hospitalized patients in Australia. Wound Repair Regen 13:462–467.

Gray D, Campbell M (1994) A Randomised Clinical Trial of Two Types of Foam Mattresses. J Tissue Viability 4:128–132.

Greenleaf JE, Vernikos J, Wade CE, Barnes PR (1992) Effect of leg exercise training on vascular volumes during 30 days of 6 degrees head-down bed rest. J Appl Physiol Bethesda Md 1985 72:1887–1894.

Griffin JW, Tooms RE, Mendius RA, Clifft JK, Vander Zwaag R, el-Zeky F (1991) Efficacy of high voltage pulsed current for healing of pressure ulcers in patients with spinal cord injury. Phys Ther 71:433–442; discussion 442-444.

Griffin M, Iqbal SA, Sebastian A, Colthurst J, Bayat A (2011) Degenerate Wave and Capacitive Coupling Increase Human MSC Invasion and Proliferation While Reducing Cytotoxicity in an In Vitro Wound Healing Model. PLoS ONE 6 Available at: https://www.ncbi.nlm.nih.gov/pmc/articles/PMC3156742/ [Accessed June 5, 2018].

Grommes J, Drechsler M, Soehnlein O (2014) CCR5 and FPR1 Mediate Neutrophil Recruitment in Endotoxin-Induced Lung Injury. J Innate Immun 6:111–116.

GROTH K (1942) Clinical observations and experimental studies of the pathogenesis of decubitus ulcers. Acta Chir Scand 87:1–209.

Guo B-S, Cheung K-K, Yeung SS, Zhang B-T, Yeung EW (2012) Electrical Stimulation Influences Satellite Cell Proliferation and Apoptosis in Unloading-Induced Muscle Atrophy in Mice. PLOS ONE 7:e30348.

Gute DC, Ishida T, Yarimizu K, Korthius RJ (1998) Inflammatory responses to ischemia, and reperfusion in skeletal muscle. Mol Cell Biochem 179:169–187.

Gyawali S, Solis L, Chong SL, Curtis C, Seres P, Kornelsen I, Thompson R, Mushahwar VK (2011) Intermittent electrical stimulation redistributes pressure and promotes tissue oxygenation in loaded muscles of individuals with spinal cord injury. J Appl Physiol 110:246–255.

Harris K, Walker PM, Mickle DA, Harding R, Gatley R, Wilson GJ, Kuzon B, McKee N, Romaschin AD (1986) Metabolic response of skeletal muscle to ischemia. Am J Physiol-Heart Circ Physiol 250:H213–H220.

Hashmi JT, Huang Y-Y, Osmani BZ, Sharma SK, Naeser MA, Hamblin MR (2010) Role of Low-Level Laser Therapy in Neurorehabilitation. PM R 2:S292–S305.

Hernandez LA, Grisham MB, Twohig B, Arfors KE, Harlan JM, Granger DN (1987) Role of neutrophils in ischemia-reperfusion-induced microvascular injury. Am J Physiol-Heart Circ Physiol 253:H699–H703.

Hesketh M, Sahin KB, West ZE, Murray RZ (2017) Macrophage Phenotypes Regulate Scar Formation and Chronic Wound Healing. Int J Mol Sci 18.

Hess R, Jaeschke A, Neubert H, Hintze V, Moeller S, Schnabelrauch M, Wiesmann H-P, Hart DA, Scharnweber D (2012) Synergistic effect of defined artificial extracellular matrices and pulsed electric fields on osteogenic differentiation of human MSCs. Biomaterials 33:8975–8985.

Holloway GA, Daly CH, Kennedy D, Chimoskey J (1976) Effects of external pressure loading on human skin blood flow measured by 133Xe clearance. J Appl Physiol 40:597–600.

Honaker JS, Forston MR, Davis EA, Weisner MM, Morgan JA, Sacca E (2016) The effect of adjunctive noncontact low frequency ultrasound on deep tissue pressure injury. Wound Repair Regen 24:1081–1088.

Horn SD, Bender SA, Ferguson ML, Smout RJ, Bergstrom N, Taler G, Cook AS, Sharkey SS, Voss AC (2004) The National Pressure Ulcer Long-Term Care Study: pressure ulcer development in long-term care residents. J Am Geriatr Soc 52:359–367.

Huang J, Hu X, Lu L, Ye Z, Zhang Q, Luo Z (2010) Electrical regulation of Schwann cells using conductive polypyrrole/chitosan polymers. J Biomed Mater Res A 93:164–174.

Huard J, Li Y, Fu FH (2002) Muscle injuries and repair: current trends in research. J Bone Joint Surg Am 84-A:822–832.

Husain T (1953) An experimental study of some pressure effects on tissues, with reference to the bed-sore problem. J Pathol Bacteriol 66:347–358.

Kabaroudis A, Gerassimidis T, Karamanos D, Papaziogas B, Antonopoulos V, Sakantamis A (2003) Metabolic alterations of skeletal muscle tissue after prolonged acute ischemia and reperfusion. J Investig Surg Off J Acad Surg Res 16:219–228.

Kaltenthaler E, Whitfield MD, Walters SJ, Akehurst RL, Paisley S (2001) UK, USA and Canada: how do their pressure ulcer prevalence and incidence data compare? J Wound Care 10:530–535.

Kaminski KA, Bonda TA, Korecki J, Musial WJ (2002) Oxidative stress and neutrophil activation—the two keystones of ischemia/reperfusion injury. Int J Cardiol 86:41–59.

Kane A, Warwaruk-Rogers R, Ho C, Chan M, Stein R, Mushahwar VK, Dukelow SP (2017) A Feasibility Study of Intermittent Electrical Stimulation to Prevent Deep Tissue Injury in the Intensive Care Unit. Adv Wound Care 6:115–124.

Kawasaki L, Mushahwar VK, Ho C, Dukelow SP, Chan LLH, Chan KM (2014) The mechanisms and evidence of efficacy of electrical stimulation for healing of pressure ulcer: a systematic review. Wound Repair Regen Off Publ Wound Heal Soc Eur Tissue Repair Soc 22:161–173.

Kelle S, Roes SD, Klein C, Kokocinski T, de Roos A, Fleck E, Bax JJ, Nagel E (2009) Prognostic value of myocardial infarct size and contractile reserve using magnetic resonance imaging. J Am Coll Cardiol 54:1770–1777.

Keller BPJA, Schuurman JP, van der Werken C (2006) Can near infrared spectroscopy measure the effect of pressure on oxygenation of sacral soft tissue? J Wound Care 15:213–217.

Kim HW, Farzaneh-Far A, Kim RJ (2009) Cardiovascular magnetic resonance in patients with myocardial infarction: current and emerging applications. J Am Coll Cardiol 55:1–16.

Kim SJ, Roy RR, Kim JA, Zhong H, Haddad F, Baldwin KM, Edgerton VR (2008) Gene expression during inactivity-induced muscle atrophy: effects of brief bouts of a forceful contraction countermeasure. J Appl Physiol Bethesda Md 1985 105:1246–1254.

Klocke FJ (2010) Cardiac magnetic resonance measurements of area at risk and infarct size in ischemic syndromes. J Am Coll Cardiol 55:2489–2490.

Kloth LC (2005) Electrical stimulation for wound healing: a review of evidence from in vitro studies, animal experiments, and clinical trials. Int J Low Extrem Wounds 4:23–44.

Kloth LC, Feedar JA (1988) Acceleration of wound healing with high voltage, monophasic, pulsed current. Phys Ther 68:503–508.

Koh TJ, DiPietro LA (2011) Inflammation and wound healing: the role of the macrophage. Expert Rev Mol Med 13:e23.

Kosiak M (1961) Etiology of decubitus ulcers. Arch Phys Med Rehabil 42:19–29.

Krapfl LA, Gray M (2008) Does regular repositioning prevent pressure ulcers? J Wound Ostomy Cont Nurs Off Publ Wound Ostomy Cont Nurses Soc 35:571–577.

Krasnoff J, Painter P (1999) The physiological consequences of bed rest and inactivity. Adv Ren Replace Ther 6:124–132.

Krause JS, Vines CL, Farley TL, Sniezek J, Coker J (2001) An exploratory study of pressure ulcers after spinal cord injury: Relationship to protective behaviors and risk factors. Arch Phys Med Rehabil 82:107–113.

Landi F, Onder G, Russo A, Bernabei R (2007) Pressure ulcer and mortality in frail elderly people living in community. Arch Gerontol Geriatr 44:217–223.

Latimer S, Chaboyer W, Gillespie BM (2015) The repositioning of hospitalized patients with reduced mobility: a prospective study. Nurs Open 2:85–93.

Leibovich SJ, Ross R (1975) The role of the macrophage in wound repair. A study with hydrocortisone and antimacrophage serum. Am J Pathol 78:71–100.

Leibovich SJ, Ross R (1976) A macrophage-dependent factor that stimulates the proliferation of fibroblasts in vitro. Am J Pathol 84:501–514.

Lente RW (1850) Cases of un-united fracture treated by electricity. NY State J Med 5:317–9.

Levine SP, Kett RL, Cederna PS, Bowers LD, Brooks SV (1989) Electrical muscle stimulation for pressure variation at the seating interface. J Rehabil Res Dev 26:1–8.

Levine SP, Kett RL, Cederna PS, Brooks SV (1990) Electric muscle stimulation for pressure sore prevention: tissue shape variation. Arch Phys Med Rehabil 71:210–215.

Li L, Zhang Y-M, Qiao W-L, Wang L, Zhang J-F (2007) Effects of hypothalamic paraventricular nuclei on apoptosis and proliferation of gastric mucosal cells induced by ischemia/reperfusion in rats. World J Gastroenterol WJG 13:874–881.

Linder-Ganz E, Engelberg S, Scheinowitz M, Gefen A (2006) Pressure–time cell death threshold for albino rat skeletal muscles as related to pressure sore biomechanics. J Biomech 39:2725–2732.

Lindsay T, Romaschin A, Walker PM (1989) Free radical mediated damage in skeletal muscle. Microcirc Endothelium Lymphatics 5:157–170.

Liu LQ, Nicholson GP, Knight SL, Chelvarajah R, Gall A, Middleton FRI, Ferguson-Pell MW, Craggs MD (2006) Pressure changes under the ischial tuberosities of seated individuals during sacral nerve root stimulation. J Rehabil Res Dev 43:209–218.

Loerakker S, Solis LR, Bader DL, Baaijens FPT, Mushahwar VK, Oomens CWJ (2013) How does muscle stiffness affect the internal deformations within the soft tissue layers of the buttocks under constant loading? Comput Methods Biomech Biomed Engin 16:520–529.

Loerakker S, Stekelenburg A, Strijkers GJ, Rijpkema JJM, Baaijens FPT, Bader DL, Nicolay K, Oomens CWJ (2010) Temporal effects of mechanical loading on deformation-induced damage in skeletal muscle tissue. Ann Biomed Eng 38:2577–2587.

Love MR, Palee S, Chattipakorn SC, Chattipakorn N (2018) Effects of electrical stimulation on cell proliferation and apoptosis. J Cell Physiol 233:1860–1876.

Lyder CH, Ayello EA (2008) Pressure Ulcers: A Patient Safety Issue. In: Patient Safety and Quality: An Evidence-Based Handbook for Nurses (Hughes RG, ed) Advances in Patient Safety. Rockville (MD): Agency for Healthcare Research and Quality (US). Available at: http://www.ncbi.nlm.nih.gov/books/NBK2650/ [Accessed March 21, 2018].

Mackey AL, Kjaer M (2017) Connective tissue regeneration in skeletal muscle after eccentric contraction-induced injury. J Appl Physiol Bethesda Md 1985 122:533–540.

Mackey AL, Magnan M, Chazaud B, Kjaer M (2017) Human skeletal muscle fibroblasts stimulate in vitro myogenesis and in vivo muscle regeneration. J Physiol 595:5115–5127.

Mahrholdt H, Wagner A, Holly TA, Elliott MD, Bonow RO, Kim RJ, Judd RM (2002) Reproducibility of Chronic Infarct Size Measurement by Contrast-Enhanced Magnetic Resonance Imaging. Circulation 106:2322–2327.

Man IOW, Morrissey MC, Cywinski JK (2007) Effect of neuromuscular electrical stimulation on ankle swelling in the early period after ankle sprain. Phys Ther 87:53–65.

Marchand S (2008) The physiology of pain mechanisms: from the periphery to the brain. Rheum Dis Clin North Am 34:285–309.

Martínez-Rodríguez A, Bello O, Fraiz M, Martinez-Bustelo S (2013) The effect of alternating and biphasic currents on humans' wound healing: a literature review. Int J Dermatol 52:1053–1062.

Mawson AR, Biundo JJ, Neville P, Linares HA, Winchester Y, Lopez A (1988) Risk factors for early occurring pressure ulcers following spinal cord injury. Am J Phys Med Rehabil 67:123–127.

May DA, Disler DG, Jones EA, Balkissoon AA, Manaster BJ (2000) Abnormal Signal Intensity in Skeletal Muscle at MR Imaging: Patterns, Pearls, and Pitfalls. RadioGraphics 20:S295–S315.

McInnes E, Jammali-Blasi A, Bell-Syer SEM, Dumville JC, Middleton V, Cullum N (2015) Support surfaces for pressure ulcer prevention. Cochrane Database Syst Rev:CD001735.

McLoughlin T, Snyder A, Brolinson P, Pizza F (2004) Sensory level electrical muscle stimulation: effect on markers of muscle injury. Br J Sports Med 38:725–729.

Merten H, Johannesma PC, Lubberding S, Zegers M, Langelaan M, Jukema GN, Heetveld MJ, Wagner C (2015) High risk of adverse events in hospitalised hip fracture patients of 65 years and older: results of a retrospective record review study. BMJ Open 5:e006663.

Mester E, Szende B, Gärtner P (1968) [The effect of laser beams on the growth of hair in mice]. Radiobiol Radiother (Berl) 9:621–626.

Michlovitz SL (2005) Is there a role for ultrasound and electrical stimulation following injury to tendon and nerve? J Hand Ther Off J Am Soc Hand Ther 18:292–296.

Miles SJ, Nowicki T, Fulbrook P (2013) Repositioning to prevent pressure injuries: evidence for practice. Aust Nurs Midwifery J 21:32.

Miller GE, Seale J (1981) Lymphatic clearance during compressive loading. Lymphology 14:161–166.

Moore Z, Cowman S, Conroy RM (2011) A randomised controlled clinical trial of repositioning, using the 30° tilt, for the prevention of pressure ulcers. J Clin Nurs 20:2633–2644.

Moore ZEH, Cowman S (2013) Wound cleansing for pressure ulcers. Cochrane Database Syst Rev:CD004983.

Mortenson W, Miller W (2008a) A review of scales for assessing the risk of developing a pressure ulcer in individuals with SCI. Spinal Cord 46:168–175.

Mortenson W, Miller W (2008b) A review of scales for assessing the risk of developing a pressure ulcer in individuals with SCI. Spinal Cord 46:168–175.

Mozdziak PE, Truong Q, Macius A, Schultz E (1998) Hindlimb suspension reduces muscle regeneration. Eur J Appl Physiol 78:136–140.

Nelson DL, Cox MM (2004) Lehninger Principles of Biochemistry.

Novak ML, Weinheimer-Haus EM, Koh TJ (2014) Macrophage activation and skeletal muscle healing following traumatic injury. J Pathol 232:344–355.

Nussbaum EL, Biemann I, Mustard B (1994) Comparison of ultrasound/ultraviolet-C and laser for treatment of pressure ulcers in patients with spinal cord injury. Phys Ther 74:812–823; discussion 824-825.

O'Connor JPB, Tofts PS, Miles KA, Parkes LM, Thompson G, Jackson A (2011) Dynamic contrast-enhanced imaging techniques: CT and MRI. Br J Radiol 84 Spec No 2:S112-120.

Ohno Y, Fujiya H, Goto A, Nakamura A, Nishiura Y, Sugiura T, Ohira Y, Yoshioka T, Goto K (2013) Microcurrent electrical nerve stimulation facilitates regrowth of mouse soleus muscle. Int J Med Sci 10:1286–1294.

Olyaee Manesh A, Flemming K, Cullum NA, Ravaghi H (2006) Electromagnetic therapy for treating pressure ulcers. Cochrane Database Syst Rev:CD002930.

Oomens CWJ, Bressers OFJT, Bosboom EMH, Bouten CVC, Bader DL (2003) Can Loaded Interface Characteristics Influence Strain Distributions in Muscle Adjacent to Bony Prominences? Comput Methods Biomech Biomed Engin 6:171–180.

Oomens CWJ, Broek M, Hemmes B, Bader DL (2016) How does lateral tilting affect the internal strains in the sacral region of bed ridden patients? - A contribution to pressure ulcer prevention. Clin Biomech Bristol Avon 35:7–13.

Oomens CWJ, Loerakker S, Bader DL (2010) The importance of internal strain as opposed to interface pressure in the prevention of pressure related deep tissue injury. J Tissue Viability 19:35–42.

Pancorbo-Hidalgo PL, Garcia-Fernandez FP, Lopez-Medina IM, Alvarez-Nieto C (2006) Risk assessment scales for pressure ulcer prevention: a systematic review. J Adv Nurs 54:94–110.

Papanikolaou P, Lyne P, Anthony D (2007) Risk assessment scales for pressure ulcers: A methodological review. Int J Nurs Stud 44:285–296.

Parks DA, Granger DN (1983) Ischemia-induced vascular changes: role of xanthine oxidase and hydroxyl radicals. Am J Physiol 245:G285-289.

Peeters E a. G, Bouten CVC, Oomens CWJ, Baaijens FPT (2003) Monitoring the biomechanical response of individual cells under compression: a new compression device. Med Biol Eng Comput 41:498–503.

Peters EJ, Lavery LA, Armstrong DG, Fleischli JG (2001) Electric stimulation as an adjunct to heal diabetic foot ulcers: a randomized clinical trial. Arch Phys Med Rehabil 82:721–725.

Polak A, Franek A, Taradaj J (2014) High-Voltage Pulsed Current Electrical Stimulation in Wound Treatment. Adv Wound Care 3:104–117.

Post F (1963) An Investigation of Geriatric Nursing Problems in Hospital. By A. N. Exton-Smith, Doreen Norton, Rhoda McLaren. Published by the Corporation for the Care of Old People, Nuffield Lodge, Regent's Park, London, N.W.1. pp. 238. Price 12s. 6d. 16.7.62. Br J Psychiatry 109:152–153.

Powell KE, Blair SN (1994) The public health burdens of sedentary living habits: theoretical but realistic estimates. Med Sci Sports Exerc 26:851–856.

Pronk JT (2000) Van kleine diertgens naar cell factories.

Qi F, Wang Y, Ma T, Zhu S, Zeng W, Hu X, Liu Z, Huang J, Luo Z (2013) Electrical regulation of olfactory ensheathing cells using conductive polypyrrole/chitosan polymers. Biomaterials 34:1799–1809.

Raman SV, Simonetti OP, Winner MW, Dickerson JA, He X, Mazzaferri EL, Ambrosio G (2010) Cardiac Magnetic Resonance With Edema Imaging Identifies Myocardium at Risk and Predicts Worse Outcome in Patients With Non–ST-Segment Elevation Acute Coronary Syndrome. J Am Coll Cardiol 55:2480–2488.

Rasero L, Simonetti M, Falciani F, Fabbri C, Collini F, Dal Molin A (2015) Pressure Ulcers in Older Adults: A Prevalence Study. Adv Skin Wound Care 28:461–464.

Reddy M, Gill SS, Kalkar SR, Wu W, Anderson PJ, Rochon PA (2008) Treatment of pressure ulcers: a systematic review. Jama 300:2647–2662.

Reddy NP, Cochran GV (1981) Interstitial fluid flow as a factor in decubitus ulcer formation. J Biomech 14:879–881.

Reed BV (1988) Effect of high voltage pulsed electrical stimulation on microvascular permeability to plasma proteins. A possible mechanism in minimizing edema. Phys Ther 68:491–495.

Richardson RR, Meyer PR (1981) Prevalence and incidence of pressure sores in acute spinal cord injuries. Spinal Cord 19:235.

Roes SD, Kelle S, Kaandorp TAM, Kokocinski T, Poldermans D, Lamb HJ, Boersma E, van der Wall EE, Fleck E, de Roos A, Nagel E, Bax JJ (2007) Comparison of myocardial infarct size assessed with contrast-enhanced magnetic resonance imaging and left ventricular function and volumes to predict mortality in patients with healed myocardial infarction. Am J Cardiol 100:930–936.

Russell LJ, Reynolds TM, Park C, Rithalia S, Gonsalkorale M, Birch J, Torgerson D, Iglesias C, PPUS-1 Study Group (2003) Randomized clinical trial comparing 2 support surfaces: results of the Prevention of Pressure Ulcers Study. Adv Skin Wound Care 16:317–327.

Russo CA, Elixhauser A (2006) Hospitalizations Related to Pressure Sores, 2003: Statistical Brief #3. In: Healthcare Cost and Utilization Project (HCUP) Statistical Briefs. Rockville (MD): Agency for Healthcare Research and Quality (US). Available at: http://www.ncbi.nlm.nih.gov/books/NBK63508/ [Accessed December 31, 2017].

Russo CA, Steiner C, Spector W (2006) Hospitalizations Related to Pressure Ulcers Among Adults 18 Years and Older, 2006: Statistical Brief #64. Available at: http://europepmc.org/abstract/med/21595131 [Accessed December 31, 2017].

Saunders LL, Krause JS, Focht KL (2012) A longitudinal study of depression in survivors of spinal cord injury. Spinal Cord 50:72–77.

Savill JS, Wyllie AH, Henson JE, Walport MJ, Henson PM, Haslett C (1989) Macrophage phagocytosis of aging neutrophils in inflammation. Programmed cell death in the neutrophil leads to its recognition by macrophages. J Clin Invest 83:865–875.

Schmid-Schoenbein GW, Fung YC, Zweifach BW (1975) Vascular endothelium-leukocyte interaction; sticking shear force in venules. Circ Res 36:173–184.

Schultz A, Bien M, Dumond K, Brown K, Myers A (1999) Etiology and incidence of pressure ulcers in surgical patients. AORN J 70:434, 437–440, 443–449.

Scivoletto G, Fuoco U, Morganti B, Cosentino E, Molinari M (2004) Pressure sores and blood and serum dysmetabolism in spinal cord injury patients. Spinal Cord 42:473–476.

Shahin ESM, Dassen T, Halfens RJG (2008) Pressure ulcer prevalence in intensive care patients: a cross-sectional study. J Eval Clin Pract 14:563–568.

Shea JD (1975) Pressure sores: classification and management. Clin Orthop:89–100.

Shields RK, Dudley-Javoroski S (2007) Musculoskeletal Adaptations in Chronic Spinal Cord Injury: Effects of Long-term Soleus Electrical Stimulation Training. Neurorehabil Neural Repair 21:169–179.

Siu PM, Alway SE (2009) Response and adaptation of skeletal muscle to denervation stress: the role of apoptosis in muscle loss. Front Biosci Landmark Ed 14:432–452.

Slade JM, Bickel CS, Dudley GA (2004) The effect of a repeat bout of exercise on muscle injury in persons with spinal cord injury. Eur J Appl Physiol 92:363–366.

Snyder AR, Perotti AL, Lam KC, Bay RC (2010) The influence of high-voltage electrical stimulation on edema formation after acute injury: a systematic review. J Sport Rehabil 19:436–451.

Solis LR, Gyawali S, Seres P, Curtis CA, Chong SL, Thompson RB, Mushahwar VK (2011) Effects of intermittent electrical stimulation on superficial pressure, tissue oxygenation, and discomfort levels for the prevention of deep tissue injury. Ann Biomed Eng 39:649–663.

Solis LR, Hallihan DP, Uwiera RRE, Thompson RB, Pehowich ED, Mushahwar VK (2007) Prevention of pressure-induced deep tissue injury using intermittent electrical stimulation. J Appl Physiol Bethesda Md 1985 102:1992–2001.

Solis LR, Liggins A, Uwiera RRE, Poppe N, Pehowich E, Seres P, Thompson RB, Mushahwar VK (2012) Distribution of Internal Pressure around Bony Prominences: Implications to Deep Tissue Injury and Effectiveness of Intermittent Electrical Stimulation. Ann Biomed Eng 40:1740–1759.

Solis LR, Twist E, Seres P, Thompson RB, Mushahwar VK (2013) Prevention of deep tissue injury through muscle contractions induced by intermittent electrical stimulation after spinal cord injury in pigs. J Appl Physiol Bethesda Md 1985 114:286–296.

Stefanovska A, Vodovnik L, Benko H, Turk R (1993) Treatment of chronic wounds by means of electric and electromagnetic fields. Med Biol Eng Comput 31:213–220.

Stekelenburg A, Gawlitta D, Bader DL, Oomens CW (2008) Deep Tissue Injury: How Deep is Our Understanding? Arch Phys Med Rehabil 89:1410–1413.

Stekelenburg A, Strijkers GJ, Parusel H, Bader DL, Nicolay K, Oomens CW (2007) Role of ischemia and deformation in the onset of compression-induced deep tissue injury: MRI-based studies in a rat model. J Appl Physiol 102:2002–2011.

Sundaram V, Lim J, Tholey DM, Iriana S, Kim I, Manne V, Nissen NN, Klein AS, Tran TT, Ayoub WS, Schlansky B (2017) The Braden Scale, A standard tool for assessing pressure ulcer risk, predicts early outcomes after liver transplantation. Liver Transplant Off Publ Am Assoc Study Liver Dis Int Liver Transplant Soc 23:1153–1160.

Sundelacruz S, Li C, Choi YJ, Levin M, Kaplan DL (2013) Bioelectric modulation of wound healing in a 3D in vitro model of tissue-engineered bone. Biomaterials 34:6695–6705.

Thakral G, LaFontaine J, Najafi B, Talal TK, Kim P, Lavery LA (2013) Electrical stimulation to accelerate wound healing. Diabet Foot Ankle 4:22081.

Thomas DR (2010) Does pressure cause pressure ulcers? An inquiry into the etiology of pressure ulcers. J Am Med Dir Assoc 11:397–405.

Tidball JG (1995) Inflammatory cell response to acute muscle injury. Med Sci Sports Exerc 27:1022–1032.

Tidball JG (2005) Inflammatory processes in muscle injury and repair. Am J Physiol Regul Integr Comp Physiol 288:R345-353.

Todd BA, Thacker JG (1994) Three-dimensional computer model of the human buttocks, in vivo. J Rehabil Res Dev 31:111–119.

Topp R, Ditmyer M, King K, Doherty K, Hornyak J (2002) The effect of bed rest and potential of prehabilitation on patients in the intensive care unit. AACN Clin Issues 13:263–276.

Trumble DR, Duan C, Magovern JA (n.d.) EFFECTS OF LONG-TERM STIMULATION ON SKELETAL MUSCLE. :8.

Tupling R, Green H, Senisterra G, Lepock J, McKee N (2001a) Effects of 4-h ischemia and 1-h reperfusion on rat muscle sarcoplasmic reticulum function. Am J Physiol-Endocrinol Metab 281:E867–E877.

Tupling R, Green H, Senisterra G, Lepock J, McKee N (2001b) Effects of ischemia on sarcoplasmic reticulum Ca2+ uptake and Ca2+ release in rat skeletal muscle. Am J Physiol-Endocrinol Metab 281:E224–E232.

van Marum RJ, Ooms ME, Ribbe MW, van Eijk JT (2000) The Dutch pressure sore assessment score or the Norton scale for identifying at-risk nursing home patients? Age Ageing 29:63–68.

Vanderwee K, Clark M, Dealey C, Gunningberg L, Defloor T (2007) Pressure ulcer prevalence in Europe: a pilot study. J Eval Clin Pract 13:227–235.

VanGilder C, Amlung S, Harrison P, Meyer S (2009) Results of the 2008-2009 International Pressure Ulcer Prevalence Survey and a 3-year, acute care, unit-specific analysis. Ostomy Wound Manage 55:39–45.

VanGilder C, MacFarlane GD, Harrison P, Lachenbruch C, Meyer S (2010) The demographics of suspected deep tissue injury in the United States: an analysis of the International Pressure Ulcer Prevalence Survey 2006-2009. Adv Skin Wound Care 23:254–261.

Vodovnik L, Karba R (1992) Treatment of chronic wounds by means of electric and electromagnetic fields. Part 1. Literature review. Med Biol Eng Comput 30:257–266.

Wan Q, Yeung SS, Cheung KK, Au SW, Lam WW, Li YH, Dai ZQ, Yeung EW (2016) Optimizing Electrical Stimulation for Promoting Satellite Cell Proliferation in Muscle Disuse Atrophy. Am J Phys Med Rehabil 95:28–38.

Waterlow J (1985) Pressure sores: a risk assessment card. Nurs Times 81:49–55.

Waterlow J (1988) Tissue viability. Prevention is cheaper than cure. Nurs Times 84:69–70.

Waterlow J (1991) A policy that protects. The Waterlow Pressure Sore Prevention/Treatment Policy. Prof Nurse Lond Engl 6:258, 260, 262–264.

Westby MJ, Dumville JC, Soares MO, Stubbs N, Norman G (2017) Dressings and topical agents for treating pressure ulcers. Cochrane Database Syst Rev 6:CD011947.

Whittington K, Patrick M, Roberts JL (2000) A National Study of Pressure Ulcer Prevalence and Incidence in Acute Care Hospitals. J Wound Ostomy Continence Nurs 27:209.

Willenborg S, Lucas T, Loo G van, Knipper JA, Krieg T, Haase I, Brachvogel B, Hammerschmidt M, Nagy A, Ferrara N, Pasparakis M, Eming SA (2012) CCR2 recruits an inflammatory macrophage subpopulation critical for angiogenesis in tissue repair. Blood 120:613–625.

Wolcott LE, Wheeler PC, Hardwicke HM, Rowley BA (1969) Accelerated healing of skin ulcer by electrotherapy: preliminary clinical results. South Med J 62:795–801.

Wood JM, Evans PE, Schallreuter KU, Jacobson WE, Sufit R, Newman J, White C, Jacobson M (1993) A Multicenter Study on the Use of Pulsed Low-Intensity Direct Current for Healing Chronic Stage II and Stage III Decubitus Ulcers. Arch Dermatol 129:999–1009.

Woodbury MG, Houghton PE (2004) Prevalence of pressure ulcers in Canadian healthcare settings. Ostomy Wound Manage 50:22–24, 26, 28, 30, 32, 34, 36–38.

Young T (2004) The 30 degree tilt position vs the 90 degree lateral and supine positions in reducing the incidence of non-blanching erythema in a hospital inpatient population: a randomised controlled trial. J Tissue Viability 14: 88, 90, 92–96.

Appendix A

Comparing the progression of deep tissue pressure injury using T_2-weighted and T_1-weighted contrast-enhanced MRI in Skeletal Muscle.

A.1. Introduction

Contrast-enhanced MRI studies the pharmacokinetics of contrast agent in the blood vessels, interstitial space, and extracellular space (Kim et al., 2009). In this MRI technique images are acquired prior to the intravenous administration of a contrast agent (baseline) and subsequently after (O'Connor et al., 2011).

T_1-weighted contrast-enhanced MRI is currently used as a method for measuring the size of a cardiac infarct in individuals with a previous or suspected myocardial infarction (MI) (Abdel-Aty et al., 2004; Roes et al., 2007; Kim et al., 2009; Klocke, 2010). Information gained from this imaging modality complements information provided by biomarkers such as troponins and creatinine kinase, and echocardiography to predict MI prognosis (Abdel-Aty et al., 2004; Roes et al., 2007). In particular, T_1-weighted contrast-enhanced MRI helps delineate very small and subendocardial infarcts that are not detected by biomarkers, with high spatial resolution and precision. Clinical outcome after an irreversible myocardial injury has been best predicted by infarct size compared to other methods (Abdel-Aty et al., 2004; Kelle et al., 2009). Moreover, while functional recovery after MI shows high correlation between infarct size and creatinine kinase levels (Kelle et al., 2009), contrast- enhanced MRI provides accurate measures of the size and location of myocardial injury.

Acute MI produces an inflammatory response within a few hours after ischemia that persists for 7 days. The initial response which occurs at 4 – 12 hours after MI, is marked by neutrophil infiltration and edema formation (Chapman et al., 2017). Subsequent reperfusion after ischemia can accentuate the myocardial injury and inflammatory response. With gradual healing of myocardial injury, edema resolves followed by scar formation. There is substantial literature on the use of T_2-weighted MRI in the first few days and weeks after MI

showing edema associated with an acute MI that resolves with time (Abdel-Aty et al., 2004; Klocke, 2010; Raman et al., 2010). However, edema after MI may not necessarily indicate irreversible myocardial injury. The injury is often followed by scar formation in the chronic phase that is best delineated with T_1-weighted contrast-enhanced MRI (Mahrholdt et al., 2002; Abdel-Aty et al., 2004; Kelle et al., 2009; Klocke, 2010). Combining the information from both T_2-weighted images and T_1-weighted contrast-enhanced images may provide extensive information about the acute and recovery phases after an ischemic myocardial injury (Abdel-Aty et al., 2004).

Previous work in the progression of musculoskeletal injury commonly used T_2-weighted MRI; however, T_1-weighted contrast enhanced MRI for injury progression has not, to the best of my knowledge, been used. In Chapter 2, I demonstrated the progression of DTPI after skeletal muscle injury using T_2-weighted MRI. The findings showed an increase in the T_2 signal intensity on day 1 after loading (induction of DTPI) compared to days 3, 5, and 7, indicative of tissue edema at DTPI onset. In this study, T_1-weighted contrast-enhanced MRI was used to study DTPI progression with/without IES on days 1, 3, 5, and 7 after the induction of DTPI and the results were compared to findings from T_2-weighted MRI.

A.2. Methods

All experimental procedures were approved by the University of Alberta Animal Care and Use Committee. The experimental timeline and protocol are as described in Chapter 2. Briefly, experiments were conducted in adult female Sprague Dawley rats, which received spinal cord transection at the T8 level resulting in paralysis of the hind limbs. The rats were randomly assigned to loading only control (Lc; n = 31), stimulation only control

(Sc; n = 25), and loading with stimulation treatment (LSt; n = 33) groups. The rats from Lc and LSt received loading to the tibialis anterior muscle two weeks after the spinal transection, to induce a DTPI (described in section 2.3.2). The progression of the DTPI was assessed on days 1, 3, 5, and 7 using MRI.

On the day of MRI assessments, the rats were positioned in Siemens Hand and Wrist RF coil with the hind limbs aligned and secured with Velcro straps. Three MRI sequences were used to acquire the images: 1) T_2-weighted turbo spin echo (TSE), T_1-weighted 2D FLASH (pre-contrast), and T_1-weighted 2D FLASH with contrast. The contrast agent (Magnavist = 0.1ml) was injected via an intravenous catheter through the jugular vein. A series of 30 images of slice thickness 1mm were obtained from knee to ankle, with the parameters described in Chapter 2.

The MR images were analysed by 2 individuals (3 trials each) using a custom written MATLAB program (Mathworks, Cambridge, MA) (described in section 2.3.5). The total pixels exhibiting increased signal intensity in slices of the tibialis anterior muscle from the knee to ankle were used to identify the percentage of muscle volume with DTPI. In this chapter, the T_2-weighted MRI and T_1-weighted contrast enhanced MRI findings for all groups are discussed.

A one-way ANOVA was performed to determine the total muscle volume exhibiting a change in signal intensity in T_2-weighted images and T_1-weighted contrast enhanced images across time points. A two-way ANOVA was conducted to compare the total muscle volume exhibiting a change in signal intensity (dependent variable) as a function of imaging technique and study group (independent variables). Least Significance Difference or Tukey's Honestly Significant Difference post-hoc tests were used for post-hoc analyses.

Differences with $p \leq 0.05$ were considered significant.

A.3. Results

A comparison of DTPI progression in a subgroup of Lc animals that had undergone both T_2-weighted imaging and T_1-weighted contrast-enhanced imaging is shown in Figure 4-1A. T_2-weighted MRI showed a significant increase in muscle volume exhibiting increased signal intensity on day 1 compared to days 3, 5, and 7 (one-way ANOVA; $*p \leq 0.002$). In contrast, the T_1-weighted contrast-enhanced MRI indicated no difference across the time points (one-way ANOVA; $p \leq 0.135$). Secondly, there was a significant difference in the percentage of muscle volume with increased signal intensity between the T_2-weighted and T_1-weighted contrast-enhanced MRI groups on day 1 time-point (two-way ANOVA; $*p \leq 0.001$).

Figure 4-1B compares the findings from T_2-weighted MRI and T_1-weighted contrast-enhanced MRI for the subgroup of Sc animals that had undergone both methods of imaging. There was no significant difference in the muscle volume with increased signal intensity of the stimulated leg obtained by both MRI sequences (one ANOVA; $p \leq 0.10$). In addition, there was no significant difference between the experimental and contralateral control leg using the two MRI sequences (two-way ANOVA; $p \leq 0.09$).

In Figure 4-2, the percentage of muscle volume with increased signal intensity was compared using T_2-weighted MRI and T_1-weighted contrast-enhanced MRI for animalswith/without IES on days 3 and 7. There was a significant difference between the Lc and LSt subgroups on day 7 using T_1-weighted contrast-enhanced MRI (independent t-test;

*$p \leq 0.026$). Interestingly, there was no significant difference between the other subgroups comparing the days 3 and 7 with/without IES using T_2-weighted and T_1-weighted contrast-enhanced MRI (independent t-test; $p \leq 0.437$).

A.4. Discussion

The overall goal of this study was to assess the progression of DTPI in skeletal muscle with and without IES using two imaging techniques: T_2-weighted and T_1-weighted contrast-enhanced MRI. The T_2-weighted MRI findings indicate a significant reduction in the percentage of muscle volume exhibiting increased signal intensity on days 3, 5, and 7 compared to day 1. There was also a significant difference between the two imaging techniques on the day 1 time point. However, T_1-weighted contrast-enhanced MRI in the same rats showed no statistical difference across time points. These results support the findings on MI progression using T_2-weighted and T_1-weighted contrast-enhanced MRI, wherein the initial response to the injury is seen as an increased signal intensity on day 1 with T_2-weighted MRI, which resolves on the subsequent days. This increase in the signal intensity is a result of tissue edema in the acute phase of injury. Whereas, the T_1-weighted contrast-enhanced MRI delineates scar formation in the chronic phase of DTPI. Collectively, the T_2-weighted and T_1-weighted contrast-enhanced MRI sequences are useful to provide information on tissue damage in both the acute and chronic stages. To the best of my knowledge, this is the first time that these two MRI sequences were compared in skeletal muscle.

In Chapter 2, I demonstrated the effect of IES, initiated on day 1 post-induction of DPTI, on the reduction of tissue edema (measured on day 3). The effect of IES initiated on

day 1 post-induction of DPTI on tissue edema measured on days 5 and 7 could not be detected (in comparison to the Lc group) using T_2-weighted MRI. In this study, the size of DTPI on day 7 was significantly different between the groups with and without IES (LSt, Lc) using T_1-weighted contrast-enhanced MRI. This suggests that the actual size of the injury on day 7 was significantly reduced by the use of IES when initiated on day 1 post-DTPI, confirming that IES may act by reducing the edema in the initial phase of DPTI and the size of injury in the chronic phase DTPI (day 7).

A.5. Figures

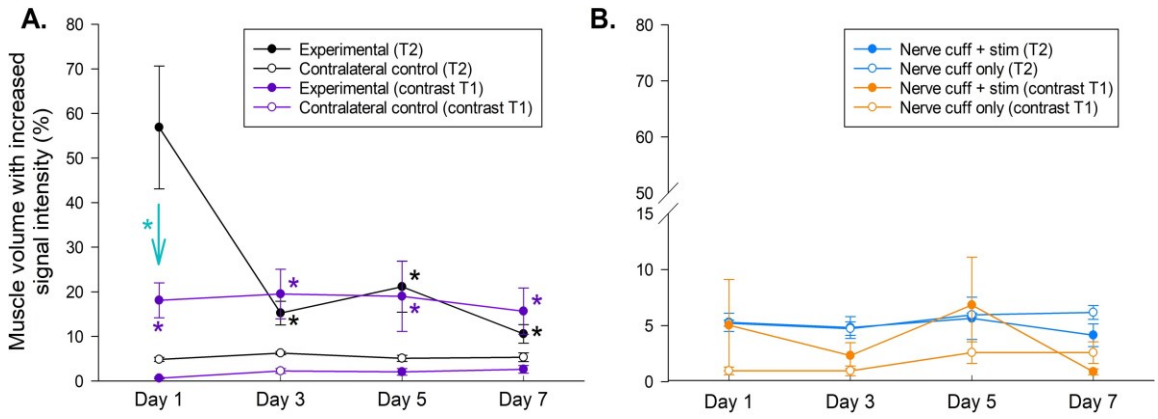

Figure A-1: Damage progression with T2-weighted & contrast-enhanced MRI. *A) Comparison of muscle volume with increased signal intensity for loading only control (Lc) subgroups on days 1, 3, 5, and 7 using T_2-weighted (black) and T_1-weighted contrast-enhanced MRI (purple) (mean ± SE). T_2-weighted MRI showed a significant decrease in signal intensity on days 3, 5, and 7 ($^*p \leq 0.002$). There was also a significant difference between the two MRI sequences on the day 1 time-point ($^*p \leq 0.001$). B) Comparison of T_2-weighted (blue) and T_1-weighted contrast-enhanced MRI (orange) for Sc subgroups (mean ± SE). There was no statistical difference between the experimental and contralateral control legs using both MRI sequences ($p \leq 0.100$).*

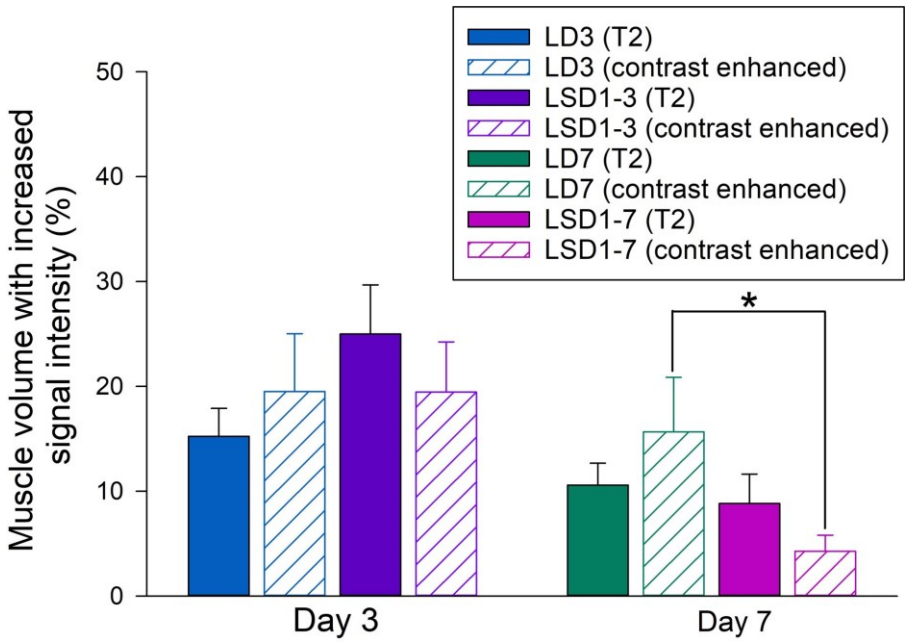

Figure A-2: Damage progression with/without IES using T2-weighted & contrast-enhanced MRI. *Comparison of T2-weighted and contrast-enhanced MRI with/without IES on days 3 and 7 (mean ± SE). The day 7 contrast-enhanced MRI (green bar) in the absence of IES was significantly different from the group that received IES initiating on day 1 and ending on day 7 (pink) (*$p \leq 0.026$).*

Bibliography

Abdel-Aty H, Zagrosek A, Schulz-Menger J, Taylor AJ, Messroghli D, Kumar A, Gross M, Dietz R, Friedrich MG (2004) Delayed enhancement and T2-weighted cardiovascular magnetic resonance imaging differentiate acute from chronic myocardial infarction. Circulation 109:2411–2416.

Chapman AR, Adamson PD, Mills NL (2017) Assessment and classification of patients with myocardial injury and infarction in clinical practice. Heart 103:10–18.

Kelle S, Roes SD, Klein C, Kokocinski T, de Roos A, Fleck E, Bax JJ, Nagel E (2009) Prognostic value of myocardial infarct size and contractile reserve using magnetic resonance imaging. J Am Coll Cardiol 54:1770–1777.

Kim HW, Farzaneh-Far A, Kim RJ (2009) Cardiovascular magnetic resonance in patients with myocardial infarction: current and emerging applications. J Am Coll Cardiol 55:1–16.

Klocke FJ (2010) Cardiac magnetic resonance measurements of area at risk and infarct size in ischemic syndromes. J Am Coll Cardiol 55:2489–2490.

Mahrholdt H, Wagner A, Holly TA, Elliott MD, Bonow RO, Kim RJ, Judd RM (2002) Reproducibility of Chronic Infarct Size Measurement by Contrast-Enhanced Magnetic Resonance Imaging. Circulation 106:2322–2327.

O'Connor JPB, Tofts PS, Miles KA, Parkes LM, Thompson G, Jackson A (2011) Dynamic contrast-enhanced imaging techniques: CT and MRI. Br J Radiol 84 Spec No 2:S112-120.

Raman SV, Simonetti OP, Winner MW, Dickerson JA, He X, Mazzaferri EL, Ambrosio G (2010) Cardiac Magnetic Resonance With Edema Imaging Identifies Myocardium at Risk and Predicts Worse Outcome in Patients With Non–ST-Segment Elevation Acute Coronary Syndrome. J Am Coll Cardiol 55:2480–2488.

Roes SD, Kelle S, Kaandorp TAM, Kokocinski T, Poldermans D, Lamb HJ, Boersma E, van der Wall EE, Fleck E, de Roos A, Nagel E, Bax JJ (2007) Comparison of myocardial infarct size assessed with contrast-enhanced magnetic resonance imaging and left ventricular function and volumes to predict mortality in patients with healed myocardial infarction. Am J Cardiol 100:930–936.